HOT STAMPING OF TITANIUM ALLOYS

By

Mateusz Kopec

Department of Mechanical Engineering

South Kensington Campus

Imperial College London

London SW7 2AZ

U.K.

A thesis submitted for the degree of Doctor of Philosophy

of

Imperial College London

2020

Please cite as: *M. Kopec, Hot stamping of titanium alloys, Imperial College London, 2020* *https://doi.org/10.25560/86389*

Declaration of originality

This thesis hereby presented is based on research by the author at the Department of Mechanical Engineering of Imperial College London. I declare the work contained in this thesis is only author's own work. Not any part of the present work has been submitted for any other degree or qualification elsewhere.

Mateusz Kopec

July 2020

Copyright declaration

Acknowledgements

'If I have seen further than other man, it is because I have stood on the shoulders of giants.'

First and foremost, I would like to express my sincerest gratitude to my supervisor, Dr Liliang Wang, who has patiently guided and supported me throughout my PhD work. I would also like to thank Prof. Jianguo Lin and Prof. Zbigniew L. Kowalewski for their ongoing support throughout the entire thesis.

I also would like to thank the Aviation Industry Corporation of China (AVIC) Beijing Aeronautical Manufacturing Technology Research Institute for their funding, and making this research possible. The research was performed at the AVIC Centre for Structural Design and Manufacture at Imperial College London.

I would like to give special thanks to my collegues and friends from Metal Forming Group: Kehuan Wang, Haitao Qu, Jun Liu, Denis J. Politis, Omer El-Fakir, Haoxiang Gao, Xiaochuan Liu, Saksham Dhawan, Xi Luan, Xiao Yang, Yiran Hu, Yang Zheng, Qunli Zhang, Yuhao Sun and Zhaoheng for the friendly co-operation, discussions and the great time we spent together during my PhD studies. Without their help, I would not have achieved such results from my experiments and simulations. I would thank to the technicians who give me a great help for setting up the experiments, Suresh and Alex.

I also wish to thank many research collaborators, especially from within my IFTR PAS research group, who supported my research and provided advice during my studies. Mirek, Pawel and Dominik, your support is much appreciated. Many thanks to my academic supervisor from Military University of Technology, Prof. Stanislaw Jozwiak. I will always be thankful for the guidance and support you have given me during my whole studies at Military University of Technology.

I would like to take this opportunity to say warm thanks to all my beloved friends, who have been so supportive along the way of doing my thesis – Michal, Monika, Artur and whole Toruszewscy family, Robert Rostkowski, Mateusz and Angela Laseccy, Arnold and Weronika Jedrale, Magda and Kamil Rzeszotarscy, I owe you so much.

I also would like to express my wholehearted thanks to my sister Marlena and my whole family for their generous support they provided me throughout my entire life and particularly through the process of pursuing my PhD degree. Because of your unconditional love, I have the chance to complete this thesis.

I would also like to thank my mother, Jolanta. You are always there for me. Thanks for being so encouraging and always allowing me to pursue my interests and passions.

I am truly grateful for the inspiration and happiness that Karolina has brought to me from the beginning and throughout my PhD studies. Without your support I would not have achieved all this. Thank you for many wonderful moments that I will remember for the rest of my life. ‘There is a corner of my heart that is yours. And I do not mean for now, or until we have found somebody else, I mean forever. I mean to say that whether we fall in love a thousand times over or once or never again, there will always be a small quiet place in my heart that belongs only to you.’ Thank you Karola for being in my life. This thesis is dedicated to you.

Mateusz Kopec

London, UK

July 2020

Abstract

Demand for low density and high strength materials in the aviation sector has expanded greatly due to ambitious carbon emission and fuel consumption targets. In order to meet these targets, manufacturers have focused on weight reduction via the use of lightweight materials. In the aerospace sector, high strength structural components are made from titanium alloys. However, the forming of complex-shaped components from titanium alloys is time, energy and cost intensive. One promising solution to overcome these difficulties proposed in the literature is using the hot stamping process to form complex-shaped components from sheet metal with cold dies, and rapidly quenching the workpiece in the dies simultaneously. The hot stamping process promises to reduce the tool wear commonly found in conventional hot forming processes and be an overall more efficient and economical process when compared to conventionally used isothermal hot forming techniques. A novel hot stamping process for titanium alloys using cold forming tools and a hot blank was studied systematically in this thesis. This work aims to investigate the microstructural evolution and flow behavior of a titanium alloy (Ti6Al4V) under hot stamping conditions experimentally, and to model these parameters using the constitutive equations proposed. The material behavior was modelled using mechanism-based viscoplastic constitutive equations to replicate the material response of a two-phase titanium alloy Ti6Al4V under hot stamping conditions. Finally, the developed model's accuracy was validated by comparing to experimental uniaxial tensile tests and microstructural maps of the deformed alloy. Microstructural analysis revealed that the heating and soaking conditions are vital to the microstructure and post-form strength, whereas the plastic deformation during the hot stamping only has a negligible effect on both recrystallization and phase transformation due to the very short deformation time. The developed material model was implemented into the Finite Element (FE) simulation to study the deformation characteristics during the hot stamping process. The verified simulation data were analysed through a novel hot stamping technique with good agreements achieved between the predicted and experimental results. A complex shaped wing stiffener panel component was successfully formed from TC4 titanium alloy, demonstrating the great potential of investigated technology in forming complex shaped titanium alloys components. Finally, Fast light Alloys Stamping Technology (FAST) is proposed for titanium alloys, where fast heating to a two-phase titanium alloy sheet with equiaxed microstructure is employed.

Nomenclature

α - titanium alpha phase

β - titanium beta phase

$\dot{\boldsymbol{\varepsilon}}_{\boldsymbol{p}}$ - plastic strain rate

$\dot{\boldsymbol{\varepsilon}}_{\boldsymbol{p\alpha}}$ - plastic strain rate for α phase

$\dot{\boldsymbol{\varepsilon}}_{\boldsymbol{p\beta}}$ - plastic strain rate

$f_{\boldsymbol{\beta}}$ - volume fraction of beta phase

σ - flow stress

H - stress due to dislocation hardening,

k - initial yield stress,

K - material parameter

$\boldsymbol{H}_{\boldsymbol{\alpha}}$ - stress due to dislocation hardening for α phase

$\boldsymbol{B}_{\boldsymbol{\alpha}}$ - α phase material constant

$\overline{\boldsymbol{\rho}}_{\boldsymbol{\alpha}}$ - normalized dislocation density for α phase

$\boldsymbol{H}_{\boldsymbol{\beta}}$ - stress due to dislocation hardening for β phase

$\boldsymbol{B}_{\boldsymbol{\beta}}$ - β phase material constant

$\overline{\boldsymbol{\rho}}_{\boldsymbol{\beta}}$ - normalized dislocation density β phase

$\boldsymbol{n}_{\boldsymbol{1}}$ - material constant for strain hardening for α phase

$\boldsymbol{n}_{\boldsymbol{2}}$ - material constant for strain hardening for β phase

$\boldsymbol{n}_{\boldsymbol{\alpha}}$ - material constant for α phase recovery

$\boldsymbol{n}_{\boldsymbol{\beta}}$ - material constant for β phase recovery

$\boldsymbol{C}_{\boldsymbol{\alpha}}$ - α phase material constant

C_{β} - β phase material constant

ε_t - the total strain

ε_p - the plastic strain

E - the Young's modulus

X - the material constant

m - the material constant;

T - the current temperature

Contents

List of Figures

Chapter 2 - Literature review on the sheet metal forming technologies of titanium alloys

Chapter 3 - Formability and microstructure evolution mechanisms of Ti6Al4V alloy during a novel hot stamping process

Chapter 4 - Experimental and modelling studies on Ti6Al4V under hot stamping conditions

Chapter 5 - Finite Element (FE) simulation of hot stamping of Ti6Al4V wing stiffener

Chapter 6 - Enhanced formability for titanium alloys by fast heating under FAST condition

Appendix A

Appendix B

List of Tables

Chapter 2 - Literature review on the sheet metal forming technologies of titanium alloys

Chapter 3 - Formability and microstructure evolution mechanisms of Ti6Al4V alloy during a novel hot stamping process

Chapter 4 - Experimental and modelling studies on Ti6Al4V under hot stamping conditions

Chapter 5 - Finite Element (FE) simulation of hot stamping of Ti6Al4V wing stiffener

Appendix B

List of Publications

Journal articles:

2018

Kopec M., Wang K, Politis D.J., Wang Y., Wang L., Lin J., Formability and microstructure evolution mechanisms of Ti6Al4V alloy during a novel hot stamping process, Materials Science and Engineering A – Structural Materials Properties, Microstructure and Processing, pp.1-20, 2018, ISSN: 0921-5093, DOI: 10.1016/j.msea.2018.02.038

2019

Kopec M., Wang K., Liu J., Politis D.J., Liu X., Qu H., Wang Y., Wang L., Kowalewski Z.L., Experimental and modelling studies on Ti6Al4V under hot stamping conditions - submitted

Levintant-Zayonts N, Starzynski G, Kucharski S, **Kopec M**, Characterization of NiTi SMA in its unusual behavior in wear tests, Tribology International, Vol.137, pp.313-323, 2019, ISSN: 0301-679X, DOI: 10.1016/j.triboint.2019.05.005

Li Z., Qu H., Chen F., Wang Y., Tan Z., **Kopec M**., Wang K., Zheng K., Deformation Behavior and Microstructural Evolution during Hot Stamping of TA15 Sheets: Experimentation and Modelling, Materials, Vol.12, No.2-223, pp.1-14, 2019, ISSN: 1996-1944, DOI: 10.3390/ma12020223

Jozwik P., **Kopec M**., Polkowski W., Bojar Z., Dynamic deformation tests of Ni_3Al based intermetallic alloy by using the split Hopkinson pressure bar technique, Journal of Mining and Metallurgy, Section B: Metallurgy, Vol.55, No.1, pp.129-134, 2019, ISSN: 1450-5339, DOI: 10.2298/JMMB181113014J

2020

Kopec M., S.Jóźwiak, Z.L.Kowalewski, A novel microstructural evolution model for growth of ultra-fine Al_2O_3 oxides from SiO_2 silica ceramic decomposition during self-propagated high temperature synthesis, Materials, ISSN: 1996-1944, 2020, DOI: 10.3390/ma13122821

Wang K., **Kopec M.**, Chang S., Qu B., Liu J., Politis D.J., Wang L., Liu G., Enhanced formability and forming efficiency for two-phase titanium alloys by Fast light Alloys Stamping Technology (FAST), Materials & Design, ISSN: 0264-1275, 2020, DOI: 10.1016/j.matdes.2020.108948

Ranachowski Z., Ranachowski P., Dębowski T., Brodecki A., **Kopec M.**, Roskosz M., Fryczowski K., Szymków M., Krawczyk E., Schabowicz K., Mechanical and non-destructive testing of plasterboards subjected to a hydration process, Materials, Vol.13, No.10, pp.2405-1-18, 2020, ISSN: 1996-1944, DOI: 10.3390/ma13102405

Liu X., **Kopec M.**, Fakir O., Qu H., Wang Y., Wang L., Li Z., Characterisation of the interfacial heat transfer coefficient in hot stamping of titanium alloys, International Communications in Heat and Mass Transfer, Vol.113, pp.104535-1-14, 2020, ISSN:0735-1933,
doi: 10.1016/j.icheatmasstransfer.2020.104535

Ranachowski Z., Ranachowski P., Brodecki A., **Kopec M.**, Kúdela Jr S., Quasi-static and dynamic testing of carbon fiber reinforced magnesium composites, Archives of Metallurgy and Materials, ISSN: 1733-3490, Vol.65, No.2, pp.893-899, 2020, DOI: 10.24425/amm.2020.132836

Conference papers:

2017

Grzywna P., Kukla D., Kowalewski Z.L., **Kopec M.**, Wyszkowski M., Zastosowanie elektronicznej interferometrii plamkowej do lokalizacji uszkodzeń zmęczeniowych (Application of Electronic Speckle Pattern Interferometry for fatigue failure location) , XXIII Seminarium NIENISZCZĄCE BADANIA MATERIAŁÓW (Seminar for non-destructive testing methods), 2017-03-15/03-17, Zakopane (Poland), pp.171-188, 2017

2018

Kopec M., Wang K., Wang Y., Wang L., Lin J., Feasibility study of a novel hot stamping process for Ti6Al4V alloy, MATEC Web of Conferences, Vol.190, pp.1-5, 2018, ISSN: 2261-236X, DOI: 10.1051/matecconf/201819008001

Wang K., **Kopec M**., Qu H., Wang Y., Wang L., Lin J., Li Z., A unified constitutive model for two-phase titanium alloys under hot stamping condition, ICNFT 2018, 5th International Conference on New Forming Technology, 2018-08-18/08-21, Bremen (DE), pp.1-1, 2018

Industrial project reports:

2017

Kopec M., Wang K., Wang L., Lin J., Hot stamping of titanium alloys, CALT – Imperial Advanced Aerospace Structure Manufacturing Technology Laboratory, Confidential.

2018

Kopec M., Wang K., Wang L., Lin J., Hot stamping of titanium alloys, Report No: AVIC-SDM-2018-03-09-KOPEC, Restricted to AVIC organisations

Kopec M., Wang K., Wang L., Lin J., Hot stamping of two-phase TC4 titanium alloy, Report No: AVIC-SDM-2018-08-15-KOPEC, Restricted to AVIC organisations

2019

Kopec M., Wang K., Wang L., Lin J., 2019, Experimental and modelling studies on Ti6Al4V deformation behavior and microstructure evolution under hot stamping conditions, Report No: AVIC-SDM-2019-03-08-KOPEC, Restricted to AVIC organisations

Kopec M., Liu, X., Wang L., Lin J., 2019, Characterisation and validation of the interfacial heat transfer coefficient in hot stamping of titanium alloys, Report No: AVIC-SDM-2019-09-08-KOPEC, Restricted to AVIC organisations

CHAPTER 1

1. Introduction

1.1 Background

Demand for low density and high strength materials in the aviation sector has expanded due to ambitious fuel consumption targets set for aircraft vehicles. In order to meet fuel consumption targets, weight reduction via the use of lightweight materials has been a key driver. In the aerospace sector, low strength structural components are commonly produced from aluminium alloys, and high strength structural components are made from titanium alloys and carbon fiber reinforced plastics (CFRP). Main advantages of CFRP include mass and part reduction, complex shape manufacture, improved fatigue life, design optimisation, and generally improved corrosion resistance. CFRP are mainly used for airframes and airplane tails constructions (Soutis 2005). On the other hand, titanium alloys are used in high operating temperatures and high stresses, for example gas turbines. The forming of complex-shaped components from titanium alloys is time, energy and cost intensive. The aircraft industry currently uses methods such as superplastic forming, superplastic forming with diffusion bonding, hot stretch forming, creep forming, hot gas-pressure forming or isothermal hot forming to produce complex-shaped components (Peters et al. 2003; Serra et al. 2009; Astarita et al. 2013; Deng et al. 2014; K. Wang et al. 2017; Raghu et al. 2011; Ermachenko et al. 2011). However, these techniques usually require a very high temperature, a very slow strain rate and simultaneous heating of tools and sheet during the process. These characteristics decrease productivity, and proportionally increase the cost of production.

Research into forming technologies with increased productivity has developed processes such as the Heat Form Quench (HFQ) (J. Liu et al. 2015), the Quick-plastic forming (Bariani et al. 2013), and the hot stamping using rapid heating (Hamedon et al 2013; Maeno et al. 2017). One promising solution to this problem proposed in the literature is the use of a hot stamping process to form complex-shaped components from sheet metal using cold dies, rapidly quenching the workpiece. The hot stamping process promises to reduce the tool wear commonly found in conventional hot forming processes and be an overall more efficient and economical process when compared to conventionally used techniques (Hamedon et al. 2013). Moreover, the mechanical properties and microstructure of the formed part can be tailored by the regulation of heating temperature, heating rate, soaking time and cooling rate.

1.2 Project driving force

Commercially pure titanium and titanium alloys are widely used in the aircraft industry as lightweight structural materials due to their good strength-to-weight ratio, high temperature performance, and corrosion resistance. However the critical issues in forming these alloys are poor formability and a

serious springback effect. As a result, the hot forming process becomes crucial to successfully form a complex-shaped part. At high temperatures, the formability of titanium alloys increases and the springback effect is reduced. However, most of the currently used hot forming techniques experience significant tool wear, a very slow strain rate and simultaneous heating of the forming tools and blank during the forming process. The relatively long forming time, high temperatures, and variation in part quality due to tool wear also impair the final mechanical properties of the formed part. In this study, the hot stamping of titanium alloys is proposed to mitigate these problems.

This work focuses on investigating the feasibility of a hot stamping process for Ti6Al4V titanium alloy using cold forming tools and a warm/hot blank. The mechanical properties and microstructure of the supplied material under different conditions are studied by uniaxial tensile tests, hardness test and scanning electron microscope to determine the possible forming windows for hot stamping. A part was formed to verify the feasibility of forming technology. Results show that this new technology has a great potential in forming titanium alloys sheet components and a qualified part (with no visible cracks observed) was formed successfully. The deformation condition had a great influence on both the mechanical property and microstructure of the material after deformation. The post-form mechanical properties and microstructure can be tailored by the adjustment of heating temperature, heating rate, soaking time and cooling rate.

1.3 Aims & Objectives

The primary aim of this PhD project is to develop a hot stamping process to form components from the Ti6Al4V titanium alloy in the warm/hot condition utilising cold forming tools in order to improve the forming efficiency and reduce tool wear found in commercial hot forming processes.

To achieve this aim, the following objectives must be met:

- Determination of mechanical properties of the Ti6Al4V alloy in varying conditions, under a range of forming parameters (temperature and strain rate). Description of flow behavior and formability of titanium alloys under high strain rate;
- Description of microstructure evolution during the hot stamping of titanium alloys;
- Development of mechanism-based constitutive equations for titanium alloys;
- Optimisation of forming process parameters via Finite Element modelling, creating a forming window of acceptable parameters
- Forming of prototype components utilising the new process and forming window (prediction and control of the defects during the forming of the typical component);
- Testing of prototype component properties (post-form strength)

1.4 Thesis structure

In this thesis, the introduction of pure titanium and its alloys, as well as a review of forming technologies for titanium alloys and their industrial applications are shown in Chapter 2. The material characterisation of the Ti6Al4V alloy, including tensile tests, microstructural investigations and forming tests are presented in Chapter 3. Detailed microstructure evolution and material modelling of the Ti6Al4V alloy under hot stamping conditions are presented in Chapter 4. The FE simulation for the forming of the Ti6Al4V wing stiffener component is shown in Chapter 5. Development of FAST technology for hot stamping of titanium alloys is presented in Chapter 6. The final conclusions of this research are summarised in Chapter 7.

CHAPTER 2

2. Literature review on the sheet metal forming technologies of titanium alloys

2.1 Titanium alloys – introductory remarks

Titanium and its alloys are known as materials for aerospace applications possessing their high strength to weight ratio and a great corrosion resistance. However, the usage of these alloys is limited due to huge costs of high temperature forming and fabrication of titanium itself, which is approximately four times greater that of stainless steel (Donachie 2001). Titanium is rarer than other metals, and it is typically found bonded to other elements only, which make it difficult to process. For that reason, the advantages of titanium applications must be balanced against their production cost (Boyer 1996).

Titanium has two allotropic varieties: low-temperature Ti_{α} with the hexagonal crystallographic compact structure and high-temperature Ti_{β} which crystallizing in a body-centered cubic (BCC) structure. A transformation of titanium occurs at a temperature of 882.5°C. This transformation depends on the purity of the titanium compound (Peters et al. 2003a; Sieniawski et al. 2013). The schematic process of the transformation is shown in **Figure 2-1.**

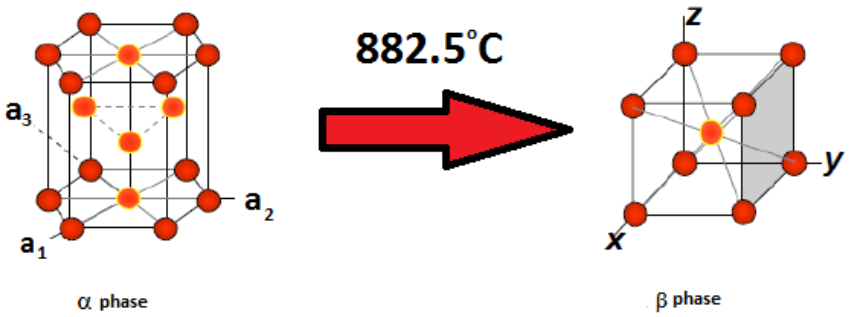

Figure 2-1. Schema of allotropic transformation Tiα into Tiβ

Titanium is one of the lightest metal because of its low density (4.51 g/cm^3), which is almost twice times lower than the density of steel, nickel or copper alloys. The density of titanium alloys depends on a type and amount of alloy additives (Beal et al. 2006). The addition of aluminium slightly reduces the density of the alloy. However, the addition of the high-density metals significantly increases this property. Titanium has a smaller thermal expansion coefficient than magnesium, aluminum, and iron. It also has a lower thermal conductivity than aluminum (approx. 15 times) or nickel-chromium steel (approx. 2.5 times). A disadvantage of pure titanium is its low mechanical strength, which significantly decreases at higher temperature. This phenomena can be eliminated by the addition of alloy additives. Some of the physical and mechanical properties are presented in **Table 2-1**.

Table 2-1. Selected physical and mechanical properties of titanium alloys (R. W. Cahn, 1995).

	Young's modulus [GPa]	Yield Strength [MPa]	Ultimate Tensile Strength [MPa]	Elongation [%]	Hardness [HV]
α alloys	100-120	170-830	240-870	15-25	120-300
Near α alloys	100-130	850-990	990-1050	6-16	340-350
α + β alloys	110-140	800-1200	900-1300	8-19	300-400
β alloys	80-120	800-1200	800-1400	6-20	250-500

Titanium is sensitive to the addition of alloying elements. This is a result of the high solubility of certain elements in one phase of titanium and titanium polymorphism. Alloy additives affect both, the microstructure and mechanical properties of titanium. However, these alloying elements are also stabilizers of phases which could decrease or increase the transition temperature in the α into β transformation (Froes 2015). The most common alloying elements using as stabilizers for α phase are oxygen, nitrogen, carbon, aluminum, gallium, lanthanum and cerium; for β phase – hydronium, niobium, vanadium, molybdenum, wolfram, tantalum (isomorphous addition) and chromium, iron, cobalt, nickel, manganese (eutectoid addition). Titanium strongly reacts with oxygen, which increases the α phase, but only by a limited value (0.10-0.12%). Impurities such as nitrogen, hydrogen or carbon have a negative effect on the properties of titanium alloys resulting in reduced ductility, creep resistance and cold brittleness. By proper selection of the alloying elements, the desired structure of the alloys with suitable mechanical properties is obtained. Changes in the structure of titanium can be obtained by heat treatment process. Technically, pure titanium and its alloys are characterized by a number of unique properties that distinguish them from conventional construction materials. First of all, they have a higher or equivalent mechanical strength compared to steel and corrosion resistant alloys based on iron and nickel. Moreover, titanium is characterized by a much higher relative strength (determined by the tensile strength to density (Rm / δ) ratio) than other construction materials. For example, the value for titanium alloys can be up to 33, where for the relative strength of the steel is 19-23. Only aluminum alloys are equal to titanium in this regard. However, the strength of aluminum decreases drastically at higher temperature. In the temperature range from 300°C to 600°C titanium alloys are 10 times stronger, and therefore, they are widely used in the aerospace industry (Peters et al. 2003a). In addition, these alloys demonstrate higher strength under long-term loads, compared to structural steel. Titanium and its alloys are characterized by high corrosion resistance in most environments oxidizing chlorides and salt water. The reason for this phenomenon is the formation of a stable oxide layer of TiO_2, which is strongly

linked with the alloy. Due to its corrosion resistance titanium compounds can work in the most agressive environments, where most of the conventional steels could not. On the other hand, titanium is not resistant to corrosion under reducing conditions, where the passive layer is broken (e.g. by hydrofluoric acid). It is crucial that titanium itself is a very strong oxidizing element at a temperatures above 500°C, when it can consume oxygen, nitrogen and hydrogen. Plastic deformation is a key factor to a large extent of titanium mechanical properties. At 80% deformation, the strength of technically pure titanium may increase three-fold, while titanium alloys will only increase two-fold. Other properties of titanium alloys are presented below (Peters et al. 2003a):

- high fatigue strength in air and chloride environments,
- high fracture toughness,
- low modulus of elasticity, which involves in reduced bending stresses,
- low coefficient of thermal expansion,
- non-magnetic - slightly paramagnetic,
- non-toxic,
- excellent cryogenic properties.

2.2 Mechanical and microstructural characterisation of titanium alloys

2.2.1 α and near α alloys

α-phase alloys include technically pure titanium and alloys containing elements stabilizing the α phase (Sn and Al) and other elements (O, C, N), which are dissolved in the α phase. They also contain limited content of β phase stabilizing elements (V, Mo, and Fe). The addition of Al and Sn increases the temperature of allotropic transformation α into β. These alloys have the structure of the solid solution α (**Figure 2-2**) (Destefani et al. 1990).

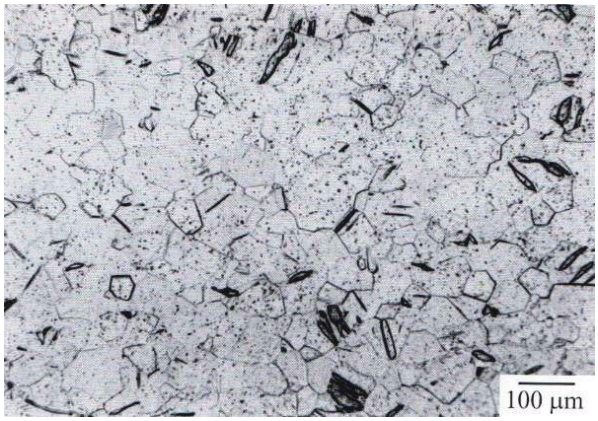

Figure 2-2. Pure titanium structure after annealing for 1 hour at a temperature of 675°C and slowly cooled in air (Arun 2006)

These alloys are not subjected to strengthen by heat treatment. In most cases, they are subjected to recrystallizing or normalized annealing in order to eliminate stresses caused by plastic deformation. Increase in strength is obtained mainly by the addition of elements (N, O, and C) which can simultaneously reduce toughness of material. With the increase of temperature, effects of material strengthening rapidly decreases. α phase titanium alloys have good casting characteristics, improved resistance to creep and are easily plastically deformed in spite of the alloys with β phase structure. They also have good weldability but do not exhibit satisfactory fatigue. Selection of this class of materials is generally based on the good corrosion resistance and ease of fabrication, not on the mechanical properties. Single α phase alloys have been used (Destefani et al. 1990):

- in the marine industry for machine parts for desalination of water and the hulls of ships,
- aircraft industry on the compressor aircraft engines,
- medical implants,
- chemical and petrochemical industries for high-pressure cryogenic and wherever required a high resistance to corrosion and a high capacity for plastic deformation (sheet metal parts).

Pseudo α alloys contain a small addition of β phase stabilizing elements (1-2%), which directly affects the strength and creep resistance. These alloys are the most commonly used titanium alloys for the production of engines in the aerospace industry because of the opportunity to work at elevated temperatures up to 550°C (Peters et al. 2003a).

The commercially pure grade could be produced with yield strength from 170 MPa to 480 MPa. The main advantages of these grades are good formability and excellent corrosion resistance. Strength of these titanium alloys is comparable to 300 series stainless steels with the 40% reduction in density achieved. Commercially pure grade titanium alloys possess good weldability and there are not heat treatable. Selected material properties were presented in **Table 2-2** and **Table 2-3** below:

Table 2-2. Selected mechanical properties of commercially pure titanium alloys (Beal et al. 2006)

Type of Ti alloy	Minimum ultimate tensile strenght [MPa]	Minimum 0.20% yield strenght [MPa]	Elongation [%]
Commerially pure titanium			
ASTM grade 2 / CP-3	345	280-450	20
ASTM grade 4 / CP-1	550	480-655	15
ASTM grade 3 / CP-2	450	380-550	18
ASTM grade 1 / CP-4	240	170-310	24

Table 2-3 Selected mechanical properties of α and near α titanium alloys (Beal et al. 2006)

Type of Ti alloy	Minimum ultimate tensile strenght [MPa]	Minimum 0.20% yield strenght [MPa]	Elongation [%]
Alpha titanium alloys			
5Al-2.5Sn / A-1	790	760	10
5Al-2.5Sn / A-2	690	657	6
8Al-1Mo-1V/ A-4	828	760	6
6Al-2Cb-1Ta-0.8Mo / A-3	711	657	10

2.2.2 β alloys

β phase alloys are characterized by a high content of β phase stabilizing elements, such as vanadium, molybdenum or niobium (above 20%). The subjection of these elements significantly reduce the temperature of phase transition (β → α), and therefore β phase alloys crystallize in the body-centered lattice system, not as α-phase in a hexagonal compact system. There are two types of β phase alloys: stable and metastable β alloys (pseudo-β). Pseudo β alloys are strengthened by heat treatment and have high tensile strength even at elevated temperatures. Stable alloys are not subjected to a heat treatment. The main features of the β-alloy are high degree of strengthening while maintaining a high yield and very good hardenability. Also, ease of shaping at temperatures lower than other titanium alloys. Some alloys may be subjected to cold working. They have a smaller thermal stability, lower corrosion resistance and creep resistance as compared with α phase alloys (Peters et al. 2003b). Through the addition of molybdenum, vanadium or iron β-alloy obtain a higher density than those with the α structure. These type of titanium alloys (include Ti10-2-3, Ti-15-3) are known from their higher strengths up to 1380MPa. They could be heat treated to obtain desirable strength/fracture toughness properties. β alloys possess good cold rolling capabilities. They also could be forged at lower temperatures which significantly reduce die cost. Selected mechanical properties of such alloys were listed in **Table 2-4** below.

Table 2-4. Selected mechanical properties of β titanium alloys (Beal et al. 2006)

Type of Ti alloy	Minimum ultimate tensile strenght [MPa]	Minimum 0.20% yield strenght [MPa]	Elongation [%]
Beta titanium alloys			
13V-11Cr-3Al / B-1	911	872	8
11.5Mo-6Zr-4.5Sn / B-2	690	623	10
3Al-8V-6Cr-4Mo-4Zr / B-3	828	796	6
8Mo-8V-2Fe-3Al / B-4	828	796	8

2.2.3 α/β alloys

These type of titanium alloys (include Ti6Al4V, Ti6Al6V2Sn and Ti6Al2Sn4Zr6Mo) are known from their good combination of mechanical properties. These type of titanium alloys could work in temperatures up to 400°C without losing its strenght. Also very good corrosion resistance made these alloys an excellent candidates for aerospace applications. Two phase titanium alloys could be strengthened through solution heat treatment below beta transus temperature and subsequent ageing process. They are also highly weldable.

Two-phase α + β alloys are obtained by adding α and β phase stabilizing elements. β phase stabilizing elements (eutectoid or isomorphic) extend the temperature range of the phase α + β → β transition. β phase fixed with eutectoid elements (Cr, Fe, Co, Ni, Mn) have better mechanical properties. Unfortunately, it also has poorer formability compared with the β phase alloys obtained as a result of adding isomorphic elements (Nb, V, Mo, Ta, and W). The solubility of the β stabilizers in α solid solution is very low, therefore, these elements cause little reinforcement of material. α phase stabilizer is mainly aluminum, which not only reinforces the α phase but also improves the heat stability of β phase. Two-phase α + β alloy structure consists of a mixture of a reinforced α solid solutions and β solid solution. The microstructure and mechanical properties depend largely on the performed processes and heat treatments. Therefore, the final equilibrium of microstructure can be categorized depending on the cooling rate. With low cooling from a temperature above the transition β → α, β phase is converted to equiaxed α phase type (**Figure 2-3a**). For fast cooling rate, β phase is transformed into α growing from grain boundaries, to the center of the grain (**Figure 2-3b**). The length and thickness of the plates depend on the cooling rate. In the case of rapid cooling (quenching) a martensitic β → α' transition occurred **(Figure 2-3c**) (Destefani 1990).

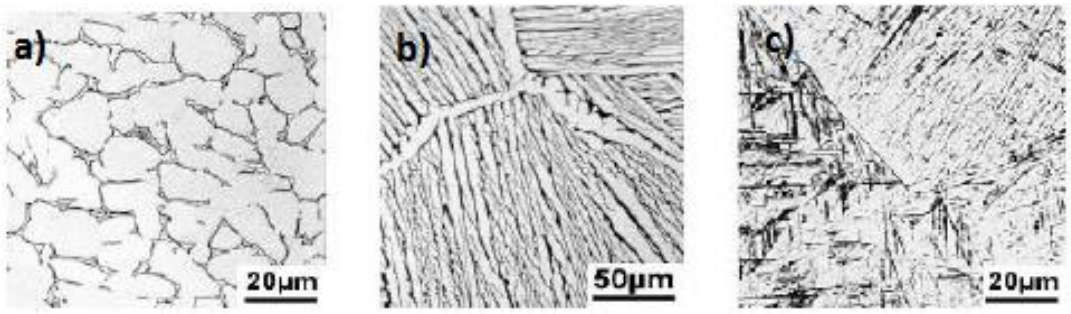

Figure 2-3. The structure of α + β alloys: equiaxed (a), the leaf (b) and martensitic (c) (Donachie 2000)

Effect of volume fraction and morphology of different phases have a great impact on mechanical properties of the biphasic alloys. The increase of β phase improves the strength of alloy, which reaches a maximum at a content of 50% of the two phases. Two-phase alloys have higher strength and ability to cold working as compared with those α single-phase alloys. Moreover, they also have good

mechanical properties at elevated temperature. These features have been applied in the aerospace industry for aircraft engine turbine blades and high-pressure cryogenic containers (Destefani et al. 1990). The most widely used α + β alloy is Ti6Al4V, where most applications include aerospace and aviation, like engine parts in airplanes and spacecraft (Peters et al. 2003a). The Ti6Al4V alloy has two-phase α + β structure with the phase stabilizers - aluminum (α) and vanadium (β). It consist of elements like aluminum (5.6-6.75%), vanadium (3.5-4.5%), carbon (<0.1%), iron (<0.3%), oxygen (<0.2%), nitrogen (<0.05%), hydrogen (<0.01%). Aluminum has a great solubility in solid α solution and strengthens it. In result, strength increase and reduction of the alloy density occurs. The Ti6Al4V alloy is one of the most intensively developed and widely used titanium alloys (more than 50% of all titanium applications). It is a result of a good balance between strength, ductility and fatigue resistance. Moreover, it has good corrosion resistance. It is recommended for use at temperatures up to 350°C (Peters et al. 2003a). Some of the mechanical properties are presented in the table below (**Table 2-5**).

Table 2-5. Selected physical and mechanical properties of the alpha-beta titanium alloys (Peters et al. 2003a)

Type of Ti alloy	Minimum ultimate tensile strenght [MPa]	Minimum 0.20% yield strenght [MPa]	Elongation [%]
Alpha-beta titanium alloys			
8Mn / AB-6	863	761	10
6Al-4V / AB-1	897	830	8
6Al-4V / AB-2	863	934	6
6Al-4V-2Sn / AB-3	1001	934	8
6Al-2Sn-4Zr-2Mo / AB-4	897	830	8
6Al-4V-SPL / AB-5	621	519	15

The Ti6Al4V titanium alloy possesses an attractive combination of material properties for the manufacture of aircraft components. As a result of its properties of yield strength, ductility, fracture toughness, high temperature strength, creep characteristics, weldability and workability, the Ti6Al4V alloy quickly found an application in many fields, such as aircraft, marine, medical, electronic and chemical industries, making it the most widely used titanium alloy. It has found many applications in aircraft airframes and engine parts (for example fan blades, fan case) (Inagaki et al. 2014; Williams et al. 2003; Peters et al. 2003a), and for this reason, the Ti6Al4V alloy is the focus of this research.

Generally, the microstructure of titanium alloy is described by the arrangement and amount of α and β phases using the phase diagram (**Figure 2-4**). At room temperature the Ti6Al4V alloy consists mainly of the hexagonal close-packed (HCP) α phase and the body centred cubic (BCC) β phase.

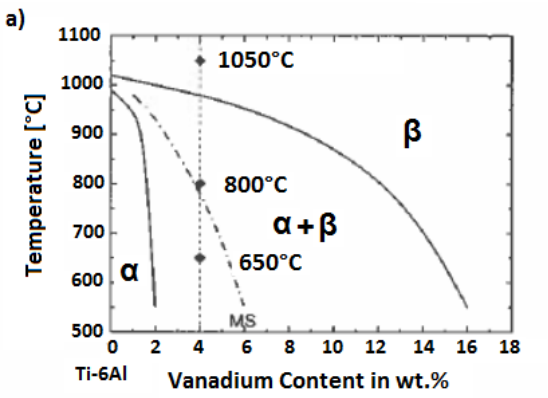

Figure 2-4. Vertical section of phase diagram for Ti alloys of type Ti-6Al-xV (Donachie 2000)

Application of different heat treatments during the forming process results in various ranges of microstructures and mechanical properties. By changing the cooling rate and the thermal processing history, many states of microstructure are observed (**Figure 2-5**) for example, plate-like α + β (**Figure 2-5a**), equiaxed α and intergranular β (**Figure 2-5b**, c), α' + β (**Figure 2-5d**), primary α and α' + β (**Figure 2-5e**) and primary α and metastable β (**Figure 2-5f**). Using a slow cooling rate above the β transition temperature, the β phase transforms into the globular type of α phase (**Figure 2-5**). In the case of rapid cooling (quenching), the β phase transforms into the martensitic α´ phase. Regarding the Ti6Al4V alloy, the amount of the martensitic HCP α' or the orthorhombic α'' phase depends on the composition of the β phase before the quenching process. Because the HCP α´ phase is enriched in the β stabilizing element, the ageing treatment in the range between the martensitic start temperature (Ms) and the β transition caused a decomposition of the HCP α´martensitic phase into α and β equilibrium phase (**Figure 2-6**). Ageing at a temperature of 700°C for about 30 minutes caused a full decomposition of the α´ phase into the equilibrium α and β phases.

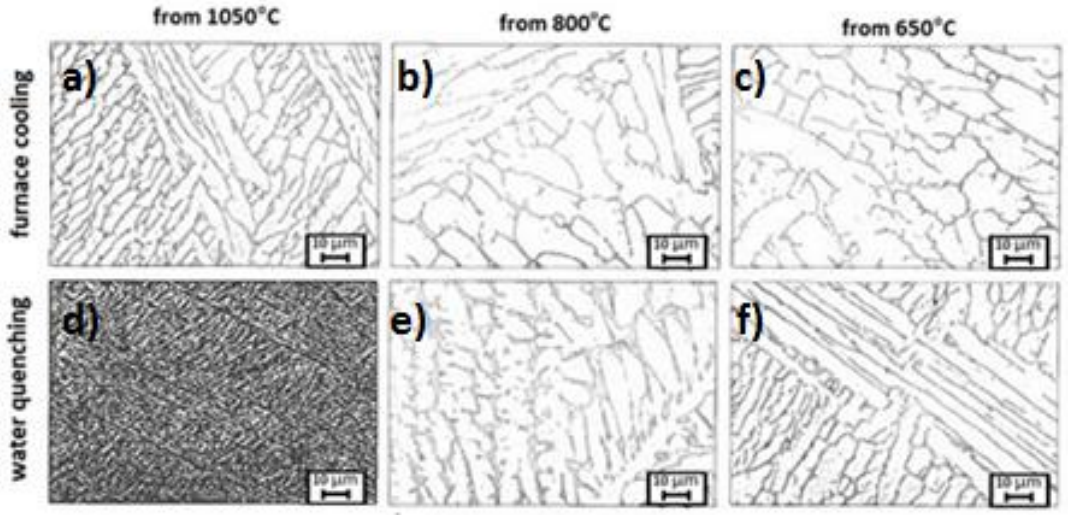

Figure 2-5. Ti6Al4V microstructures after furnace slow cooling (50°C/h) and water quenching (Donachie 2001)

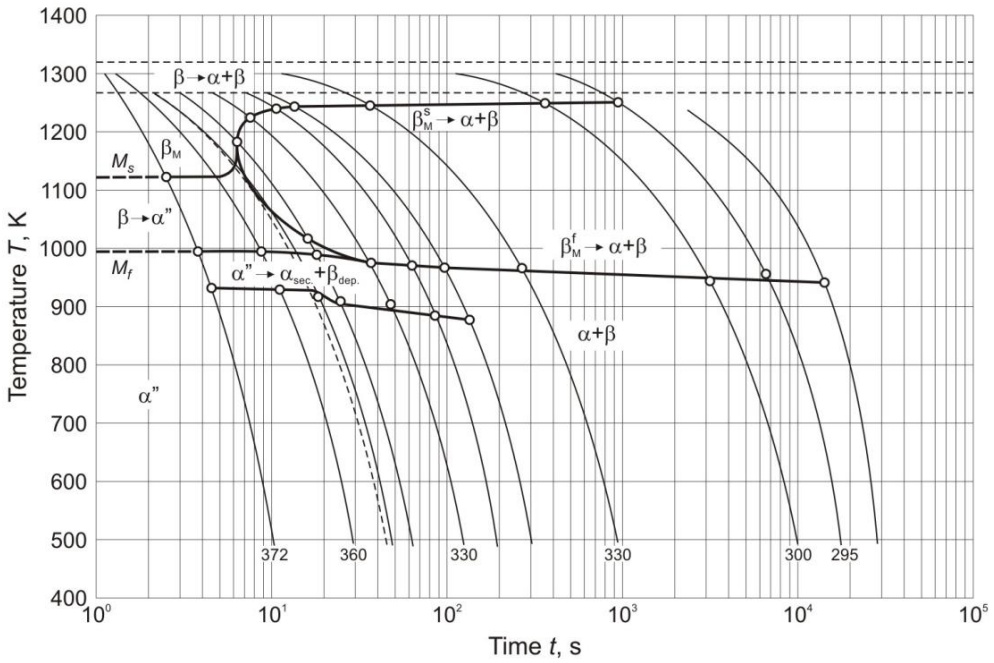

Figure 2-6. CCT diagram for Ti-6Al-4V alloy (Sieniawski et al., 2000.).

2.3 Applications of titanium alloys

Titanium alloys are widely known as "space" materials and they are used in aerospace and aviation, from the beginning of the 50s. Over the past 10 years, titanium materials were use in chemical engineering, medicine for bone implants, the marine industry, automotive and energy sector and many others (Peters et al. 2003a). In the aerospace titanium is used thank such characteristics as high relative strength, corrosion resistance, creep resistance, load carrying capabilities at elevated and cryogenic temperature, a capacity to create alloys, composites, and intermetallic phases. Commonly used applications of titanium alloys are pressure vessels in spacecraft, gas turbine components, connectors, brackets, springs, undercarriage components, fuselage, wings and other components of airplanes and helicopters. Aerospace, military and civil aviation industry demand continuous work on obtaining better and better properties of titanium alloys, titanium materials with an intermetallic matrix, powder materials or composites. For this purpose, are increasingly being used unconventional manufacturing technologies which also leads to a reduction in production costs. These technologies include the formation of objects in superplastic conditions so called hydrogen and incremental laser technologies (Peters et al. 2003a). The use of titanium has solved a technically complicated problem of heat exchangers manufactured in the chemical industry. It is also used for the production of steam condensers for turbines in nuclear power plants. Titanium effectively supplanted the graphite as the material for the tube heat exchanger for cooling the chlorine solution. Other applications in the chemical industry are chemical reactors, filters, dryers, pumps, pipelines, separators and more (Beal et al. 2006). In the automotive industry, use of titanium reduces the weight of vehicles, which directly affect the decrease

in fuel consumption and reduction of carbon emissions. For example, a reduction in weight of 1.1% reduces fuel consumption by 0.7%. Special titanium alloys have a high strength to density ratio in temperatures to 600°C which is so much better in comparison to aluminum and steel. Initially, titanium alloys have been introduced to racing cars on elements such as connecting rods, valves, axles (front and rear), suspension components, bearings and others. Today, many car companies such as Volkswagen, General Motors, Mitsubishi Motors, Honda Motors and Toyota expands a range of components manufactured from titanium alloys (Beal et al. 2006). In the marine industry, titanium was applied because of good surface corrosion resistance in the sea water, resistance to pitting and biological corrosion. The disadvantage of titanium materials is that at elevated temperatures, they lose the anticorrosion properties for example Ti_2Ni alloy, used for pipes to pump sea water in nuclear power plants. Other applications in the marine industry are elements of submarines, ships surfaces and hulls deep-sea cameras. Quite new application of titanium alloys is to use them for parts of oil rigs and mining, pipes and pipelines operating in the marine environment under high load (Destefani 1990; Peters et al. 2003a). There has been a high increase in the use of titanium in the manufacture of common use objects, such as bicycle frames, eyeglass frames, bodies' watches and cameras, fishing equipment, golf club heads, climbing equipment, etc. The use of titanium in the manufacture of consumer products will grow through nontoxic nature of this material (Peters et al. 2003a). Applications of titanium alloys are presented in **Table 2-6** below (Singh et al. 2017; Boyer 1996):

Table 2-6. Industrial applications of titanium alloys

Type of Ti	Advantages	Grade	Applications
α alloys	Formability, corrosion resistance, operating at high temperatures, 40% weight savings	Commercially pure Ti	floor support structure in the galley and lavatory areas, tubes or pipes in the lavatory system, clips and brackets, and ducting for the anti-icing and environmental control systems (ECS).
	40% weight savings	Ti-3AI-2.SV	hydraulic tubing, honeycomb core structures,
	good fracture toughness and ductility down to cryogenic temperatures	Ti-5-2.5,	Cryogenic applications, high pressure fuel turbo-pump of the space shuttle.
	low density and high modulus	Ti-8-1-1	blades in turbine engines; fan blades for military engines, tear straps on commercial airframes
	good properties retention and creep resistance at elevated temperatures	Ti-6-2-4-2S,	gas turbine engine industry, rotating components such blades, discs and rotors at temperatures up to about 540 °C. high pressure compressor

α/β alloys	good balance of characteristics: strength, ductility, fracture toughness, high temperature strength, creep characteristics, weldability, workability, and thermal processability	Ti-6-4	airframe and engine parts, static and rotating components in gas turbine engines, fuselage, fan blades, fan case, nacelles, landing gear, wing, and empennage.
	higher weight savings, though the fracture toughness and stress corrosion resistance are reduced.	Ti-6-6-2	landing gear support structures
	oxidation resistance and creep property	Ti-6Al-2Sn-4Zr-2Mo	compressor discs
	Thermal stability	Ti-5AI-2Sn-2Zr-4Mo-4Cr.	fan and compressor discs
	Thermal stability	Ti-17/ Ti-6-2-4-6	high pressure compressor
β alloys	Thermal stability, operating temperatures, about 250-315°C	Ti- 13V- 11Cr-3A1 (Ti- 13-11-3)	It was used for wing and body skins, frames, longerons, bulkheads, ribs, rivets and essentially the complete main and nose landing gears. Nowadays - coil springs, down-lock landing gear springs, feel and centering , springs for the yoke, pedal return springs for the brakes, hydraulic return springs, and flight control springs are common aircraft applications of titanium springs
	strip producibility, cold formability, and the ability to heat treat to high strengths	Ti-15-3.	fire extinguisher bottles, springs, clips and brackets in the floor support structures
	excellent fatigue properties	Ti-10-2-3	landing gear, flap tracks. rotor systems

2.4 Manufacturing techniques of titanium alloys

In general, hot forming is expensive technology and requires special tools and procedures. Nevertheless, hot forming has many attributes compared to cold forming of metal alloys (**Table 2-7**). Highest quality of derived elements is achieved by using the appropriate steps at every stage of processing. Starting from a proper clean work surface, the selection of the annealing temperature, the use of lubricants, appropriate tools and methods for processing. To prevent damage during processing, each element undergo for hot forming method must be clean and free from surface defects. To avoid reducing the strength of materials after heat treatment it is recommended to remove the oxidized surface. All kinds of lubricants and oils should be also removed before due to thermal susceptibility to corrosion. Also heavily oxidized surfaces shall be applied to alkaline and acid baths. Surface specimens before testing should be cleaned sandpaper. Only properly cleaned material can be used for studies of mechanical properties, containing tensile and yield strength (Froes 2015).

Table 2-7. Advantages and disadvantages of hot forming and cold forming/hot sizing (Froes 2015)

Hot forming	Cold forming/hot sizing
Advantages	
Fewer operations	Forming can be done on all available types of forming machines
Lower forming pressures	Reduced dwell time in cold forming press
Material is at elevated temperature for shorter time than hot sizing	Parts are stress relieved on hot sizing
Parts can be made in most alloys that could not be produced by cold forming	Can use lower-cost tooling materials in cold forming
Disadvantages	
Requires heat-resistant tool materials	Requires additional equipment (hot sizing presses)
Tools must be adapted for heating	Long dwell times in hot sizing press (30 min)
Requires use of slow press with some dwell time (5 min or more)	Requires two sets of dies (one set heat resistant)
Limited to forming operations on equipment that can use heated tools	Some parts cannot be made by cold forming procedures

Depending on the type of titanium alloy, suitable processing temperature must be applied. Most used are three ranges of temperatures - 200°C to 315°C, 480°C to 540°C and 650°C to 815°C for the most difficult-to-form alloys. The behavior of the material under load determines the selection of the appropriate temperature. Typical processing temperature for titanium alloys are presented in **Table 2-8**. There are many methods for heating blanks and tools for forming. Due to degradation of mechanical properties and subsequent destruction, overheating of the treated material or tools material should be avoided. Both the temperature and heating time should be minimized. Below are listed some heating methods:

- furnace heating - electric furnaces with air atmosphere are the most useful for heating titanium blanks. Flame-Gas furnaces are acceptable but only if the flame does not touch the surface and the atmosphere is slightly oxidizing. Especially important is to preserve the purity of the atmosphere. Every change of the hydrogen content results in catastrophic degradation of material properties;
- resistance heating - this type of heating is commonly used because of titanium high electrical conductivity. Problems caused by the change of current density may happen in this case. Also, higher temperatures occur in areas where the cross-section is smaller. Nevertheless, it is an effective method for many types of hot forming. Process can be done properly even with the loss of heat or handling time;

- hot die heating - blank and heated die are in contact till forming part does not reach the desired temperature. Once it is reached, it is followed by compressing and giving the desired shape. Heated forming die are often used, especially at high temperatures (Peters et al. 2003a).

Table 2-8. Temperatures for forming processes (Froes 2015)

Alloy	Forming temperature ['C]		Forming method								
	mild forming	severe forming	drop hammer	Hydropress[1]	brake	spin	draw	matched die	Hydroform[1]	finish die	creep form
Unalloyed titanium	205-316	…	x	x	x	x	x	x	x	…	…
	…	482-538	x	…	…	…	x	…	…	x	x
	…	538-705	…	…	…	x	…	…	…	…	…
Ti6Al4V	205-316	…	…	x	…	…	…	…	…	…	…
	…	482-538	…	…	…	…	…	x	x	x	…
	…	538-649	…	…	x	…	…	…	…	…	x
	…	538-788	x	…	…	x	x	x	…	…	…
Ti5Al2.5Sn	205-316	…	…	x	…	…	…	…	…	…	…
	…	482-538	…	…	…	…	…	x	x	…	…
	…	538-760	x	…	x	x	x	…	…	…	x
Ti8AlMoV	…	to 732	x	x	x	…	…	…	…	…	…
	343	649-760	x	…	…	…	…	…	…	…	…
	…	788	…	…	…	…	x	x	…	…	x

[1]In hydropress process, the flat sheet and the protective rubber pad placed on it are deformed to die shape under pressure applied by the hydraulic fluid bag. In hydroform, a high pressure hydraulic fluid is used to press working material into a die.

To reduce energy expenditure, heat transfer and friction between blank and tool surfaces some lubricants are applied. Most used are combinations of solid additives with oils (**Table 2-9**). Using of appropriate tool material is also a crucial factor. Typical tool materials are listed in the **Table 2-10**.

Table 2-9. Lubricants for forming processes (Froes 2015)

Forming operation	Forming temperature	Lubricants used
Stretch forming skins	Cold	Grease-oil combinations, Wax-type lubricant
	Hot	Colloidal graphite
Stretch forming sections	Cold	Wax-type lubricant plus flake graphite (10:1 by volume)

Stretch forming extrusions	Hot	Molybdenum disulphide, Colloidal graphite
Brake forming	Cold	Colloidal graphite
Contour rolling sections	Cold	Colloidal graphite
Roll forming	Cold	Heavy oil (SAE 60)
	Hot	Colloidal graphite
Hot sizing	Hot	Colloidal graphite
Draw forming	Hot	Colloidal graphite plus alcohol, xylene
Hammer forming	Hot	Colloidal graphite
Hydropress forming	Hot	Colloidal graphite

Table 2-10. Tooling materials for forming processes (Froes 2015)

Forming operation	Forming temperature	Tool material
Stretch forming skins	Cold	Cast aluminium with epoxy face
	Hot	Cast ceramic
Stretch forming sections	Cold	Kirksite form block; Ampco Bronze No. 21 wiper die
	Hot	H11, H15 tool steels; high-silicon cast iron
Stretch forming extrusions	Cold	Mild steel; AISI 4130 steel
	Hot	AISI 4130 steel; type 310 stainless steel
Brake forming	Cold	AISI 4340 steel (36–40 HRC)
	Hot	H11, H13 tool steels; Incoloy 802
Contour rolling sections	Cold	O2 tool steel
Hot sizing	Hot	Mild steel; high-silicon cast iron; high-silicon nodular cast iron; H13 tool steel; type 310 stainless steel; RA 330 stainless steel; Inconel X; Hastelloy X; Incoloy 802
Draw forming	Hot	High silicon cast iron; Incoloy 802
Hammer forming	Hot	Kirksite dies with stainless steel caps; lead punches with stainless steel caps; high silicon cast iron; RA 330 stainless steel; Inconel X; Incoloy 802
Hydropress forming	Cold or hot	High silicon cast iron; Incoloy 802

Among the hot forming techniques for titanium alloys, the most common are listed below:

- **Break forming** - which is similar to break forming of stainless steel with the exception of titanium alloys are characterized by higher springback effect. Typical die for brake forming titanium is presented in **Figure 2-7**. The channel punch and die are made from various types of steels. Materials used for

these tools are based on zinc alloys and other inexpensive steels. Blank and tool can also be heated for hot forming break.

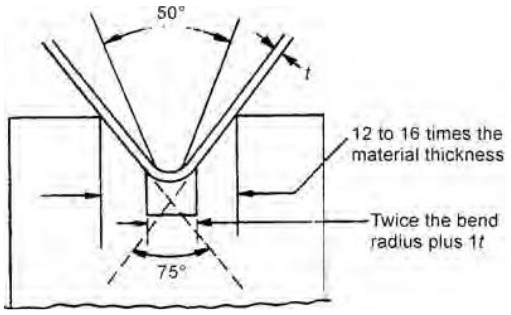

Figure 2-7. Schema of typical die for brake forming (Froes 2015)

- **Stretch forming -** this technology allows the production of single-curved contours and more complex contours in a sheet. During process, metal streches around the die. Blank is holding by grips as it is pulled into desire shape. Typical setup is presented in **Figure 2-8**. This type of processing is typically carried out in the cold to die eliminate expensive materials and to Obtain the best properties in the formed part,

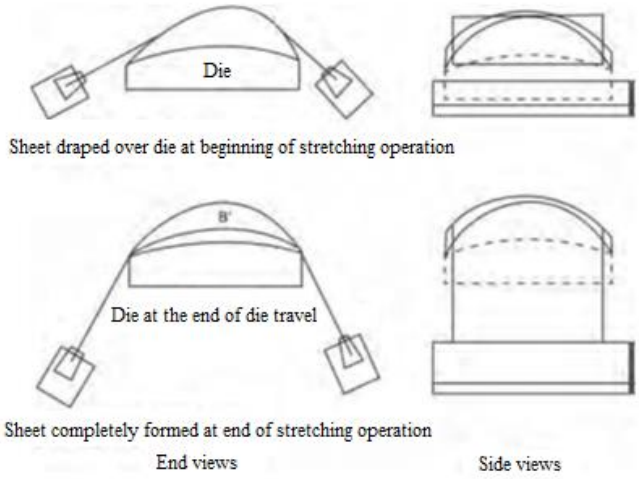

Figure 2-8. Stretch forming sheet (Froes 2015)

- **deep drawing** – in this technology punch pulls a metal blank through the die surrounding metal punch and then reduce the diameter, length of the part or thickness of the wall (redraw). Some types of deep drawing like single action without hold down **(Figure 2-9a**), double-action with recessed hold down (**Figure 2-9b**), single-action inverted with die-cushion hold-down reverse redraw (**Figure 2-9c**), double-action with flat hold down push-through (**Figure 2-9d**), double-action redraw push-through (**Figure 2-9**), and single-action redraw with die cushion hold-down (**Figure 2-9**) are presented below. Typically, the titanium blank is located between the draw ring and pressure pad. In order to prevent the buckling during this process, a proper pressure must be applied. Deep drawing could be used at elevated temperatures by heating the blank or the dies, or both of them. Unfortunately drawing speed is rather slow (254 mm / min) and forming forces on the part held for five or more minutes after forming,

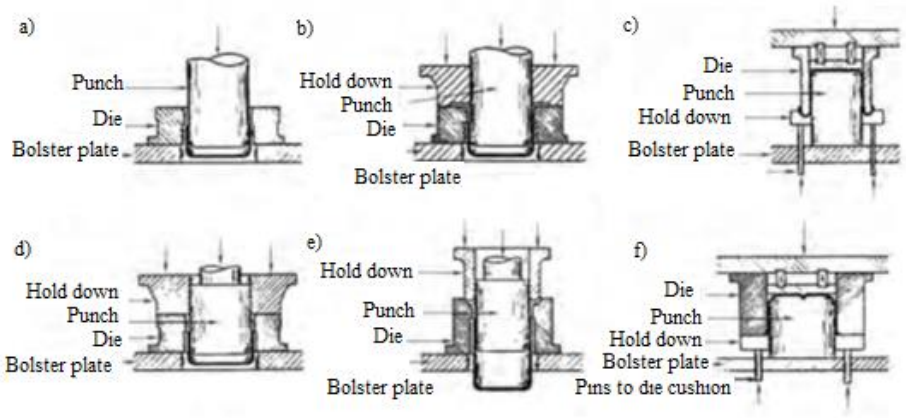

Figure 2-9. Various deep-drawing operations (Froes 2015)

- drop-hammer forming - method which consists of using gravity or pneumatic drop-hammer to presses titanium by progressive deformation with repeated blows in matched dies. Typical part produced by means of drop-hammer method is presented in **Figure 2-10**. Forming energy depends on the mass of the ram, tool and its striking velocity. Hammer is typically made of lead or other soft material that will cause deformation of the female die contour. Dies are usually made from steel, stainless steel and Inconel. Execution of complex shapes requires the use of high temperatures (Froes 2015; Peters et al. 2003a).

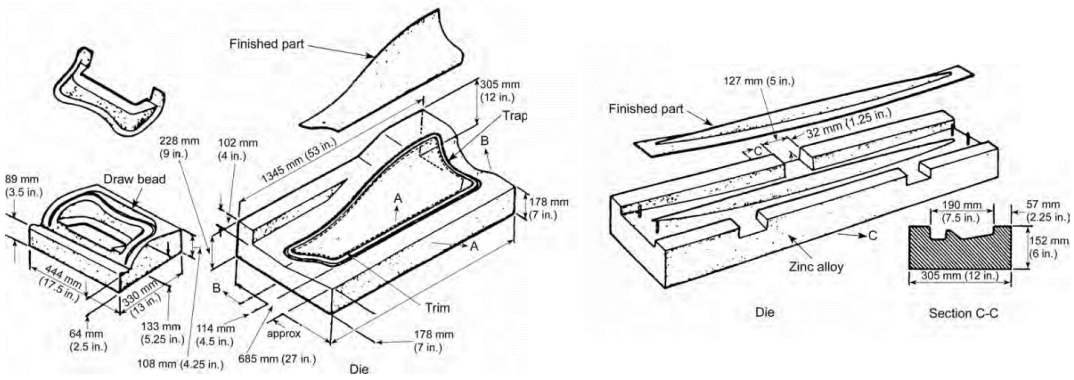

Figure 2-10. Drop-hammer and formed parts (Froes 2015)

With increasing demand for high strength lightweight parts in the aircraft industry, a number of techniques for forming titanium alloys have been developed and commercially used. Since the formability of titanium alloy sheets at room temperature is low, the sheets are commonly formed at elevated temperatures. Processes such as hot stretch forming, creep forming, hot gas-pressure forming have become promising methods to overcome the springback effect (Destefani 1990), however these processes have long processing times and thus high per-unit costs. Recent research into new manufacturing processes for the hot forming of titanium has led to the development of processes, with superplastic forming gaining the most traction in the aircraft industry. Titanium super-plastic formed parts are used in military and commercial engines for fan blades, casings, ducts and exhaust nozzles (Serra 2009). Superplasticity is the ability of materials to reach the elongation over 200% at an elevated

temperature (higher than 0.5 value of the melting point) prior to failure without necking (H. Yang et al. 2011). Superplastic forming is commonly used in aircraft part fabrication. At approx. 900°C a solid titanium is deformed beyond its usual breaking point. Superplastic materials deform by getting thinner. There is no behavior like necking leading to fracture. Superplastic forming process required the optimal size of alpha grain <10um and well-dispersed beta phase at the grain boundaries. Generally, as a superplastic mechanism is based on the diffusion and sliding of grains past each other. Obtained parts are completely springback and stress-free. During one cycle, several parts of varying shape can be obtained. It significantly reduces the cost of the process. Thank to this technique large amount of part may be produced during one machine cycle so cost savings and time reduction are significant. Another advantages of the SPF include very complex geometry of produced parts; lighter and more efficient structures; applied force is supplied by a gas so there is equal pressure in the whole sheet of work-piece. During the SPF process, the gas pressure is controlled by a computer programme to keep a constant strain rate of deformed sheet. The most common used titanium alloy for such kind of process is the Ti6Al4V. This alloy should have microstructure of fine and equiaxed grains (usually less than 10 μm) and high elongation at the elevated temperatures (Beal et al. 2006). At the beginning of the SPF the forming part is placed on top of cavity die (**Figure 2-11a**). As soon as the tool and blank reach the forming temperature in the superplastic range, proper gas pressure is applied to hold a constant strain rate during the process. When the part is at its final stage of deformation, the gas pressure increase to preserve the strain rate and the thickness of the sheet decreases. The final part has a geometry based on the die shape (**Figure 2-11b**).

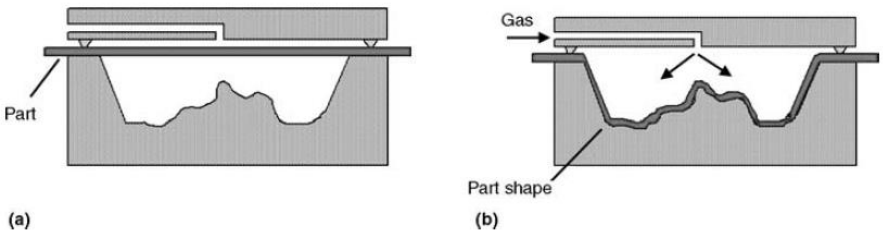

Figure 2-11. Superplastic forming of titanium alloys at the beginning of the forming cycle (a) and after forming (b) (Beal et al. 2006)

The main disadvantages of the SPF process include requirement of heat-resistant tool materials; a specialized forming machines which provide high temperature and high pressure during process; relatively long preheat time to obtain the forming temperature; a protective atmosphere. However, even above mentioned limitations SPF process is still very attractive method to produce complex shaped parts. Some of most interesting investigations were reported in literature. Comparison tests between sub-micron grained (0.3 μm grain size) Ti6Al4V sheets of 0.8 and 1.8 mm thickness and commercially available superplastic Ti6Al4V sheets of 0.8 mm thickness (5 μm grain size) and 1.36 mm thickness (3 μm grain size) were carried out. Tensile tests were performed using three types of specimens (according

to the rolling direction by 0, 45 and 90°) by means of screw driven tensile testing machine equipped with split type resistance furnace. Tests were conducted at various temperatures and different strain rate range in an inert atmosphere. Because sub-microcrystalline type of titanium has an average size of grain less than 1µm, it shows it superplastic behavior at lower temperatures (600-700°C) than commercially available one (850-950°C) (Beal et al. 2006).

The superplastic forming process has a relatively slow forming rate, as compared to the other hot forming methods. Time of one cycle vary from 30 min to 2h. That is why a new attempts to reducing a forming time are investigating. In paper (Liu et al. 2013) a new superplastic-like forming method is presented. The Ti6Al4V alloy sheets were successfully formed at 800°C in 16 min. Titanium alloy sheets of 1.6mm thickness were tested under forming conditions by means of presented machine (**Figure 2-12**).

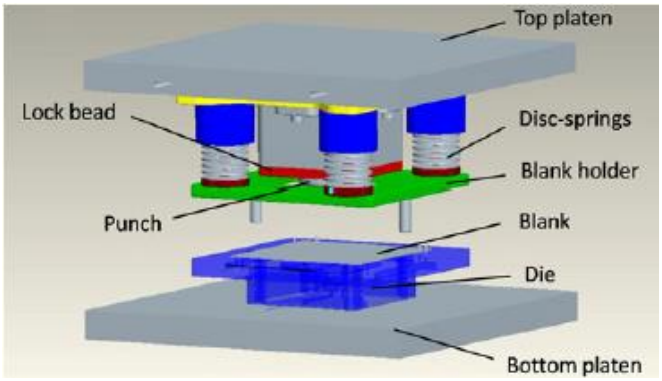

Figure 2-12. Schema of superplastic-like forming machine (Liu et al. 2013)

Several parts under various operating temperature (750, 800 and 825°C) were formed (**Figure 2-13**). As it shown the surface is shining with some little oxidations areas at 750°C. The one obtained at 800°C is darker than previous and also a little oxidation formed on the surface. At the highest temperature of 825°C, more oxide film were observed.

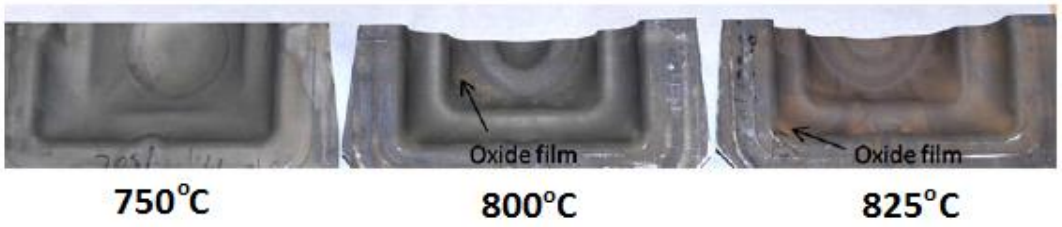

Figure 2-13. Surface finish after superplastic-like forming process at different temperatures (Liu et al. 2013)

As it is well known, the oxidation effect occurred on the Ti6Al4V alloy surface above temperature of 650°C. At temperature of 800°C in air atmosphere the weight of gain is about 1.2mg/mm^2. The thickness of the oxide film is around 5µm in this case. When temperature increase to 900°C, the weight of gain is about 2mg/mm^2 and the thickness of the oxide film was 25µm (Guleryuz and Cimenoglu 2009). As

the superplastic-like process consist of the hot drawing and the blow forming processes (**Figure 2-14**), the thickness measurements after each process were conducted.

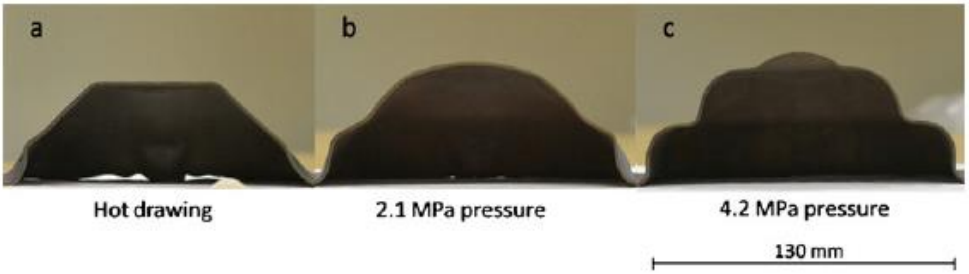

Figure 2-14. Bulge height profiles after hot drawing (a), and blow forming (c,d) (Liu et al. 2013)

Because the sheet was formed without any visible fracture on the surface, the thickness were measured from the dome centre to the edge along the cross section. Each measurement was named by its location (numbers 1 to 11) (**Figure 2-15a**). The thickness profiles are presented in the graph (**Figure 2-15b**). The maximum reduction is located at location 4, where thinning was about 54%. The reason of such kind of behavior was influenced by the forming process. When the sheet came into contact with the punch during hot drawing, material adjacent to this area was locked against the die surface by friction and gas pressure.

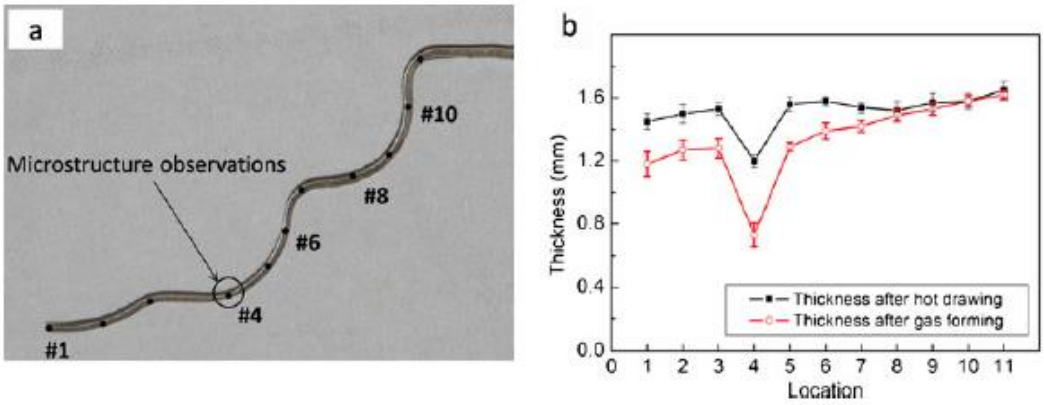

Figure 2-15. Cross section of obtained Ti-6Al-4V part at 800°C (a); Distribution of thickness after two forming operations (Liu et al. 2013)

Undeniable advantages of superplastic forming including very complex geometry of produced parts and lighter and more efficient structures. Moreover, depending on the initial sheet size, more than one piece may be successfully produced during one forming cycle. Force applied during superplastic forming is supplied by a gas so there is equal pressure in the whole sheet of work-piece and thus minimal thinning of the sheet material occurs during forming. However, this process requires heat-resistant tool materials and specialized forming machines which provide high temperature, high pressure and a protective atmosphere. Despite the use of a protective atmosphere during forming, an oxide layer can still form on the material surface as a result of the long timescale of the process. Moreover, the superplastic forming process has a relatively slow forming rate, as compared to other hot forming methods such as hot stretch forming or isothermal hot forming (Froes 2015) .

2.5 Hot stamping technology

Hot stamping is a hybrid process which combines a sheet metal forming and a heat treatment process in order to obtain comparable mechanical properties between the formed metal part and initial blank (Chen et al. 2014). The main advantages of this process include a desirable material microstructure, reduction of the springback effect, and a good formability at elevated temperatures. Due to these benefits, very thin and complex shaped sheet metal parts with a high strength-to-mass ratio and a high geometrical accuracy can be produced (Karbasian et al. 2010). Applications of titanium hot stamped components for the aircraft industry (Maeno et al. 2017) mainly focus on curved extruded profiles, load carrying structures, fan frame structures and airframes.

By controlling the process parameters and changing the thermo-mechanical sequence of operations during the forming process, production of components with different mechanical properties is possible (Karbasian et al. 2010). The standard temperature versus time diagram of the hot stamping cycle for steel components is presented in **Figure 2-16.** The blank of the material, with a ferritic-pearlitic microstructure and relatively low mechanical properties at room temperature, is heated in a furnace above the austenitization temperature. The blank is soaked until a homogeneous austenitic microstructure is formed throughout the material. Afterwards the blank is rapidly transferred into the forming press, where it is formed and quenched at a controlled cooling rate. At the end of the process, the formed component has a fully martensitic microstructure, with a strength of over 1500 MPa and a good ductility (Karbasian et al. 2010).

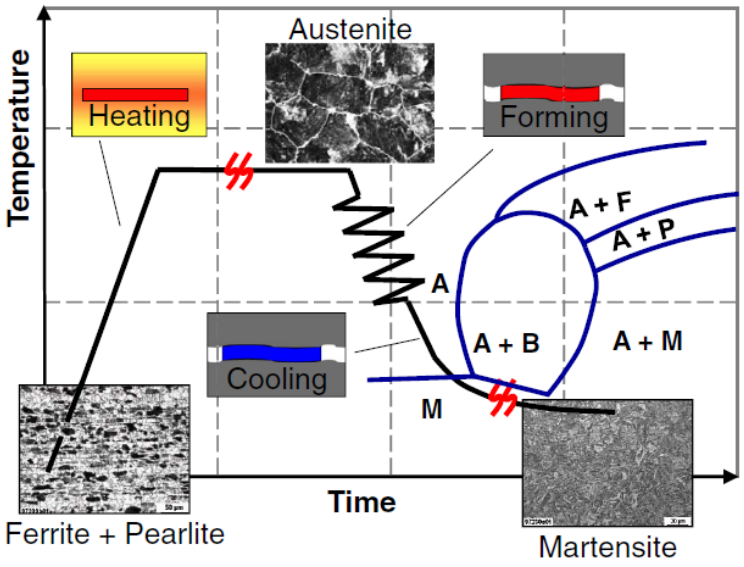

Figure 2-16. The temperature versus time diagram of the hot stamping process (Bruschi et al. 2014a).

The hot stamping technology has two variants: direct and indirect hot stamping (**Figure 2-17**). In the direct hot stamping process, the blank of the material is heated up and then transferred to the press.

Then, it is pressed and formed at the temperature higher than the austenitization temperature and quenched at a controlled cooling rate by the same dies that are cooled (**Figure 2-17a**). In the indirect hot stamping process, the blank of the material is pre-formed at room temperature and then heated up to the austenitization temperature. The part is then transferred to the press where it is quenched in the die, followed by ejection and trimming (**Figure 2-17b**). The direct hot stamping process is devoted to the production of components with a relatively small drawing depth or with a limited formability. The indirect process is commonly used for the production of more complex-shaped parts (Bruschi et al. 2014a).

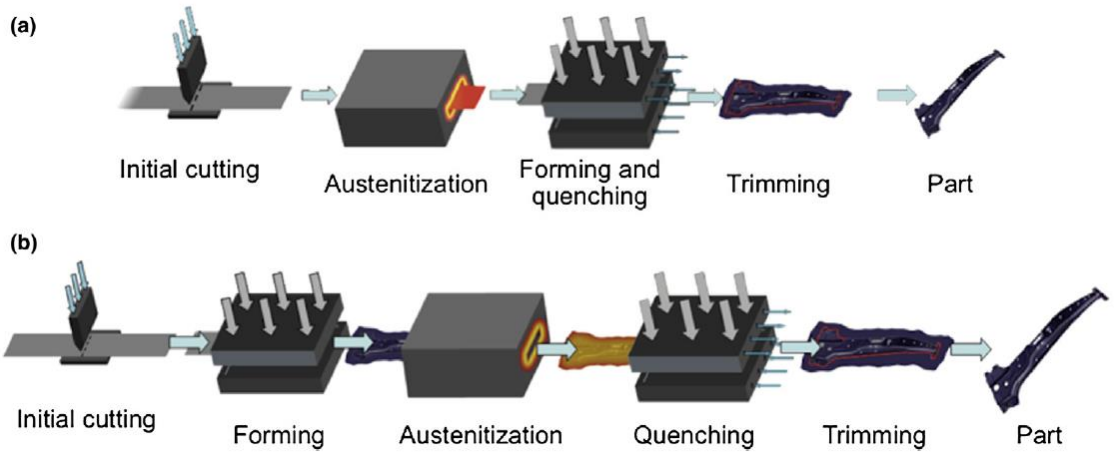

Figure 2-17. The hot stamping process variants: (a) direct hot stamping, (b) indirect hot stamping (Bruschi et al. 2014a).

Titanium alloys may be formed using mechanical or hydraulic presses, however this process has the inherent disadvantages of poor material ductility, dimensional accuracy, and significant springback. A hot forming process improves these common issues in the stamping processes. The successful hot stamping of titanium components requires the additional consideration of: notch sensitivity (causing cracking and tearing), galling, poor ability to shrink, embrittlement from overheating and from absorption gasses (hydrogen and oxygen), limited workability and the springback effect (Beal et al. 2006).

The high temperatures used during the hot stamping process increase formability, reduce the springback effect and enable maximum deformation with minimal annealing time between forming operations. In most cases, a forming process must be executed in hot dies with a preheated blank. A flat metal sheet is located in the die and heated up to a high temperature. The punch is activated to deform the blank into the die, and is held for 10 minutes under pressure. Research has been conducted in the use of a combination of a hot/warm blank and cold dies and in the hot forming process of titanium alloys. In the literature (Hamedon et al. 2013), hot hat-shaped bending of the Ti6Al4V alloy sheet using resistance heating was carried out. The conditions and general schematic of the process are presented below (**Figure 2-18**).

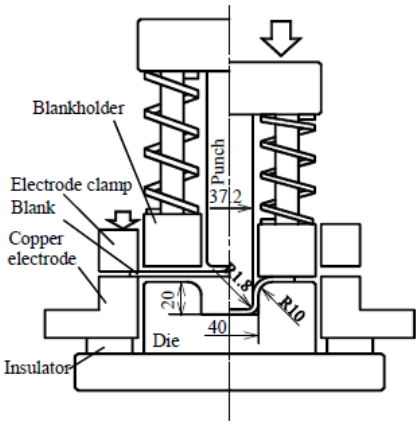

Sheet holder pressure [MPa]	0.6
Electrode clamping pressure [MPa]	4
Holding time at bottom dead centre [s]	0, 3, 6
Bending speed [mm/s]	150
Current density [A/mm2]	12.5
Heating temperature [°C]	370, 550, 690, 790, 880
Heating time [s]	2.8, 4.9, 6.1, 7.3, 8.0

Figure 2-18. Hot hat-shaped bending using resistance heating of titanium alloy sheet and the experimental conditions (Hamedon et al. 2013)

The productivity of the bending process was improved by resistance heating. Die heating was eliminated and the heating time of the titanium sheet was reduced. To prevent the heating of the die, the punch, blank holders and the sheet were not in contact with these tools during the forming process. The sheet (130mm length and 20mm width) was successfully formed at temperatures above 370°C. To evaluate the success of the forming, cracking was investigated via the use of non-destructive fluorescent penetrant test, and no cracks were observed on the sheet (**Figure 2-19a**). In the final stages of forming, the bending load was reduced from 6.5kN at room temperature to 1.8kN at a heating temperature of 880°C. The performed studies reveal no significant microstructural changes after the forming process indicating that heating rate was too high to entirely transform the structure of formed part (**Figure 2-20**); and almost constant hardness values measured in the longitudinal direction of the formed part (**Figure 2-19b**). The hardness at temperatures of 550°C and 880°C were similar to the hardness of the as-received sheet. The hardness increased from 320HV20 to 370HV20 when the heating temperature was approximately 880°C (Hamedon et al. 2013). The strength increase was caused by phase transformation however no analysis of the phase transformation or deformation mechanisms was presented.

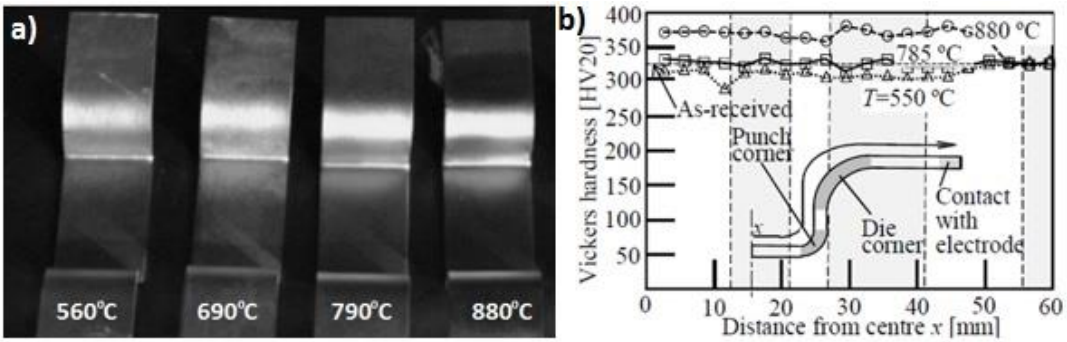

Figure 2-19. Hot stamped sheets formed at various temperatures (a) and Vickers hardness distribution in the longitudinal direction for various heating temperatures (b) (Hamedon et al. 2013).

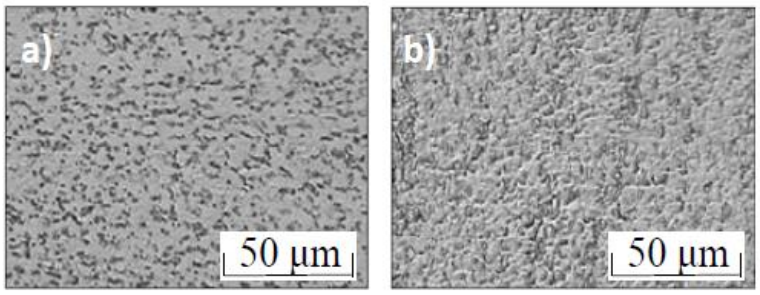

Figure 2-20. Microstructure of the formed sheet: as-received (a) and formed at 880°C (b) (Hamedon et al. 2013).

Resistance heating was also evaluated by Fahrettin et al. (Ozturk et al. 2016) who found that no microstructural change occurred during forming at 600°C, 650°C and 680°C. DIN WL 3.7024 titanium sheets with a thickness of 0.6mm in the range of temperatures from 600 to 680°C were formed under a press force of 1100kN and a punch speed of 45mm/s. No contact between tools and blank occurred during the heating process. As a result, an industrial part was successfully produced (**Figure 2-21**).

Figure 2-21. Example of an industrial part formed by electric resistance method (Ozturk et al. 2016).

Under these processing conditions, it was found that the part was free from tearing and cracks and the springback effect was eliminated. The highest ductility and property uniformity throughout the part occurred at temperatures above 540°C. Above 870°C the forming process is most effective in a vacuum or under a protective atmosphere to minimize oxidation.

To obtain the highest values of ductility, temperatures below 425°C should be avoided. Moreover, alpha-beta alloys should be formed under the β-transition temperature. Generally, to avoid deterioration of the mechanical properties, the temperature during the forming process should be lower than 815°C (Sieniawski et al. 2013). The most important conclusion is that no significant microstructure and no phase changes occurred during the forming process at 600°C, 650°C and 680°C. The average grain size of the as-received material was 10µm (**Figure 2-22a**) and after forming all specimens had an equiaxed-grain microstructure with a grain size of 12µm (**Figure 2-22b-d**). Nevertheless, different temperatures only slightly changed the grain size and elongation of grains was observed as the temperature approached 882°C (β-transition temperature). Therefore, there was no significant change in the grain size at forming temperatures below 882°C and short heating (30s) and forming (10s) times. Subsequently, X-ray diffraction (XRD) analysis showed that the microstructure of the formed parts are extremely close to the as-received material (**Figure 2-23**). These studies confirmed that no phase

transformation occurred, and thus this method can be successfully applied for the titanium alloys. However, heated specimens have negligible amounts of titanium dioxide and titanium oxide only on their surfaces, which is a result of oxidation kinetics during heating in air.

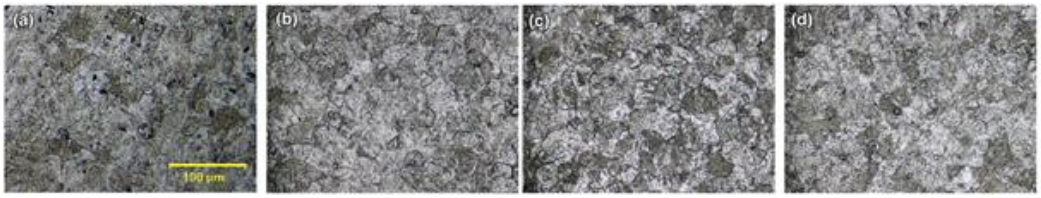

Figure 2-22. Optical microscope images of the as-received material (a), and formed at 600°C (b), 650°C (c), and 680°C (d) (Ozturk et al. 2016)

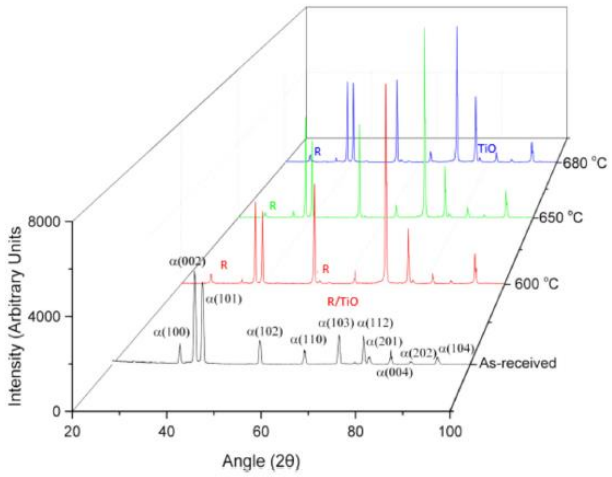

Figure 2-23. XRD analysis of the specimens formed at various temperatures (Ozturk et al. 2016)

The mechanical properties of titanium alloys are strongly dependent on the thermo-mechanical history, initial microstructure, alloy concentration and impurities within the structure. At room temperature and temperatures up to 600°C the common microstructure of the Ti6Al4V alloy consists of equiaxed alpha and elongated α (HCP crystal structure) phase in a minor volume of β phase matrix (BCC crystal structure). In order to understand and model the mechanical behavior of titanium alloys under varying temperatures and strain rates, a number of studies were performed (Zherebtsov et al. 2016; Oh et al. 2015; Majorell, et al 2002a; 2002b; Semiatin et al 1998; W. S. Lee and Huang, n.d.; Moćko, et al 2017). Due to the high yield strength and low elastic modulus, the springback effect and shape distortion was found to be extensive upon forming thin sheets. The formability of titanium alloys could be increased with increasing temperature and decreased with an increase of strain rate in the lower temperature region. At elevated temperatures, the compressive flow behavior is characterized by a peak stress followed by strain softening. The strain softening may occur as a result of temperature increase during deformation, phase transformation and microstructural changes resulting from dynamic recovery, dynamic recrystallization and local necking (Rollett, A; Humphreys, F; Rohrer, G.S; Hatherly 2013). Despite the

difficulties of titanium forming, the benefits of the material properties result in an ever increasing demand for titanium alloys in airframes and engines (Bridges and Magnus 2001; Ermachenko, Lutfullin, and Mulyukov 2011; Boyer 1996; Peters et al. 2003b; 2003a).

2.6 From hot stamping to FAST – the development of new technology

Titanium alloys are widely used in the aviation industry due to their outstanding mechanical properties (K. Wang et al. 2018). However, titanium alloys are seldomly used in the commercial field due to the prohibitively high cost (Peters et al. 2003a). It is reported that the cost of a product made from titanium alloy is 40 times greater than steels and 20 times greater than Aluminium alloys (Sikirica 2016). The price pressure of titanium alloy products is becoming more pronounced with the continued expansion of the aviation and aerospace industry. The cost contribution to manufacturing titanium alloy products can be subdivided into sponge titanium, additive alloys, melting and manufacturing cost (Sengupta et al 2017). It is difficult to further reduce the price of processes such as sponge titanium, additive alloys and melting due to the mature production lines and increasing environmental pressure (Cui et al. 2011). Therefore, reducing the manufacturing cost of titanium alloy products is becoming increasingly important as it is the area that can benefit most from new technologies.

Titanium alloys have strong deformation resistance at room temperature and a high level of springback, resulting in titanium alloy sheet components being generally formed at elevated temperatures (H. Yang et al. 2011). In the traditional hot pressing process, both forming tools and blank are heated in a furnace attached to the press (Velay et al. 2016). When the forming tools have a large mass, significant amounts of energy and time are required. Extended heating times also impose strict requirements on the tool material, as it must exhibit high temperature performance including high strength at elevated temperature, creep resistance and oxidation resistance, which results in high tooling cost. Moreover, tool wear and galling are also critical at elevated temperatures, which will reduce tool life. Due to these reasons, it is necessary to develop new technologies to improve the forming efficiency and reduce the cost of manufacturing titanium alloy components.

Hot stamping technology is widely used in the automobile industry (Karbasian et al. 2010), which uses cold forming tools to form and quench the hot (austenized) steel blank. In this hybrid forming technology, forming and heat treatment are conducted simultaneously, and one could obtain a part with martensite structure after forming (Maeno et al. 2017) . However, the application of hot stamping to titanium alloys has not yet achieved widespread adoption in industry. Compared with the traditional hot forming process for titanium alloys, hot stamping has the advantages of higher heating and energy efficiency, improved production efficiency, lower tool cost and improved post-form properties. Hot stamping of titanium alloys is used to produce components of complex geometry and superior mechanical properties. Ozturk et al. (Ozturk et al. 2013; 2011; 2016) investigated the application of electric resistance heating methods on titanium hot forming by using cold forming tools at industrial scale. In the authors' work, hot forming of commercially pure titanium and the Ti6Al4V alloy was found

to be applicable for industrial size part production with effective elimination of springback. It was observed that the combination of high deformation speed (45 mm/s) and relatively low forming temperature (< 700˚C) prevented grain size growth during forming. A hot stamping process of a titanium alloy sheet using resistance heating and cold forming tools was also studied by Hamedon et al. (Hamedon, et al 2013) where the sheet was successfully formed at elevated temperatures above 370˚C. It was also found that at the optimum heating temperature of 880˚C, the springback effect was successfully reduced and hardness of sheet improved. Meng et al. (Meng et al. 2017) proposed a near isothermal forming technique to manufacture a titanium alloy component, aiming to reduce cost and obtain a specific microstructure for the formed component. In this study, the dies were heated to a temperature approximately 150˚C lower than that of the workpiece. The results show that the microstructure morphology of the deformed titanium alloy can be changed by control of the strain rate and thermal path

In the authors' previous work (Kopec et al. 2018a; Kopec et al. 2018b), a feasibility study on hot stamping of titanium alloy was performed. The results show that the processing windows for TC4 titanium alloy during hot stamping are very narrow and one could only achieve a qualified part without surface cracking between 750°C and 850°C. During the hot stamping process, the sheet blank was first heated in a furnace to the target temperature and soaked for approximately 2 minutes to enhance the ductility, followed by rapid transfer to the cold forming dies and forming. During the transfer and forming process, the temperature decreased rapidly. It is known that the microstructure of titanium alloys is sensitive to the thermal-mechanical processing conditions. During the heating and soaking process, phase transformation of α to β would occur; and the reverse phase transformation of β to α would occur during the subsequent forming and cold die quenching processes. The heating temperature and soaking time will determine the volume fraction of β phase at the specific heating temperature; the cooling path will determine the volume fraction and morphology of different phases after quenching. Hence, the formability and post-form properties of titanium alloys are mainly determined by the material heating and cooling history. When the heating temperature is low (<750°C), titanium alloys have limited elongation under the hot stamping condition, which will lead to crack failure and severe springback. In the hot stamping of steels, the material is heated to the single-phase zone, where all the other phases are transformed to austenite. However, if the titanium alloy is heated to the single-phase zone and formed at a lower temperature, forming will be unsuccessful due to the poor ductility caused by the martensite, which is different from steel (Bruschi et al. 2014a). The authors' results showed that a qualified part could not be formed if the microstructure of the blank is β phase dominant which reduced ductility. On the other hand, increasing the forming temperature is one of the most effective approaches to reduce the springback (Hamedon et al. 2013). However, for titanium alloys, the rates of β phase transformation, grain coarsening and oxidation increase with temperature, especially when the temperature is near the β phase transus temperature. Therefore, there is a dilemma between reducing

the springback and improving the formability. Due to the above limitations, it is challenging to form complex-shaped components through hot stamping technologies.

Recently, a novel data driven forming technology, namely the FAST (Fast light Alloys Stamping Technology) (Zhang et al. 2019), was proposed to address the technological challenges of hot stamping (Cai, Z.-H., et al 2019) and to support the multi-material mix for the next-generation vehicles (Sun et al., 2019). In this new technology, a sheet blank is heated to the target temperature at an ultra-fast rate and immediately formed and quenched in the cold dies. The innovation of the FAST technology lies in the precise control of the phase transformation, grain growth and oxidation at elevated temperatures by the combination of tailored initial microstructure, precisely controlled heating, transfer, forming and in-die quenching, which could solve the dilemma discussed above. More importantly, it improves the formability and reduces the springback simultaneously. In addition, the forming efficiency could also be improved.

Ozturk et al. (2016) and Maeno et al. (2016) studied the hot stamping of titanium alloys utilising resistance heating, where the heating rates ranged from 108°C/s to 132°C/s. During the resistance heating, the materials in contact with the electrodes were not heated, and as a consequence, when the shape of the blank was not rectangular, the temperature was non-uniform (Maeno et al. 2018). Therefore, significant efforts have been devoted to solving this heating problem (Maeno et al. 2016). However, in these studies, the effect of heating rate on the formability and post-form properties was not studied. Other studies regarding fast heating of titanium alloys focused on the kinetics of the phase transformation from α to β (Elmer et al. 2004), and it is reported, that the diffusion distance of β stabilizer elements, such as V, decreases with the increasing heating rate (Elmer et al. 2005). This leads to a higher β-transus temperature under fast heating conditions (Rhaipu 2002). The microstructure of the rapidly heated titanium alloy does not have sufficient time to reach equilibrium, and therefore, affects the formability and post-form properties significantly. However, limited research has been performed in this field, particularly under the FAST conditions.

2.7 Deformation mechanisms in titanium alloys

The deformation mechanisms in titanium alloys can vary widely depending on the specific alloy composition (Karasevskaya et al. 2003) and the temperature of its deformation (Vanderhasten et al. 2007). These mechanisms include grain boundary sliding, dislocation slip, twining, dynamic recovery, dynamic recrystallization and dynamic grain growth.

The deformation mechanisms could be considered globally, for the material as a whole structure, or locally, when the deformation in each phase is investigated separately. In general, the occurrence of plastic deformation is determined by the movement of dislocations defined as defects or irregularities within the structure. It is affected by the alloying elements, strain rate and temperature (Sandala 2012). The movement of dislocations in a crystallographic direction can be executed by mechanisms of slip or

dislocation climb when an edge dislocation moves perpendicular to its slip plane (Barrett 1952). Dislocation slip has a little dependence on temperature while the dislocation climb occurs at high temperatures due to increase in mobility of vacancies. Dislocation slip occurs in particular planes and directions that are called dominant slip systems. The homogeneous plastic deformation requires five active and independent slip systems, according to Von Mises theory (Von Mises 1928). In two phase titanium alloy, twelve slip systems in the β phase and primarily three in the α phase were defined (Lutjering 2007). It was reported (Leo Prakash et al. 2010)**,** that activation of secondary slip and twining is possible in α phase, however, twining rarely occurred in two phase titanium alloys due to the high content of aluminium.

Historicaly, the deformation mechanisms for titanium alloys were summarised by Sargent and Ashby (1982) and presented in Figure 2-23 in form of the deformation maps.

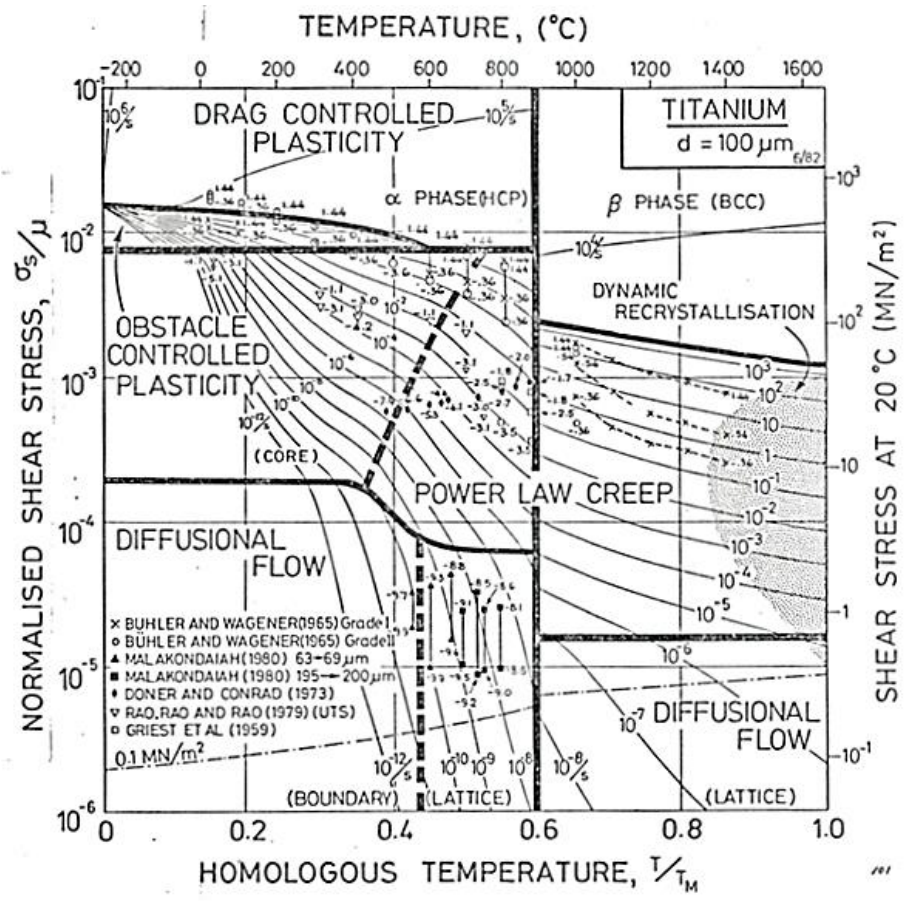

Figure 2-24 The deformation map for titanium alloys (Sargent 1982)

A compressive summary reported by (Vanderhasten et al. 2007) and (Wu et al. 2017; Souza et al. 2015) allows a categorisation of the deformation mechanisms based on the deformation temperature (Table 2-11). It was presented, that classical work hardening was a dominant mechanism if the temperature did not exceed 650°C. The work hardening rate increases with strain rate and decreases with temperature (Fitzner et al. 2019). With the temperature increase up to 750°C, an enhancement in elongation was observed due to dynamic recrystallization (DRX) promoted by grain boundary sliding. Additionally,

dynamic recrystallization led to grain refinement and significant decrease in grain size was observed of approximately 50%. The two types of dynamic recrystallization can be distinguished: discontinuous DRX (DDRX) and continuous DRX (CDRX) (Raja et al. 2020). Nucleation of new grains and growth of new fine grains in the high dislocated areas are called DDRX (Knauer et al. 2013). This mechanism is mostly observed during hot deformation of materials with low to medium stacking fault energy. On the other hand, in materials with high stacking fault energy, the new fine grains with low-angle grain boundaries formed during deformation are gradually transformed into high-angle grain boundaries due to efficient dynamic recovery (CDRX) (Raja et al. 2020). Subsequent increase of the deformation temperature above 800°C resulted in increasing domination of dynamic grain growth and continued α to β phase transformation. The deformation at the temperature higher than 900°C led to the formation of β phase in the whole volume of material investigated.

Table 2-11 Deformation mechanisms of titanium alloys

Temperature range	**Room temperature - 650°C**	**650°C - 750°C**	**750°C - 900°C**	**900°C - 1050°C**
Deformation mechanisms	work hardening	Dynamic recrystallization promoted by grain boundary sliding	Dynamic recrystallization and dynamic grain growth promoted by grain boundary sliding	Static and dynamic grain growth

2.8 The modelling of deformation behavior of titanium alloys

The deformation behavior experienced by materials during component forming can be predicted using mathematical and computational modelling. By application of such modelling techniques, cost savings can be achieved due to the reduced requirement for forming trials before successful manufacture (Mosleh et al. 2019). Hence, modelling of the flow behavior and microstructure evolution during deformation has been investigated by many research groups. Yang et al. (L. Yang et al. 2016) developed a set of unified viscoplastic constitutive equations for the determination of flow stress and globularisation evolution in the Ti6Al4V alloy with initial lamellar microstructure. Due to the application of Ti6Al4V, mainly for superplastic forming purposes, low strain rates were considered in many studies (Velay et al. 2016; Guo et al. 2014; K. Wang et al. 2017; Liu et al. 2013). Large strain deformation response of Ti6Al4V has been evaluated over the strain rates ranging from 10^{-4} to over 10^{-4} s^{-1} by Lesuer et al. (Biennial et al 2001) and the Johnson-Cook (JC) material model was used to describe

the flow behavior of titanium alloys. Generally, such models as Johnson-Cook or Arrhenius could precisely describe the mechanical behavior of titanium alloys during plastic deformation at high temperatures (> 850˚C) and wide range of strain rates (10^{-4} - 1 s^{-1}) (Hu et al. 2018; W.-S. Lee et al 1998; Jha et al. 2017). A dislocation density based model for plastic deformation and globularization of Ti6Al4V developed by Babu et al. (Babu et al 2013) investigated plastic deformation of the alloy at strain rates ranging from 10^{-3} to 1 s^{-1} and temperatures between 20°C and 1100˚C. The model is capable of describing the plastic flow of the alloy in a wide range of temperature and strain rates by including the dominant deformation mechanisms such as dislocation pile-up, dislocation gliding, thermally activated dislocation climbing, and globularization. In this model, recovery and recrystallization are two competing restoration mechanisms and counteract strain hardening. In order to compute the evolution of dislocations, density and vacancy concentration are used as the internal state variables. However, the model assumes that the α - β phase composition of the alloy is in the equilibrium state at all temperatures which is only sound for the low heating or cooling rates used in hot stamping. Velay et al. (Velay et al. 2016) developed a material model which considers initial equiaxed microstructures (grain sizes of 0.5 and 3 μm) to predict their influence on the viscous flow and strain hardening. In this model, the dynamic recrystallization can be assumed negligible whereas, in contrast, grain boundary sliding and grain growth play a predominant role on the flow stress and hardening. The constitutive equations proposed were capable of modelling viscoplasticity, strain hardening and grain size evolution for a wide range of strain rates (10^{-4} to over 10^{-2} s^{-1}) and forming temperatures (650°C - 870˚C). The developed model could also accurately replicate the flow behavior of titanium alloys under superplastic forming conditions. In the last dacade, great efforts have been made in terms of modelling of viscoplastic behavior of titanium alloys in high temperatures and low strain rates (< 1 s^{-1}). With the development of new forming technologies, it has become increasingly important to understand the behavior of titanium alloys deformed at high temperatures and high strain rate conditions. Thus, such behavior was considered in this thesis.

Finite element (FE) modelling has been widely used to analyse and optimise sheet metal forming processes (A. Wang et al. 2017). Under warm and hot stamping conditions, the formability of sheet metal varies depending on temperature, strain rate and strain path. These variables were analysed by Sirvin et al (Sirvin et al. 2017) in order to identify modelling potential to predict the mechanical behavior of the Ti6Al4V alloy under hot stamping conditions. The hardening plastic model identified in the study was introduced in FEM to simulate an omega shape forming operation. Chen et al (Chen et al. 2019) developed a numerical simulation model for the thero-plastic forming process of a high-temperature titanium alloy of TA32. In this study, the viscoplastic properties of the TA32 titanium alloy at high temperatures were described by the hyperbolic sinusoidal Arrhenius equation and verified by experimental and FE simulation work. Fiorentino et al (Fiorentino et al 2015) developed experimental and numerical methods for the analysis of cold (20°C) and warm (300°C) CP titanium sheet stamping which were vertified through the production of an automotive component. Despite of the number of

papers on the hot stamping of titanium alloys (Sirvin et al. 2017; C. Chen et al. 2019; Fiorentino et al 2015; Ozturk et al. 2010; Ma et al. 2016; Odenberger et al. 2011; Bruschi et al. 2014; Adamus 2009), the actual industrial practice in designing plastic deformation processes to obtained titanium complex shaped parts is based on empirical approaches. In order to verify these aproaches, several forming trials are required to solve the potential production errors and to identify the best forming parameters before full scale production.

2.9 Conlusions

The mass commercialization of titanium alloys in the aircraft industry is leading to a greater development of tools, testing machines and processing. Conventional hot forming processes require hot tools and hot blanks to form a final part. New trends have now focused on using cold dies and hot/warm blanks to form titanium components to overcome the high cost, low productivity and reduce the tool wear found in commercially used hot forming processes. In this thesis, the novel hot stamping process and evolution of microstructure and mechanical properties of the Ti6Al4V titanium alloy was studied in details.

CHAPTER 3

3. Formability and microstructure evolution mechanisms of the Ti6Al4V alloy during a novel hot stamping process*

A novel hot stamping process for titanium alloys using cold forming tools and a hot blank was studied systematically in this chapter. Uniaxial tensile tests at temperatures ranging from 600°C to 900°C and strain rates ranging from 0.1 s^{-1} to 5 s^{-1} were conducted to investigate the formability of the Ti6Al4V alloy. The microstructure and post-form properties of the material were characterised to identify the deformation mechanisms that occur at these test conditions. Hot stamping tests were performed in a wide temperature range to verify the feasibility of the novel process for the Ti6Al4V alloy. Results showed that the flow stress of the Ti6Al4V alloy was sensitive of both temperature and strain rate. The formability of the material under isothermal conditions increased with the increasing temperature and decreasing strain rate. A satisfactory elongation ranging from 30% to 60% could be achieved at temperatures ranging from 750°C to 900°C, respectively. The phenomenon of material hardening and softening varied with temperature due to the different deformation mechanisms present at different test conditions. For example, from 600°C to 700°C, the main mechanism was recovery; whereas from 750°C to 950°C, the main mechanism was transformation and recrystallization. Refinement of α grains was observed from 750°C to 900°C, although α grains tended to grow with temperatures exceeding 900°C. The hardness of the material after deformation first decreased with the temperature due to recovery at 750°C, and subsequently increased due to the phase transformation and recrystallization at 900°C. During the hot stamping tests, qualified parts without visible cracks could be formed successfully at heating temperatures ranging from 750°C to 850°C, although the forming failed beyond this temperature range. At lower temperatures, the forming failed due to the limited ductility of the material. At higher temperatures (900°C - 950°C), extensive phase transformation of α to β occurred during the heating. During the transfer and forming, the temperature dropped significantly which led to the formation of transformed β, reduced the formability and caused the failure. The post-form hardness distribution demonstrated the same tendency as that after uniaxial tensile tests.

3.1 Experimental details - Determination of mechanical properties and microstructure characterization

Tensile specimens made of the Ti6Al4V titanium alloy, were supplied by AVIC Beijing Aeronautical Manufacturing Technology Research Institute. A dog-bone shaped specimen was used with a gauge length of 46 mm, a width of 12 mm and a thickness of 1.5 mm **(Figure 3-1)**. A Gleeble 3800 thermo-

* Chapter 3 is based on paper work Kopec M., Wang K, Politis D.J., Wang Y., Wang L., Lin J., Formability and microstructure evolution mechanisms of Ti6Al4V alloy during a novel hot stamping process, MSAE

mechanical testing machine (**Figure 3-2a**) was used to conduct uniaxial tensile tests at elevated temperatures to characterize the properties of Ti6Al4V specimens at a range of strain rates and temperatures. Ti6Al4V flat specimens were heated at a rate of 2°C/s to the testing temperature and deformed immediately. The value of heating rate was chosen to ensure that the deformation temperature is as close as possible to target, testing temperature. After failure, specimens were cooled to room temperature at the cooling rate of 40°C/s. The test matrix for the uniaxial tensile tests is shown in **Table 3-1**. Before each test, the width and thickness of the specimen was measured at three different locations and recorded, due to the stress and strain during each test could be calculated during post-processing of the data. Subsequently, the center of the specimen was marked out to locate the position of the pair of thermocouples that were welded to the surface of specimen. The thermocouples were used to control and monitor the temperature of the specimen during the tensile test. The equipment used to spot weld the thermocouples is present in **Figure 3-2b**. The voltage used was based on previous experience and it was equal to 40V.

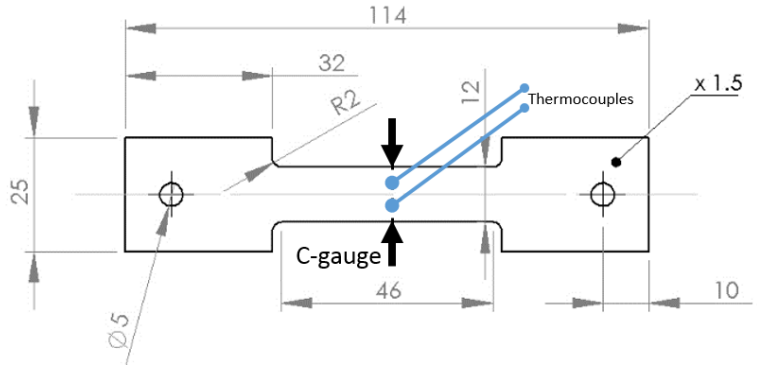

Figure 3-1 Specimen geometry for the uniaxial tensile test.

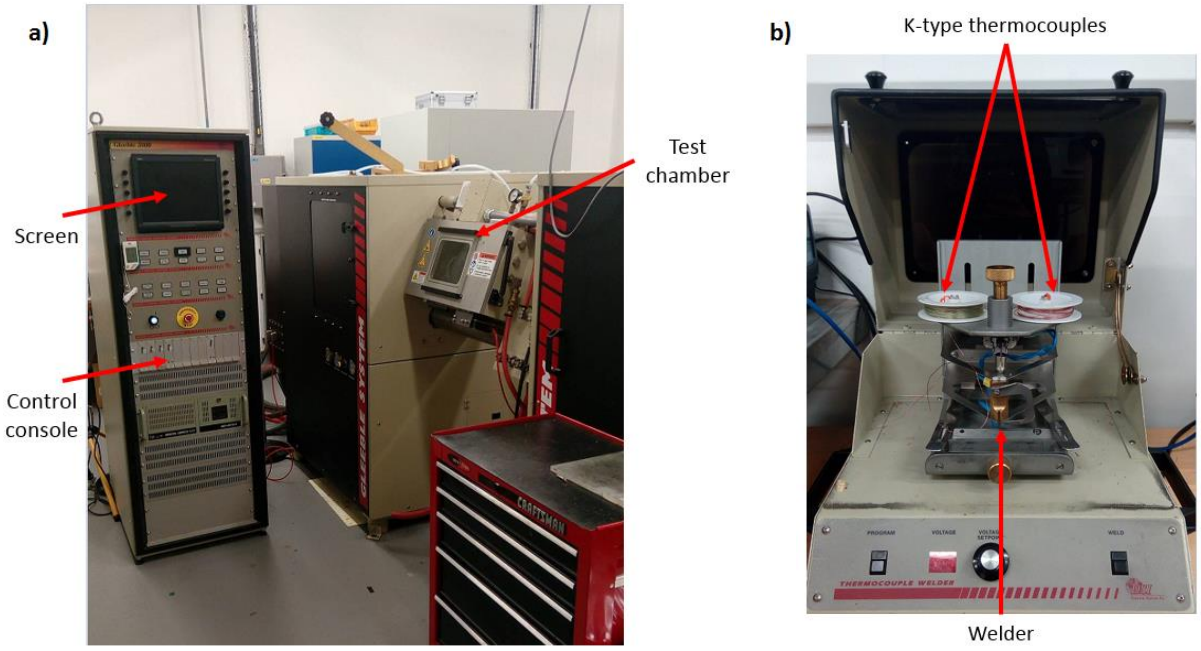

Figure 3-2 The Gleeble 3800 simulator (a) and spot welding equipment used during specimen setup (b).

Table 3-1 Test matrix for uniaxial tensile tests of the Ti6Al4V

Temperature (°C) / Strain rate (s^{-1})	600	650	700	750	800	850	900
0.1				×	×	×	
1	×	×	×	×	×	×	×
5				×	×	×	

The surfaces and the edges of the specimen were ground with fine sanding paper in order to provide a clean surface to weld the thermocouple and to stress concentrations elimination. Subsequently, the specimen was put between two low thermal conductivity stainless steel grips, which were positioned and clamped between the Gleeble jaws. A C-Gauge transducer was used to measure and record the width at the center of the specimen throughout the tensile test. The force was measured by a load cell fixed to the static jaw of the Gleeble. The full test setup is shown in **Figure 3-3.**

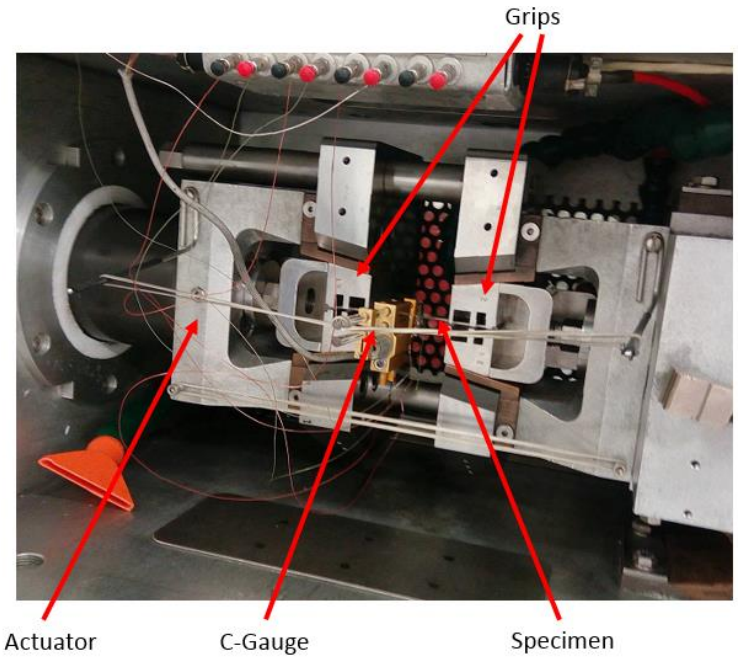

Figure 3-3 The specimen setup in the test chamber.

During heating, the system was put in 'force control' mode and the force set to zero in order to allow expansion of the specimen during the heating process. This prevents compressive stresses from developing in the specimen by enabling the actuator to compensate for any expansion. During deformation, the target temperature of the specimen is maintained, and the system put in 'stroke control'. Here, the required actuator stroke (in mm) was set at each time increment of the test to achieve the target strain rate. This was done by assuming an initial gauge length of 10 mm in the specimen. The size of gauge length was determined by identification of isothermal zone and was presented in Appendix A. The most critical data acquired and recorded during the tests included the C-Gauge readings of the

width and the load history. True stress was calculated as the applied load divided by the actual cross-sectional area (the changing area measured with c-gauge with respect to time) of the specimen at that load. True strain was calculated from the axial displacement data as the natural log of the quotient of current length over the original length.

The hardness values of the specimens after the uniaxial tensile tests and hot stamping forming were measured by means of a Zwick hardness tester at room temperature with 6 measurements per condition. Each hardness measurement was performed using a 10 kgf force and the dwelling time of 10 seconds. Microstructure investigations were made for tensile test specimens tested at room temperature and in the range of 600°C - 900°C. The microstructure of investigated material was observed using a Scanning Electron Microscope (SEM) and backscattered electrons (BSE) mode. The specimens for microstructural characterization were prepared by conventional metallographic procedures for titanium. Prior to study, the specimens were first hot mounted and then ground using 600, 800, 1200 and 4000 SiC paper. The polishing was performed using Metrep® MD-Chem cloth and 0.04 μm Colloidal Silica solution. The microstructural characterization was performed on a Zeiss Sigma300 scanning electron microscope (SEM) under Backscattered Electron (BSE) mode operated at 20 kV. Volume fraction of coexisting phases was measured by ImageJ software. Three SEM pictures were measured to get the average value. The average grain size was obtained by using Esprit software from single EBSD map of scanned material, where over 100 grains were calculated.

3.1 Initial material

The tensile test results for the as-received Ti6Al4V titanium alloy specimen cut in the rolling direction at room temperature and strain rate of $1s^{-1}$ is shown in **Figure 3-4.** The results show an ultimate tensile stress for the tested material of 1120 MPa, a yield strength of 850 MPa and Young's modulus of 97 GPa. Yield strenght was determined for the 0.2% offset strain from the experimental stress-strain curve. The hardness of the as-received material was 380HV10. Hardness tests details were presented in **Appendix B** respectively.

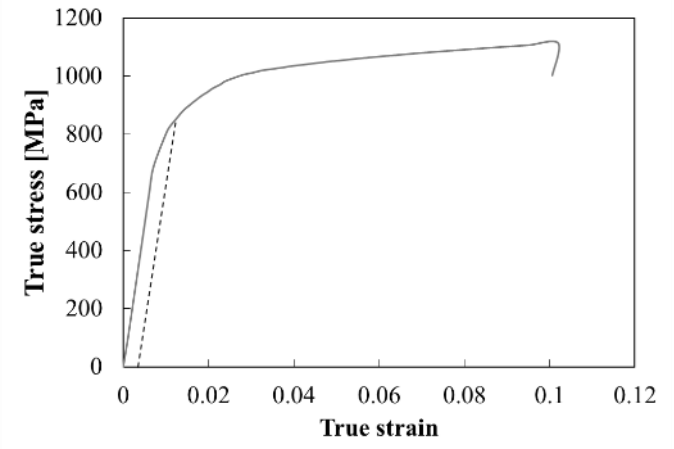

Figure 3-4. Stress - strain curve obtained for the as received material at room temperature.

A microstructural investigation of the as-received material was performed on the SEM using Backscattered Electron (BSE) mode. The initial microstructure of material in the rolling direction is presented in **Figure 3-5.** The microstructure of the investigated titanium alloy contains the α-phase matrix and small particles of β-phase. The specific chemical composition of as-received material is presented in **Table 3-2.**

Table 3-2. Chemical composition of the as-received Ti6Al4V.

Wt. %	C	N	O	H	Fe	Al	V	Ti
Ti6Al4V	0.08	0.05	0.2	0.15	0.4	6.8	4.5	Bal.

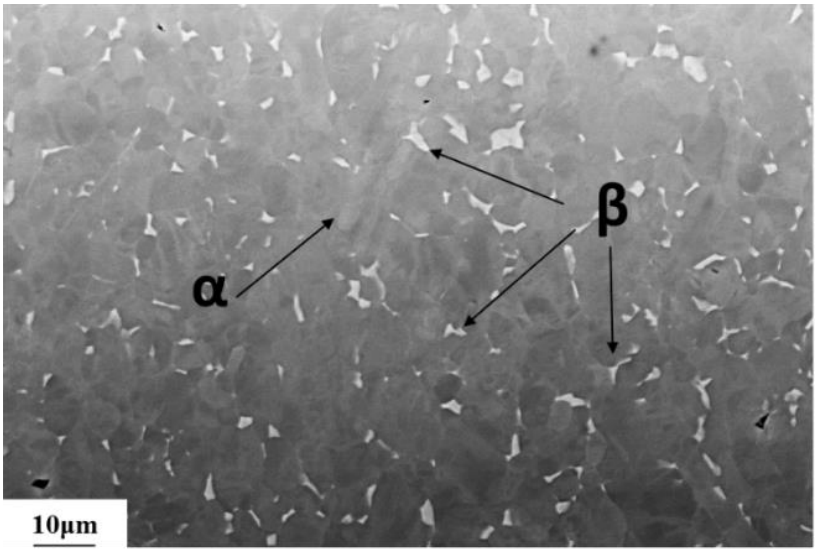

Figure 3-5. SEM microstructure images of the as-received material.

3.2 Effect of temperature on mechanical properties of the Ti6Al4V alloy

To investigate the formability of the Ti6Al4V alloy, tensile tests were performed under a range of temperatures (600°C - 900°C) with a strain rate of $1s^{-1}$ on specimens cut in rolling direction (**Figure 3-6**). It was observed that the temperature has a great influence on the elongation. In the range of temperatures from 600°C to 700°C, there is little change in elongation. However, for temperatures greater than 700°C, the elongation increased dramatically from 30% at 750°C to 60% at 900°C as shown in **Figure 3-7**. At elevated temperatures, high dislocation mobility led to an increase in ductility (Chang 2017) as well **Figure 3-7**. It should be mentioned that in the range of temperatures from 600°C - 700°C, strain hardening occurs. At 600°C significant strain hardening is observed, leading to an UTS of 600 MPa. At 750°C and higher temperatures, the flow stress curve became flat due to the occurrence of materials softening, indicating that the deformation mechanisms vary with the deformation temperature.

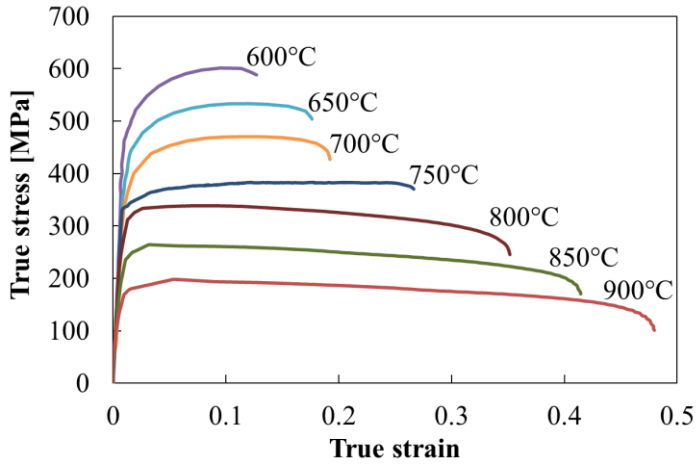

Figure 3-6. Stress - strain curves obtained for the Ti6Al4V specimens at the range of 600°C - 900°C.

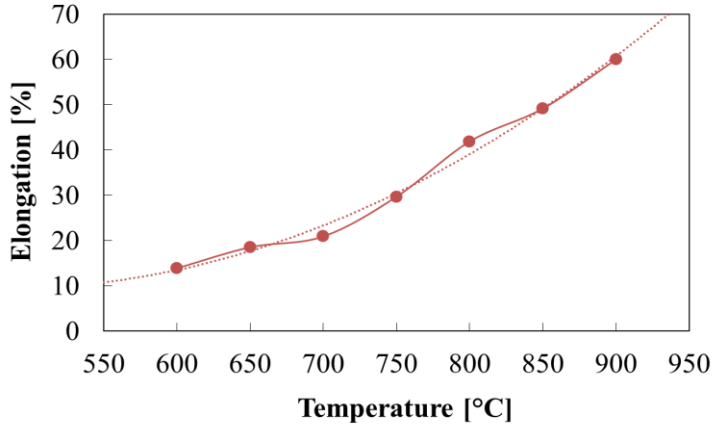

Figure 3-7. Ductility obtained for the Ti6Al4V specimens at the range of 600°C - 900°C.

It can be concluded from the above tensile test results that the material exhibits good ductility at temperatures greater than 700°C. However as the strain rate during actual forming is not constant, the material behavior was studied through tensile tests conducted at temperatures ranging from 750°C to 850°C, and strain rates ranging from 0.1 s^{-1} to 5 s^{-1} . **Figure 3-8** presents the stress-strain curves of the initial material under different testing conditions. The ductility of the investigated material increased with increasing temperature and decreasing strain rate from 0.2 at 750°C (strain rate of $5s^{-1}$) to 0.3 at strain rate of $0.1s^{-1}$ and from 0.4 at 850°C (strain rate of to $5s^{-1}$) to 0.47 at strain rate of $0.1s^{-1}$. Peak stress decreased with temperature increase and strain rate decrease from 445 MPa at 750°C to 200 MPa at 850°C. Material softening during the hot deformation process was observed, and it was found that the softening rate increased with decreasing strain rate. It could be observed that the investigated material was strongly strain rate sensitive. It was concluded that both strain rate and temperature have a great influence on deformation behavior and mechanism of the material. The elongation increase and peak stress decrease with decreasing strain rate was observed during the tensile tests. This phenomenon is related to the dislocation mobility and atom diffusion at higher temperatures and lower strain rate resulting in larger elongation and lower stress.

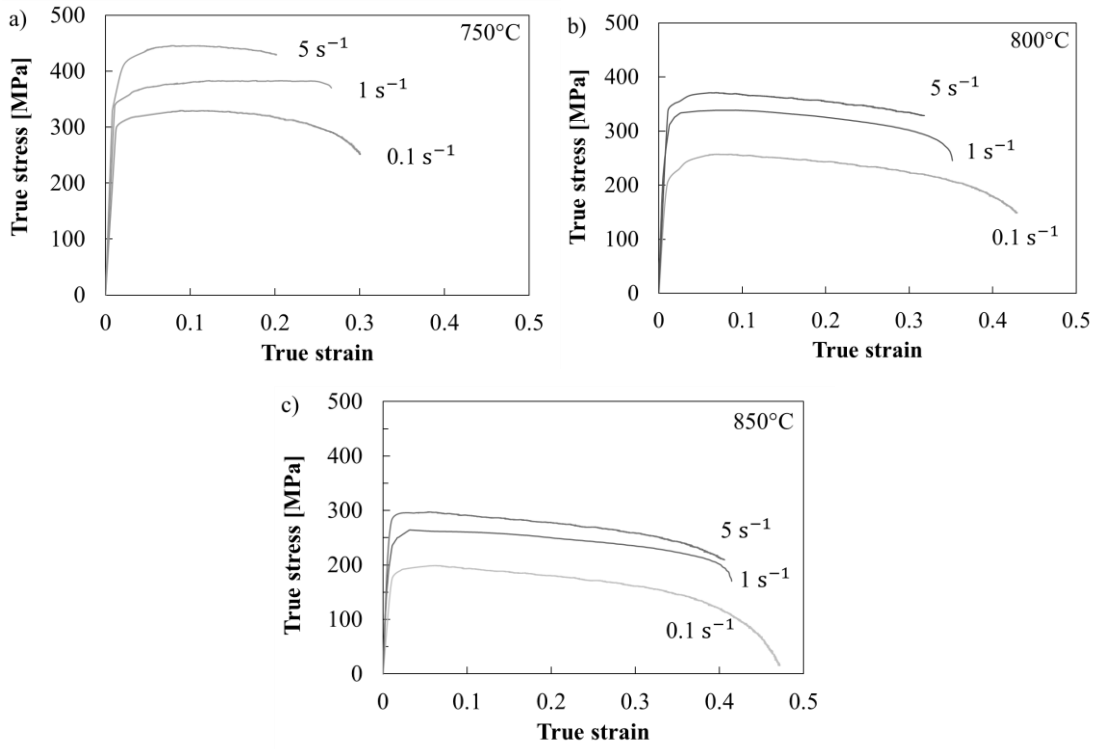

Figure 3-8. Ti6Al4V stress - strain curves obtained by tensile test at different strain rate conditions for temperature values of 750°C (a), 800°C (b) and 850°C (c).

3.3 Evolution of microstructure and post form strength after deformation

Following tensile testing, the hardness distribution of all specimens after completed tensile tests performed was evaluated. The detailed hardness measurements of the Ti6Al4V alloy were presented in **Appendix B**. A microstructural investigation of specimens was performed on a SEM using BSE mode. The distribution of Vickers hardness of specimens following deformation at a strain rate of 1 s^{-1} for different temperatures is shown in **Figure 3-9**, and the corresponding microstructure and fraction of various phases presented in **Figure 3-10** and **Figure 3-11** respectively. It can be seen that the hardness of the material decreased at first and then increased with increasing temperature. The microstructure of the investigated material showed limited change after tensile testing at temperatures of 600°C and 650°C. The dimension of the β-phase particles and their content in the whole volume of the material were almost the same in comparison to the initial microstructure (**Figure 10a-b**, **Figure 11**). This may be because the temperature was too low to initiate phase transformation. However, increased dynamic recovery occurred at higher temperature with the consumption of more dislocations, and as a result the hardness and flow stress began to decrease gradually with the increasing temperature before 750°C. When the temperature was greater than 750°C, both the content and size of β-phase increased with increasing temperature (**Figure 10d-f, Figure 11**) which caused material softening during the tensile tests. Both phase transformation and recovery reduced the dislocation density resulting in a reduction in material's strength and a simultaneous increase in elongation. When the specimen was cooled after tensile tests, transformed beta phase formed during the cooling process which could improve the

hardness of the material at room temperature. The fraction of transformed beta increased with temperature, resulting in the simultaneous increase in hardness (Jadhav et al. 2017). It is worth noting that dynamic recrystallization of α grains may also occur during the deformation, which could refine the microstructure and improve the hardness (Furuhara et al. 2007).

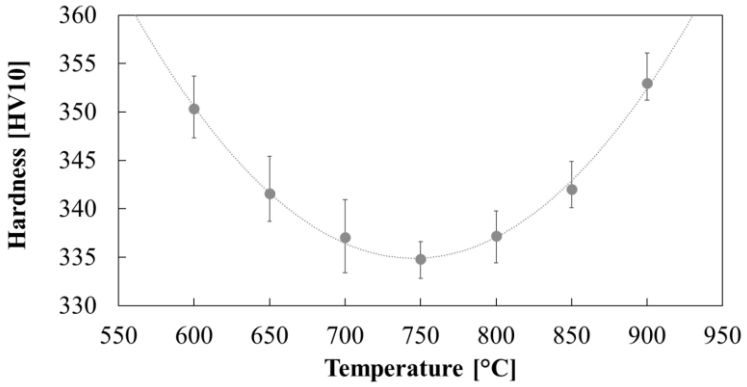

Figure 3-9. Evolution of Vickers hardness of tensile tested specimens conducted at different temperatures.

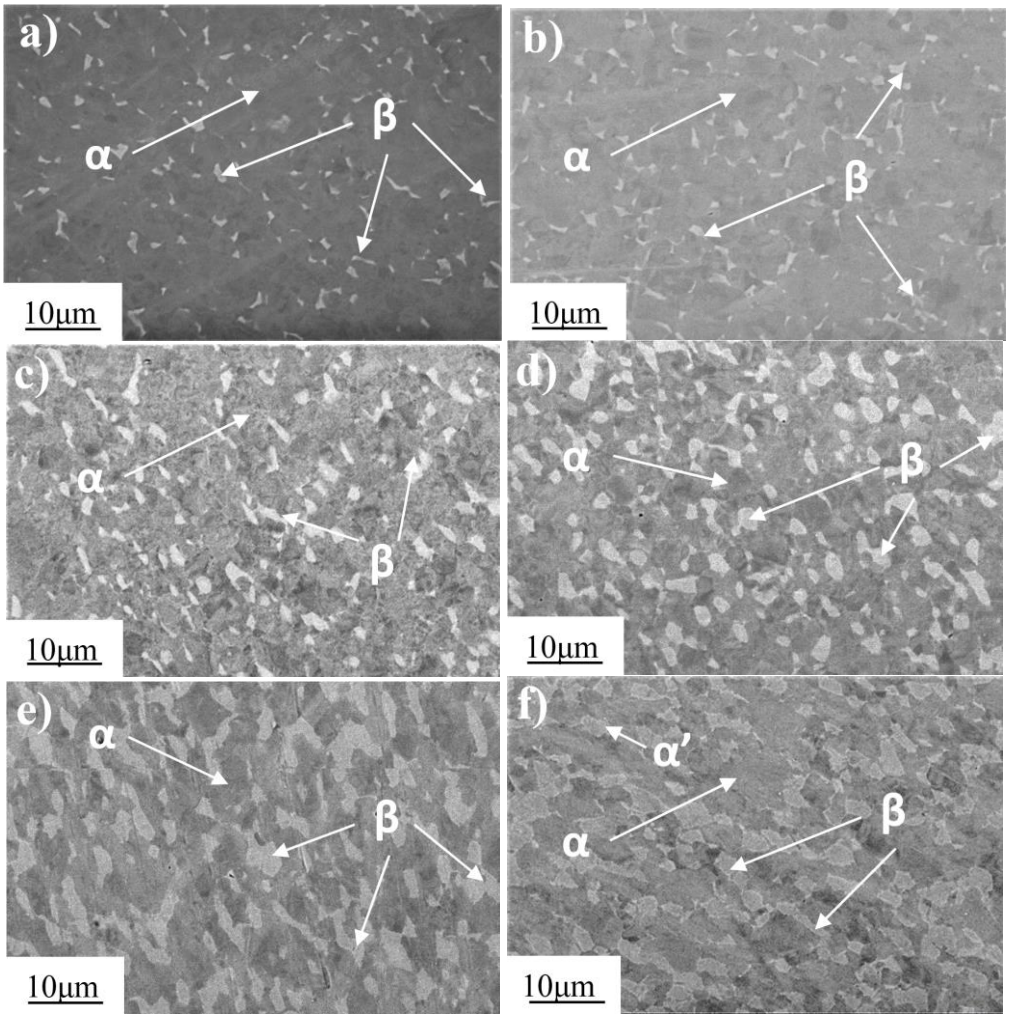

Figure 3-10. SEM microstructure images of the Ti6Al4V specimens after completed tensile tests performed at 600°C (a), 650°C (b), 750°C (c), 800°C (d), 850°C (e) and 900°C (f).

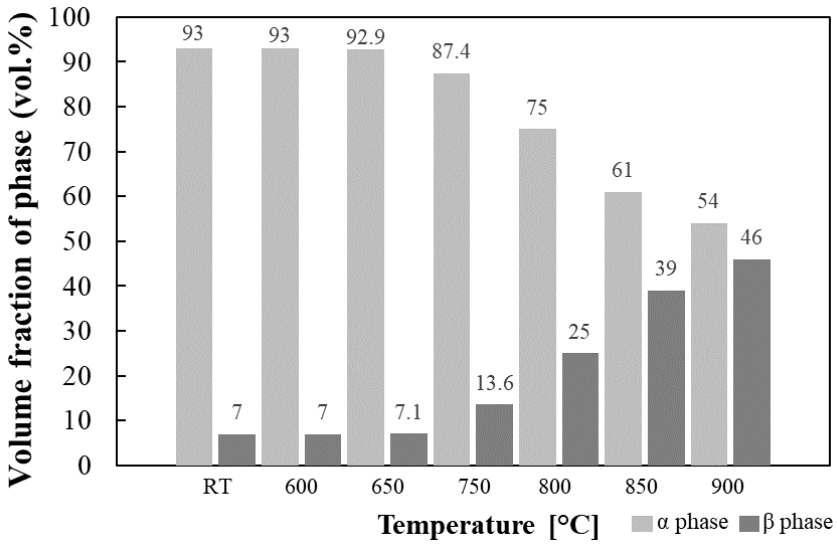

Figure 3-11. Evolution of α and β phase fraction after completed tensile tests at different temperatures.

3.4 Feasibility of hot stamping technology – forming test of m-shaped component

To verify the feasibility of the proposed technology, forming tests were conducted on a 250 Ton Instron press. The setup of facilities for hot stamping is presented in **Figure 3-12**. These tests were conducted under loading frame velocity of 10 mm/s at room temperature and at temperatures ranging from 600°C to 950°C. The specimen size was 90 x 8 x 1.5 mm. The heating and forming temperature was monitored by thermocouple wire welded to the specimen. Once the temperature of the specimen was stable, it was removed from the furnace, transferred to the forming tool and formed immediately by cold dies. The transfer time from the furnace to the cold die was controlled to be around 2s. The formed specimen was held for 10s within the die. Subsequently, the formed specimen was removed from the stamping tool to allow further cooling in air to room temperature.

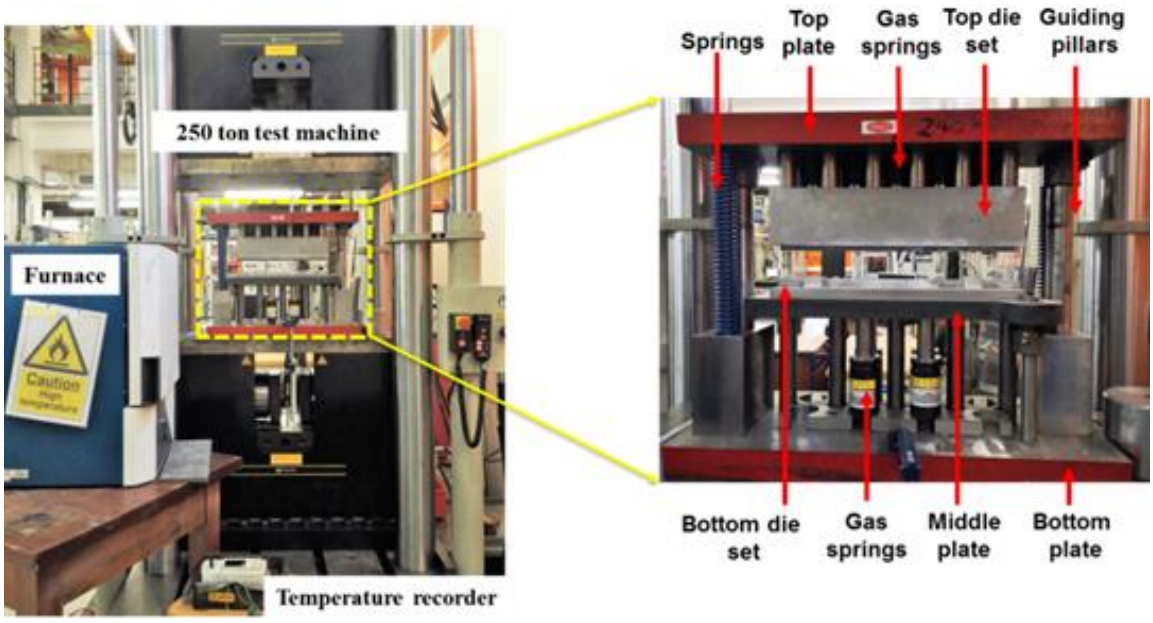

Figure 3-12 Setup of facilities for hot stamping experiment.

From the above tensile tests, it can be found that the Ti6Al4V alloy has a good formability at elevated temperature even with a high strain rate and the deformation conditions have a huge impact on the material properties. In order to further verify the feasibility of the hot stamping of titanium alloys and determine the processing windows, forming tests were conducted. The hot stamping of titanium alloy includes three main steps: heating, transfer, and simultaneously forming and quenching as shown in **Figure 3-13** During the whole forming process, temperature is one of the most important parameters, which will affect not only the formability of the material but also the post-form properties of the formed part. Therefore, a thermocouple wire was welded on the sidewall of the specimen to monitor the temperature evolution during the whole process. **Figure 3-14a** presents the typical temperature history of one specimen. The specimen was heated to 850°C and then soaked until the temperature became stable. The total time for heating and soaking was 180 s approximately. Subsequently, it was transferred from the furnace to forming tool, formed immediately by cold dies and quenched. During the transfer, the actual temperature of the specimen reduced from 850°C to approximately 700°C just before forming. During forming the temperature rapidly dropped to approximately 350°C and then gradually decreased to room temperature. **Figure 3-14b** shows the load and displacement information during the forming process. The displacement curve could be divided into two parts: forming and holding. In the forming part, the press moved at a constant speed of 10 mm/s, but the load curve represented different characteristics. Before the punch contacted with the specimen, the movement of the press would compress the gas spring in the dies, which led to the slow increase of load to around 10 kN. After the punch contacted with the specimen, the load increased dramatically as the specimen was deformed within cold dies (**Figure 3-14c)**. After displacement reached its maximum value, the specimen was held for 5 seconds within the forming tools.

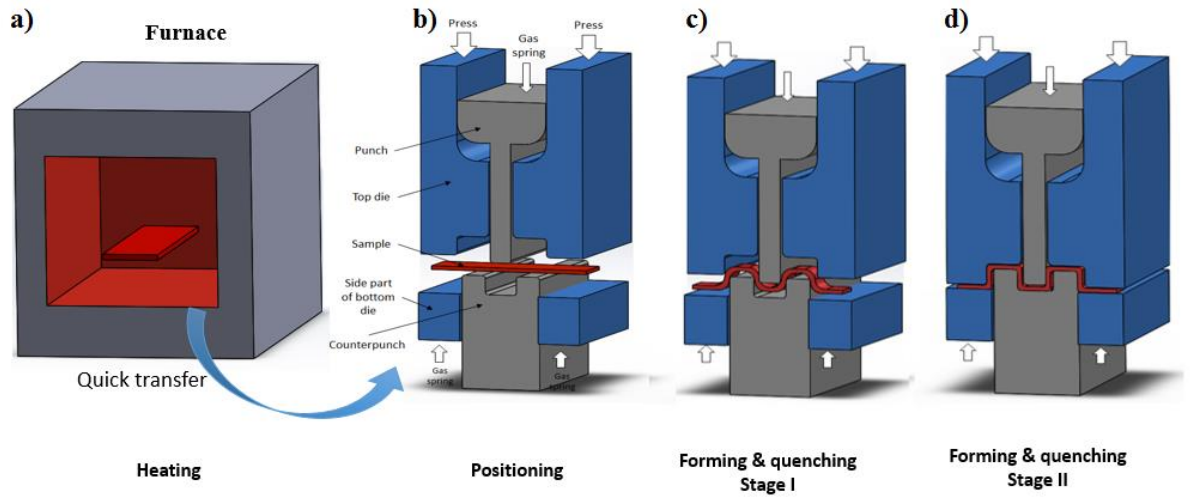

Figure 3-13. Schematic of the forming process during heating of the specimen (a), at the positioning stage (b), during forming (c) and at the final stage (d).

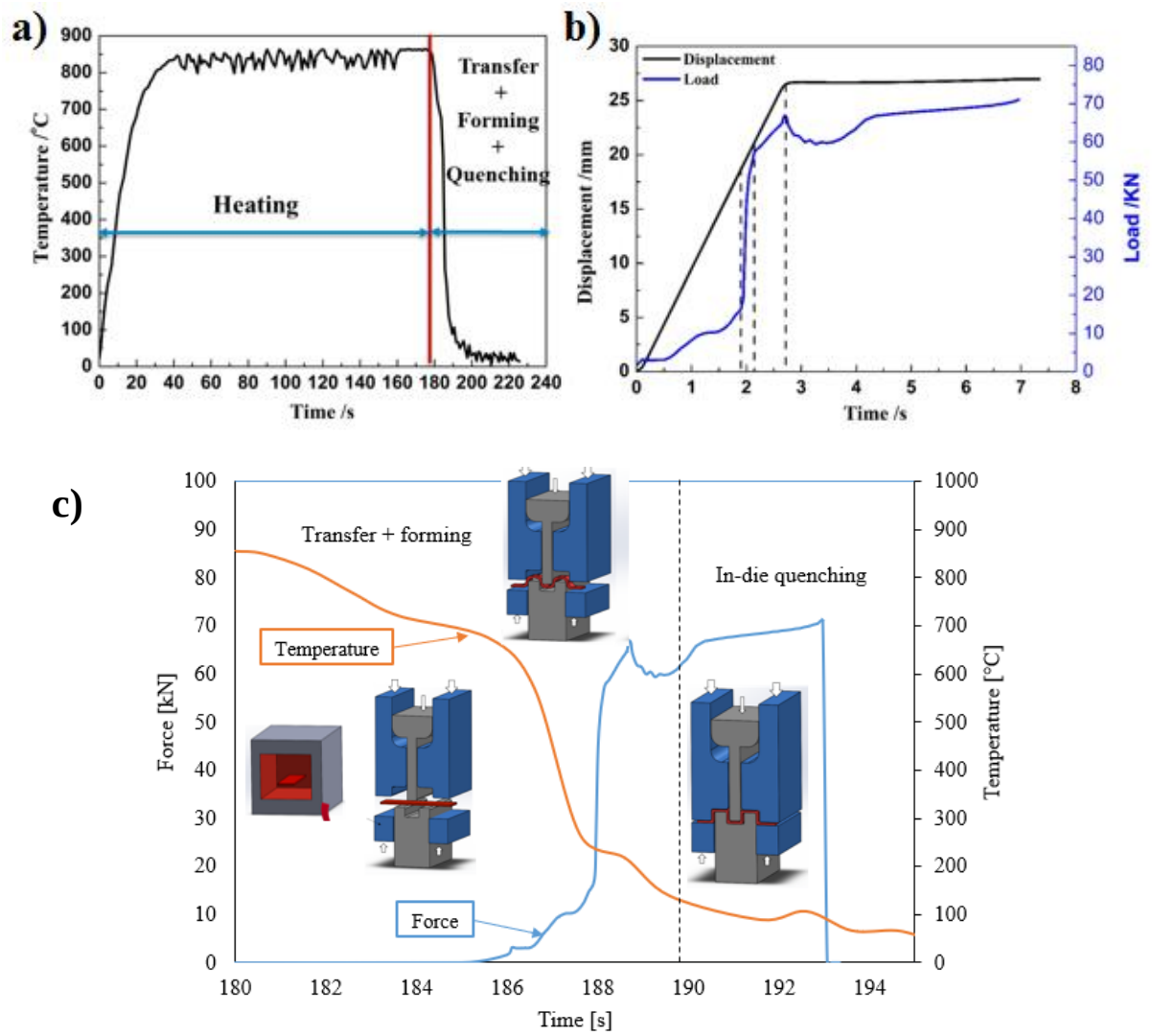

Figure 3-14. Evolution of temperature (a), load/displacement (b) during forming process and load/temperature (c).

Figure 3-15 shows the cross-section of the formed parts using cold forming tools at different temperatures. Titanium features have been formed at temperatures ranging from 600°C to 950°C (**Figure 3-15b-f**) since room temperature forming led to the fracture of the specimen into several pieces (**Figure 3-15a**). A qualified part without visible cracks could only be formed between 750°C to 850°C with specimen formed at 600°C displaying cracks on the surface indicating that forming temperature was too low to form the component (**Figure 3-16a**). Obvious cracks (**Figure 3-16b**) were also observed in parts formed at 900°C. When the heating temperature was increased to 950°C, the forming also failed due to the occurrence of cracking **(Figure 3-15f).** This tendency is different to the uniaxial tensile tests, where the elongation increased with increasing temperature. During the tensile tests, the specimen was deformed under isothermal condition, whereas the temperature reduced significantly during the transfer and forming stages of hot stamping. The formability of the material is determined by its microstructure under certain conditions, therefore one can infer that the crack and failure that occurred at 900°C and 950°C was caused by the temperature dropping and the corresponding microstructure alteration. The detailed explanation of this can be found in Section 3.6.

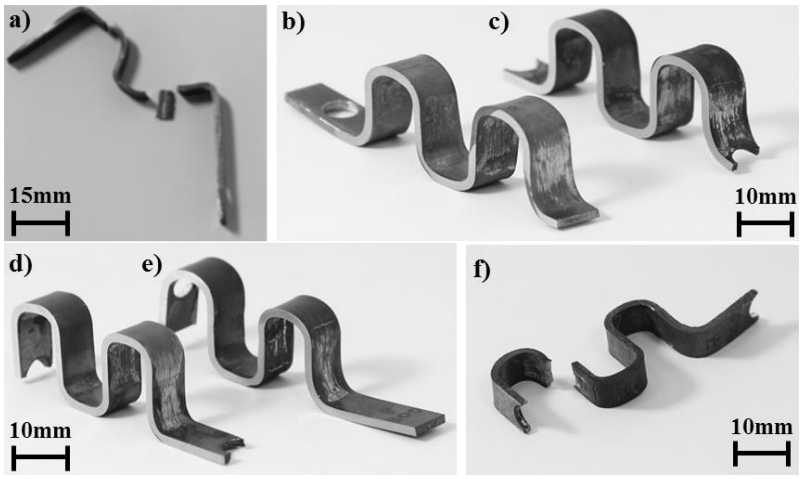

Figure 3-15. View of parts formed at room temperature (a), 600°C (b), 750°C (c), 850°C (d), 900°C (e) and 950°C (f).

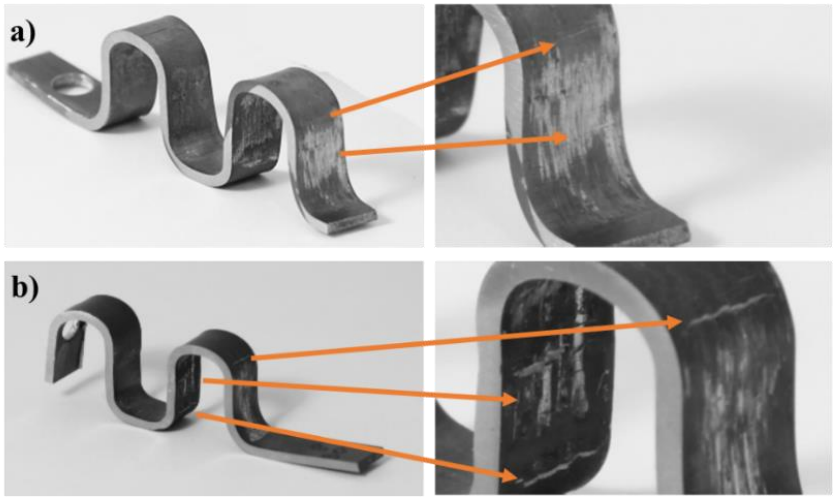

Figure 3-16. View of cracks of parts formed at 600°C (a) and 900°C (b).

3.5 Evolution of post-strength of components formed at different heating temperatures

Hardness tests were conducted on the formed parts to evaluate the post-form properties of the as-formed part, and the results are shown in **Figure 3-17.** The detailed hardness measurements of formed parts were presented in **Appendix A** The microstructure of the formed parts and the fraction of different phases are shown in **Figure 3-18** and **Figure 3-19**, respectively. It can be seen that the hardness values increased from 341HV10 at 750°C to 392HV10 at 950°C (**Figure 3-17**) due to phase transformation **(Figure 3-18, Figure 3-19),** which is in good agreement with the tensile test results (**Figure 3-7**). It could be observed that the microstructure of the formed part changed little after forming at temperature of 600°C. The fraction of the β-phase in the whole volume of the material and the dimension of its particles were almost the same as compared with the initial microstructure (**Figure 3-12**). When the heating temperature was increased, significant phase transformation occurred and the content of β-phase increased dramatically from 6.7% at 600°C to 58% at 950°C as shown in **Figure 3-17**.

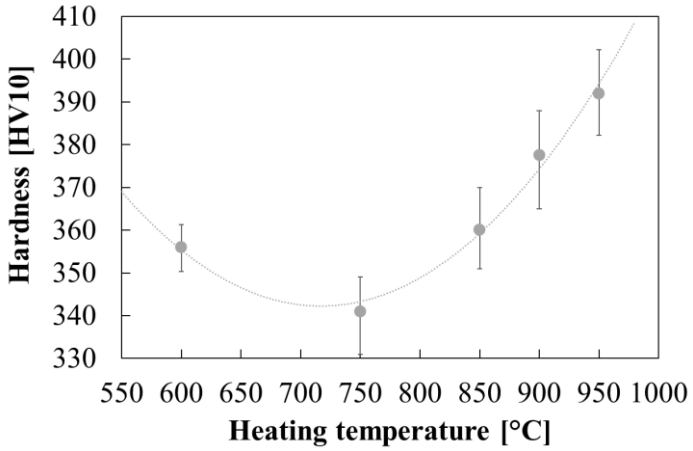

Figure 3-17. Post-form strength of components formed at different heating temperatures.

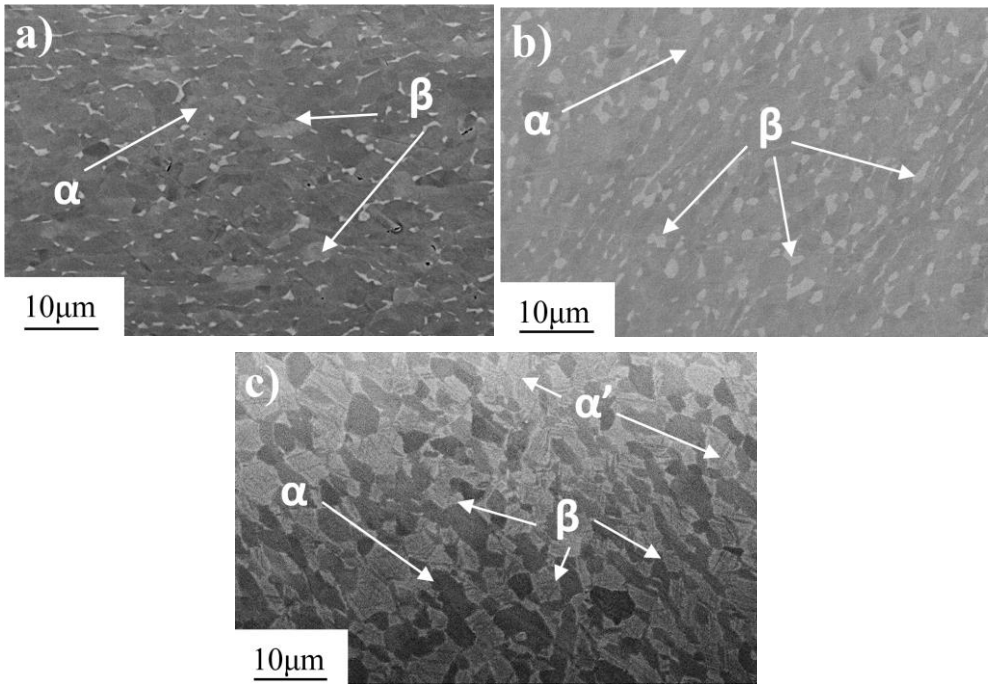

Figure 3-18. SEM microstructure images of the Ti6Al4V specimens formed at temperatures 600°C (a), 850°C (b), and 950°C (c).

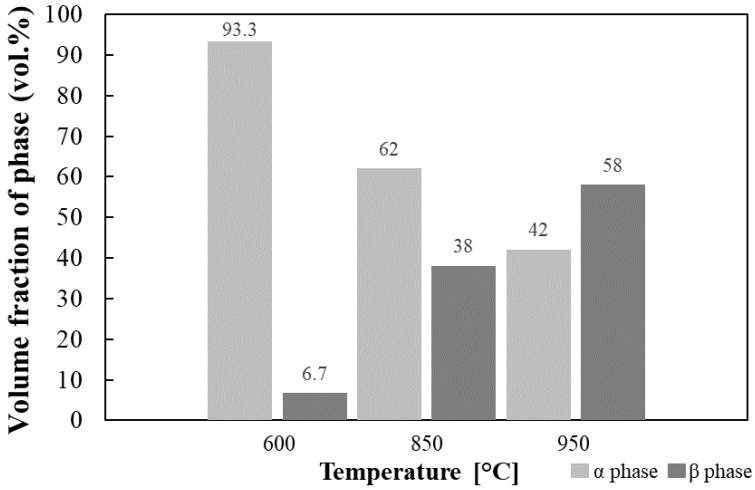

Figure 3-19. Evolution of α and β phase fraction during forming at different heating temperatures.

During thermo-mechanical processing of metals, recovery, recrystallization and phase transformation are three important microstructure evolution mechanisms. The SEM results above revealed that obvious phase transformation took place when the temperature was greater than 750°C. To further verify whether recrystallization occurred, Kernel Average Misorientation (KAM) map was captured by EBSD as shown in **Figure 3-20**, where the blue colour represents low values of misorientation while the green colour represents large values. It can be observed that the average KAM values tended to decrease with increasing heating temperature and the average grain size of α grains decreased first (**Figure 3-20**) and then increased (**Figure 3-20d**). The initial material (**Figure 3-20a**) before the forming process consisted of grains with relatively high KAM value. It indicates that the dislocation density of the initial material was high. When the forming temperature increased to 850°C (**Figure 3-20b**), many fine grains with low KAM value appeared, demonstrating the occurrence of recrystallization. At this stage, the temperature was high enough to initiate the recrystallization nucleation. With the temperature increasing to 900°C (**Figure 3-20c**), recrystallization became more obvious, leading to grain refinement. At the temperature of 950°C (**Figure 3-20d**), secondary α precipitated in the β matrix and the equiaxed α grains grew coarser. This is because significant phase transformation of α to β took place at 950°C, which led to the secondary α phase precipitates during the cooling stage. The high temperature also intensified the diffusion process and led to the merging of adjacent α grains (Jiao 2010), which resulted in the noticeable increase of the α phase grain size. Both refinement of microstructure and transformed β phase could improve the hardness at room temperature. Therefore when the temperature was lower than 900°C, the hardness increase may be caused by the recrystallization and phase transformation. At 950°C, the hardness increase was mainly caused by the phase transformation (Quan et al. 2015; Rollett, et al 2013). Both the possible grain growth during heating and the transformed β formed during the stamping process reduced the formability of the material, which led to the forming failure when the heating temperature was greater than 900°C.

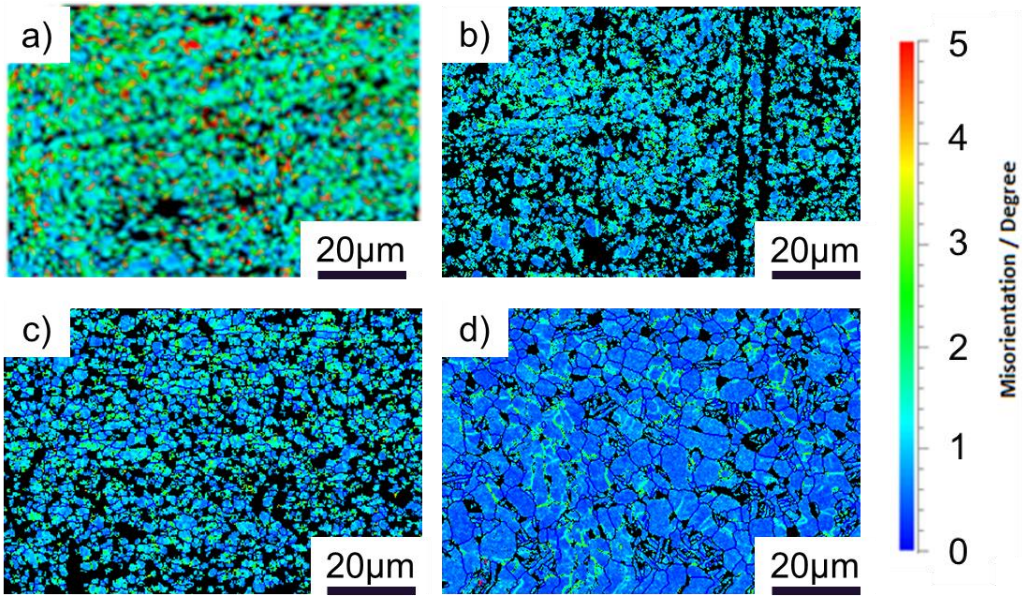

Figure 3-20. KAM maps of the material in as-received state (a) and after forming at different heating temperature values equal to: 850°C (b), 900°C (c) and 950°C.

3.6 Deformation mechanisms of titanium alloys under hot stamping conditions

One can find from both tensile and hot stamping test results that both the formability and post-form properties varied greatly with the deformation conditions, indicating that deformation mechanisms under different conditions may be different. Based on the obtained results, the mechanisms for the Ti6Al4V alloy under hot stamping conditions were summarized in **Table 3-3**. At heating temperature ranging from 600°C to 700°C, work hardening was observed (**Figure 3-7**) during tensile tests, and the microstructure morphology changed little after deformation, indicating that the main mechanism was recovery. At heating temperature values ranging from 750°C to 900°C, work hardening disappeared and material softening appeared during the tensile tests. After the deformation, the fraction of β phase and post-form hardness increased with the temperature; recrystallization of α grains was also observed, and therefore the main mechanism at this temperature range would be phase transformation and recrystallization. When the heating temperature was greater than 900°C, significant phase transformation of α to β and noticeable grain growth of α grains occurred, which increased the post-form hardness and simultaneously reduced the formability of the material. Therefore, the main mechanism at this temperature range would be phase transformation and recrystallization. Similar conclusions were also reported by Ning et al. (Ning et al. 2015).

Table 3-3. Deformation mechanisms for the Ti6Al4V alloy under hot stamping conditions

Temperature (°C)	600 - 700	750 - 900	> 900
Microstructure morphology evolution	Little change	Phase transformation of α to β and recrystallization of α grains	Phase transformation of α to β and grain growth of α grains
Post-form hardness	Decrease with the temperature	Increase with the temperature	Increase with the temperature
Main mechanisms	Recovery	Phase transformation and recrystallization	Phase transformation and recrystallization

3.7 Determination of processing windows for hot stamping of the Ti6Al4V alloy

It can be seen from the hot stamping tests, that the qualified part cannot be formed when the heating temperature was lower than 750°C or higher than 850°C, but can be formed between 750°C and 850°C as shown in **Figure 3-21**. The formability of the material was determined by both deformation conditions and the corresponding microstructure. Therefore, it is very important to fully understand the relationship between the forming process and microstructure evolution. The hot stamping process is a non-isothermal forming process, and the temperature varied in different stages as shown in **Figure 3-14**. The heating temperature was higher than the temperature before forming due to the temperature drop during the transfer. There would be microstructure evolution during the heating, soaking and

transfer stages before forming. Hence, the heating and soaking condition would determine the microstructure before forming, and the heating temperature and temperature drop during transfer would determine the initial forming temperature. The microstructures of the material at different stages formed at heating temperatures of 850°C and 950°C are shown in **Figure 3-21**. It can be seen that despite the considerable drop of temperature during manual transfer from furnace to forming tools during the forming process, the microstructure changed little during the transfer. Moreover, the microstructure of the material after heating and soaking was also very similar with that after forming, even at the heating temperature of 950°C. It can be concluded that both formability and post-form properties of the material were mainly determined by the heating temperature and soaking time. Therefore, both formability and post-form properties of the material could be tailored through the control of the forming process and material microstructure.

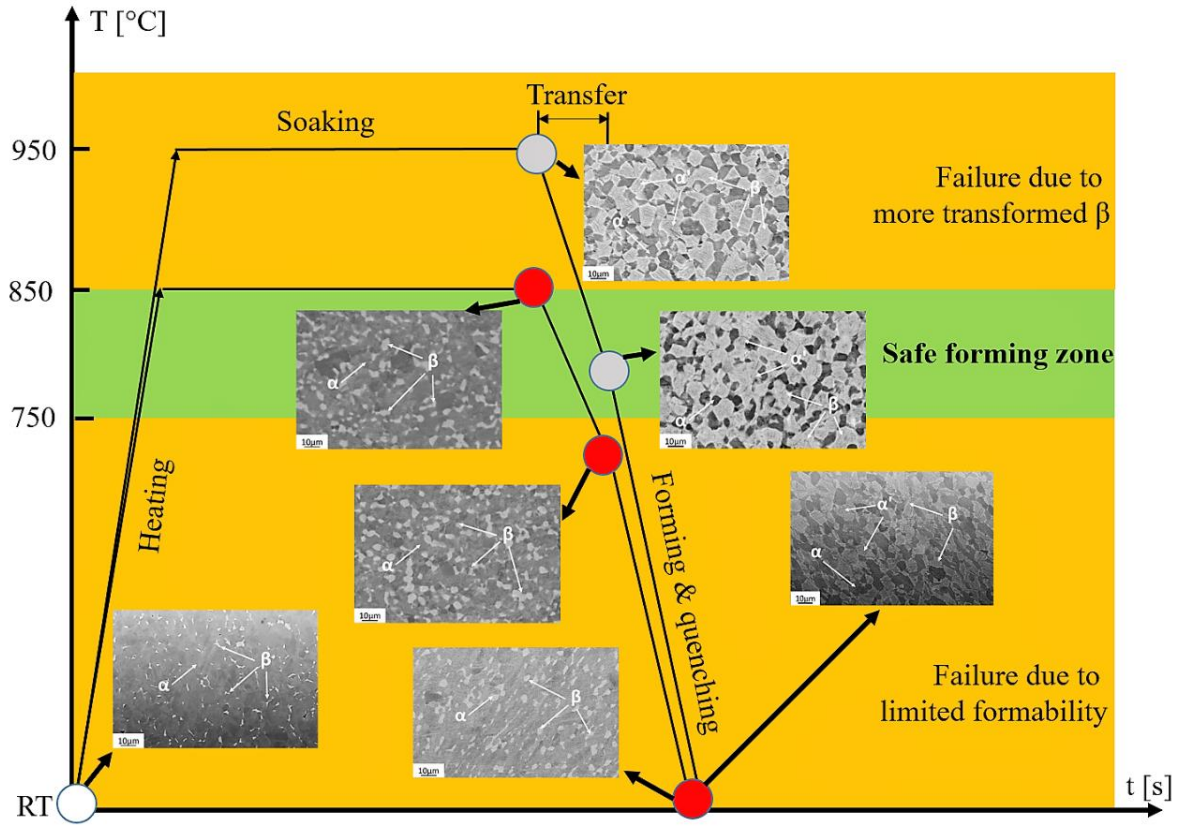

Figure 3-21. Evolution of microstructure during the forming process at 850°C and 950°C.

Control of the phase transformation during heating and improving the forming temperature are the two basic guidelines to further extend the forming window. The transformed β would impair the ductility of the material, therefore in order to reduce the phase transformation during heating, a reduction of soaking time should be considered. It will also prevent the precipitation of secondary α phase within the structure, when the temperature will be great enough to initiate the phase transformation. On the other hand, the formability of the material could also be improved by using warm forming tools to reduce the temperature reduction during the forming process. It also should be mentioned that at elevated

temperatures, oxidation became an obvious problem. This phenomenon reduced the formability and increased the hardness of material during forming. In order to prevent oxidation during the forming, the use of high quality oxidation resistant lubricant coating should be considered.

3.8 Conclusions

In this chapter, the formability and deformation mechanisms during a novel hot stamping process for titanium alloys using cold forming tools and a hot blank were investigated. During uniaxial tensile tests at temperatures from 600°C to 900°C with the strain rate of $1s^{-1}$, a satisfactory elongation of the material ranging from 30% to 60% was achieved at temperatures ranging from 750°C to 900°C. The main conclusions were formulated as follows:

- During deformation at temperatures from 600°C to 700°C, work hardening occurred. The hardening rate decreased with the increasing temperature resulting in the hardness reduction from 350HV10 at 600°C to 335HV10 at 750°C, indicating that the main deformation mechanism may be recovery. As the temperature increased to 900°C, phase transformation and grain refinement caused by recrystallization occurred resulting in the hardness increase to 352HV10.
- During the hot stamping tests, titanium parts were successfully formed at heating temperatures ranging from 750°C to 850°C. After forming at temperatures up to 750°C, cracks were observed on the component surface due to limited ductility of the material. On the other hand, the forming failed at heating temperatures above 850°C. It was found that heating to such high temperatures led to $\alpha \rightarrow \beta$ phase transformation. During the following transfer and forming, temperature reduction occurred. As a result of such a reduction, formation of transformed β reduced the formability significantly and caused failure. The post-form hardness distribution demonstrated the same tendency as that after uniaxial tensile test, which dropped from 357HV10 at 600°C to 341HV10 at 750°C indicating dynamic recovery of material and then increased to 392HV10 at 950°C due to phase transformation.
- The deformation condition had a great influence on both the mechanical properties and microstructure of the material. The post-form mechanical properties and microstructure were mainly determined by heating temperature and soaking time, hence formability and post-form properties of the material could be tailored through the adjustment of the forming process. In order to extend the processing window, measures such as reduction of soaking time, use of warm forming tools and oxidation resistant lubricants during the hot stamping process should be considered.

CHAPTER 4

4. Experimental and modelling studies on the Ti6Al4V alloy under hot stamping conditions *

The chapter aims to investigate the microstructural evolution and flow behavior of a titanium alloy (Ti6Al4V) under hot stamping conditions experimentally, and to model these parameters using the constitutive equations proposed. In order to determine the material behavior, uniaxial tensile tests were conducted on the Ti6Al4V specimens at different temperatures ranging from 750°C to 850˚C and at strain rates ranging from 0.1 to 10 s^{-1}. The material behavior was modelled using mechanism-based viscoplastic constitutive equations to replicate the material response of a two-phase titanium alloy Ti6Al4V under hot stamping conditions. Finally, the developed model's accuracy was validated by comparing to experimental uniaxial tensile tests and microstructural maps of the deformed alloy. Microstructural analysis revealed that the heating and soaking conditions are vital to the microstructure and post-form strength, whereas the plastic deformation during the hot stamping only has a negligible effect on both recrystallization and phase transformation due to the very short deformation time. The developed material model was implemented into the Finite Element (FE) simulation to study the deformation characteristics during the hot stamping process. The material model was verified experimentally through hot stamping of a demonstrator component, with good agreement achieved between the predicted and experimental results.

4.1 Experimental details - High temperature uniaxial tensile tests and microstructure characterization

Commercial Ti6Al4V titanium alloy was used for this study and uniaxial tensile tests were performed at elevated temperatures using a Gleeble 3800 thermo-mechanical testing machine. To analyse in details of the mechanical response and microstructural changes in the defined forming window, an additional set of uniaxial tensile tests was carried out. The mechanical properties of the titanium alloy were characterized at wider range of strain rates ranging from 0.1 to 10 s^{-1} and temperatures within the range from 750°C to 850˚C. Titanium specimens were heated at a higher and constant rate of 4˚C/s up to the test temperature and deformed immediately. After failure, the specimens were cooled to room temperature with an average cooling rate of 40˚C/s which was obtained by using air quenching pipes mounted in Gleeble chamber. The initial pressure of the compressed air was set as 2 bars in order to

* Chapter 4 is based on paper work - Kopec, M., Wang, K., Qu, H., Politis, D.J., Liu, J., Wang, Y., Kowalewski, Z.L. Wang, L., Lin, J., Experimental and modelling studies on Ti6Al4V under hot stamping conditions

obtain an average cooling rate of 40˚C/s. Evolution of microstructure during deformation was monitored via interrupted tensile tests and subsequent SEM analysis. The interrupted tensile tests were performed at a temperature of 850˚C. Specimens were deformed to strain values equal to 0.1, 0.3 and 0.7 at a range of strain rates (0.1 – 10 s^{-1}) and cooled immediately by water quenching after deformation. The microstructure of the deformed specimens was characterized by SEM by using the same methods described in chapter 3.3.1.

4.2 Determination of Ti6Al4V flow stress at elevated temperatures

The geometry of the tensile specimens made of the Ti6Al4V titanium alloy were presented in **Figure 3-1** and the initial thickness of specimens was 1.6 mm. The results of uniaxial tensile tests performed on the specimens for the evaluated temperatures and strain rates are shown in **Figure 4-1**. The ductility of the material increased with increasing temperature and decreasing strain rate. This phenomenon is attributed to the improvement of dislocation mobility and atom diffusion at high temperatures and low strain rates resulting in higher elongation and decrease in the peak stress. During deformation at high strain rate conditions (10 s^{-1}), ductility increased by 42% from 0.4 to 0.7 whereas at low strain rate conditions (0.1 s^{-1}), ductility increased by 30% from 0.78 to 1.1. As such, temperature effects on the ductility enhancement were more pronounced at high strain rate conditions. It can also be seen that peak stress decreased with increasing temperature and decreasing strain rate from 455 MPa at 750˚C to 120 MPa at 850˚C. At 750˚C (**Figure 4-1a**), the stress first reached a peak value, followed by a plateau, indicating that recovery may be the dominant softening mechanism (Takaki et al 2015). With the increasing temperature (for example at 850˚C) (**Figure 4-1c**), the stress first reached a peak value, followed by a gradual decrease, indicating that dynamic recrystallization may be the dominant softening mechanism. During deformation under lower strain rates, a sufficient deformation time for diffusion and dislocation polygonization is provided (Tan et al. 2015). Increasing temperature and decreasing strain rate result in an increase of elongation during deformation.

The reduction in flow stress with an increase in the deformation temperature and a decrease in the strain rate is caused by the presence of higher volume fraction of the β phase with a bcc crystal structure. Such higher volume fraction of the β phase lowers the flow stress as it has more slip systems than the hcp α phase (Rollett et al 2013). The larger number of slip systems promote the dynamic recovery. Additionally, the β phase was found to be more ductile at high temperature than the α phase, and thus, with the increase of its volume, the elongation of material increased accordingly. On the other hand, the increase of flow stress at high strain rates is also related to the high volume fraction of dislocations, which inhibit the movement of mobile dislocations and result in a resistance to the plastic deformation and subsequent higher flow stress requirement. Such material behavior was also reported by Souza et al. (Souza et al. 2015) .

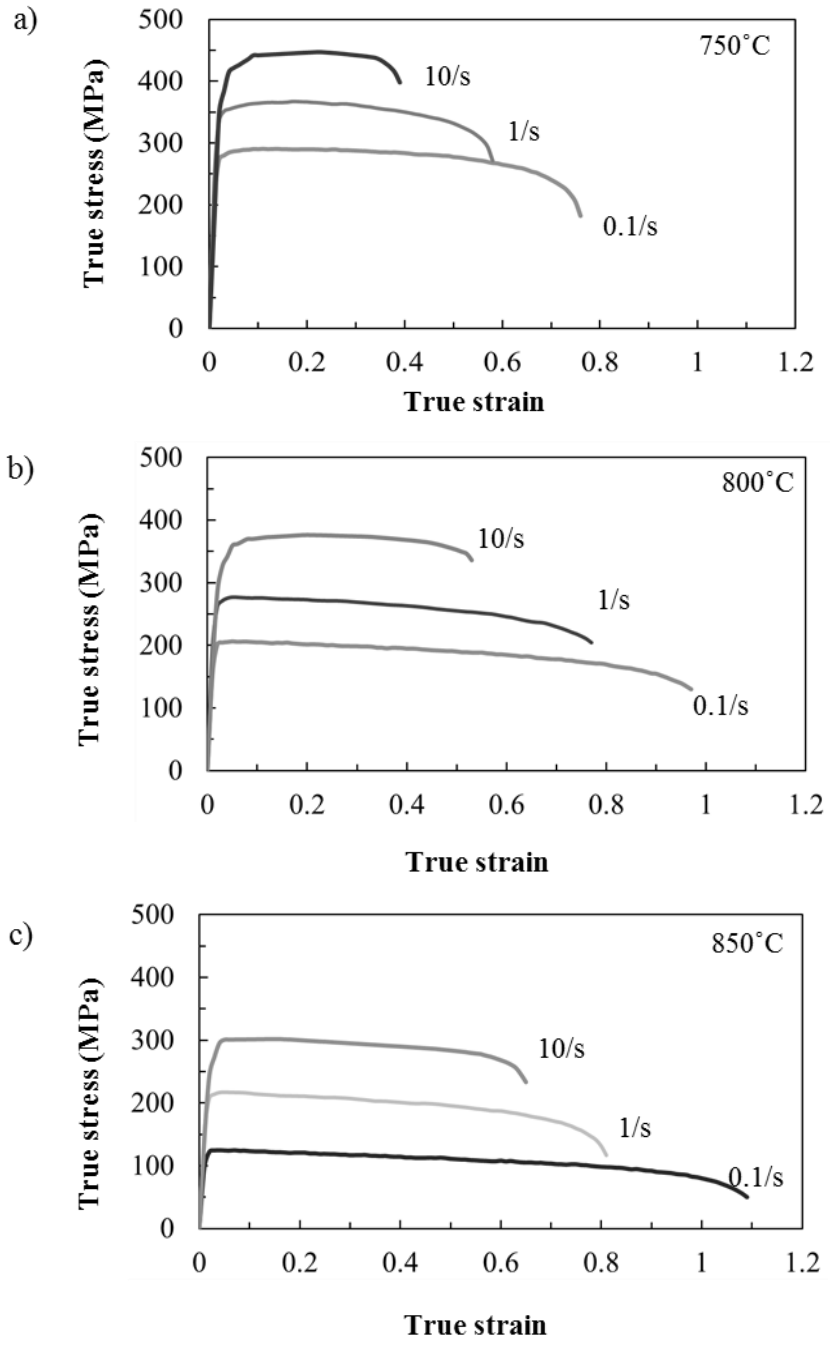

Figure 4-1 True stress-strain curves of the as-received material tested under different strain rate and temperature conditions.

It was reported in Ref (Kopec et al. 2018a) that after the deformation, the fraction of β phase and post-form hardness increased with the deformation temperature. When the heating temperature was 900°C and higher, significant phase transformation of α to β and noticeable grain growth of α grains was observed. Such behavior resulted in increase of the post-form hardness and simultaneous reduction of the material formability. During feasibility studies of hot stamping of the Ti6Al4V alloy reported by authors elsewhere (Kopec et al. 2018b), the qualified part can be formed between 750°C and 850°C thus the temperature of 850°C was selected as optimal for hot stamping of full scale component.

Therefore, microstructure evolution during the deformation at 850°C was studied in the following study. In order to maintain the initial grain size during forming at such high temperature, relatively high strain rates during deformation should be used during the process.

4.3 Microstructure evolution of the Ti6Al4V alloy during high temperature deformation

4.3.1 Phase transformation during high temperature deformation

It is widely reported that more phase transformation occurred with the increasing temperature for titanium alloys. More information about this could be found in Ref (Kopec et al. 2018). The microstructural evolution with strain is shown in **Figure 4-2**. **Figure 4-2a** shows the microstructure of a specimen heated to 850˚C, with a heating rate of 4˚C/s. After heating to 850˚C, a typical microstructure consisted of the finely transformed β (β_t) and primary α phases. During deformation at a strain rate of 1 s^{-1} (**Figure 4-2b**), additional deformation filaments characterized by deflated α phase among elongated β grain boundaries were observed. On the contrary, at the strain rate of 0.1 s^{-1}, elongated and intermittent β phase grains in α phase matrix were observed (**Figure 4-2c**). At such high temperatures (850˚C), some α phase dissolved through α to β transformation. The volume fraction of β phase in the specimens tested at 850˚C was approximately 42% and remained almost constant during deformation (**Figure 4-2**) indicating that phase transformation occurred mainly during the heating stage (Kopec et al. 2018). Based on above results, it could be concluded that deformation below β transus temperature within investigated range of strain rates did not influence the volume fraction of β phase due to relatively short time of deformation.

An evolution of the titanium alloy microstructure at 850˚C is presented schematically in **Figure 4-3**. The material initially containing 7% β phase was heated to the target temperature. During the heating and soaking stage, the fraction of β phase increased to 42% and slightly increased during forming as reported in a previous study of the authors (Kopec et al. 2018). After hot deformation at 850˚C, the microstructure of titanium alloy consisted of deflated α phase among elongated β grain being observed on the grain boundaries.

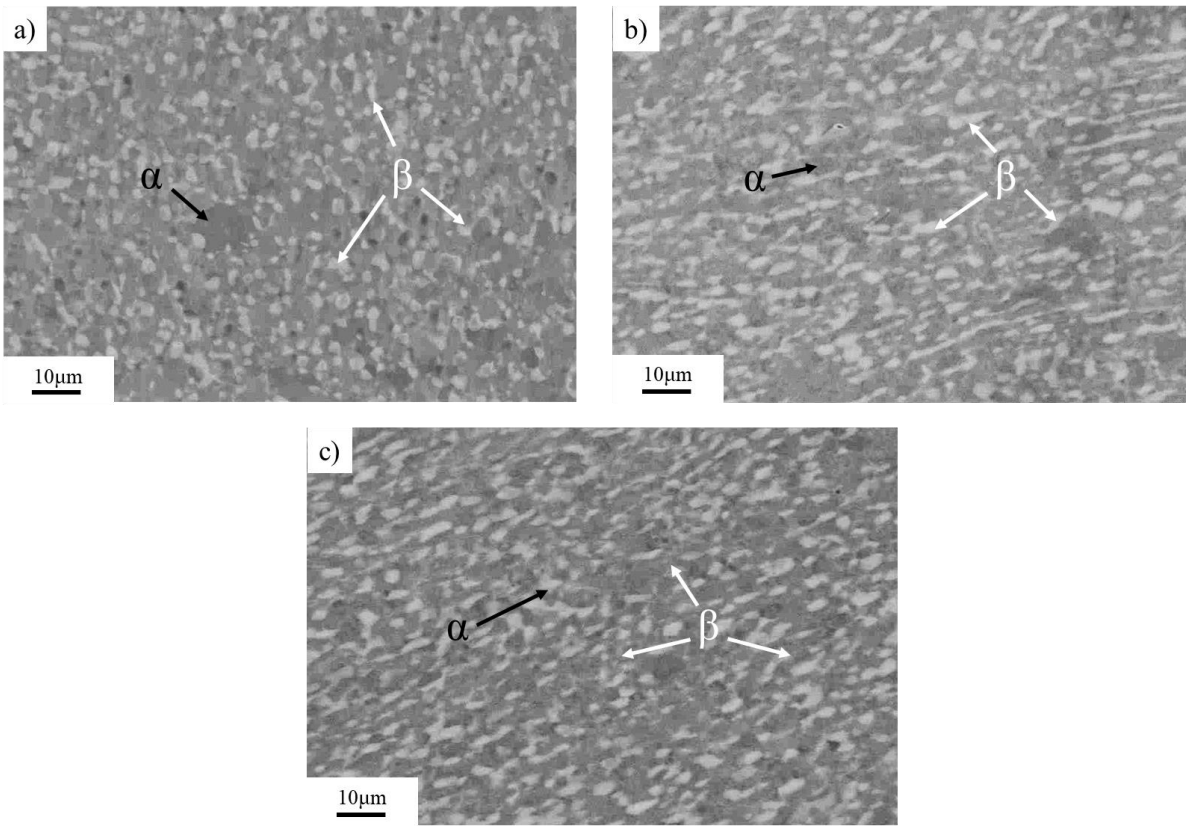

Figure 4-2. Microstructure of specimens heated to: (a) 850˚C, (b) 850˚C and deformed at strain rate of $1s^{-1}$ to strain value of 0.7, and (c) 850˚C and deformed at strain rate of $0.1s^{-1}$ to strain value of 0.7 (dark field - α phase, bright field - β phase).

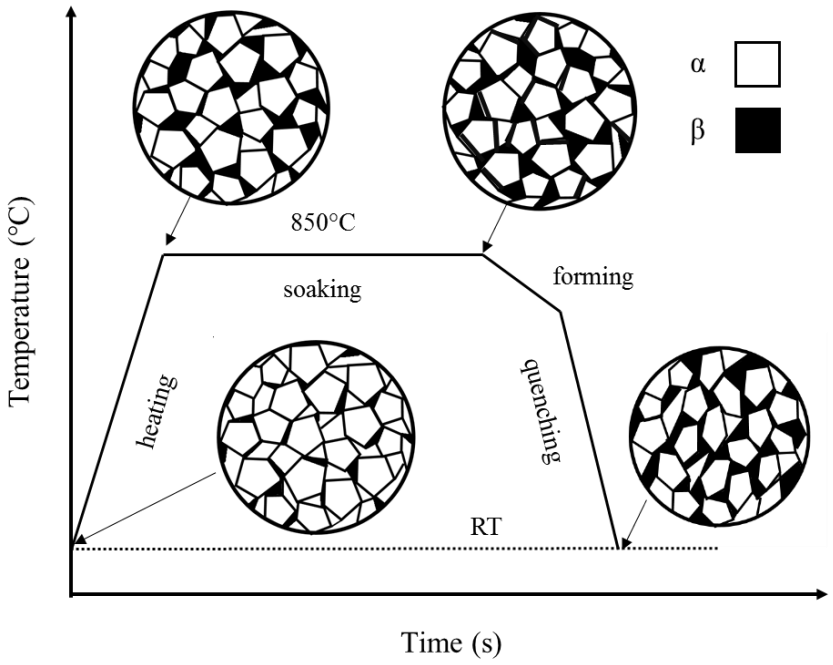

Figure 4-3. Schematic diagram of the microstructure evolution during a hot stamping process (Kopec et al. 2018).

4.3.2 Grain size evolutions during hot plastic deformation

The grain size evolution of the specimen deformed at 850˚C with different strain rates are presented in the form of grain boundary maps and grain size distribution graphs in **Figure 4-4** and **Figure 4-5**, respectively. It was confirmed that the high strain rate (above 1 s^{-1}) enables the microstructure of the material obtained after heating to be maintained without any change in the grain size. As expected, during deformation at the strain rate of 1 s^{-1} (**Figure 4-4a-b**), only slight changes of the grain size were observed. Even after deformation to a strain value of 0.7, the grain size remained at its initial value of 3 μm approximately.

On the contrary, during deformation at the strain rate of 0.1 s^{-1} with increasing deformation, the grain size gradually decreased due to the occurrence of dynamic recrystallization (**Figure 4-4c-e**). Deformation under lower strain rates provides a sufficient deformation time for diffusion and dislocation polygonization and accelerate the occurrence of dynamic recrystallization (Tan et al. 2015). Dynamic recrystallization phenomenon is characterized by the nucleation and growth of new fine grains during deformation. Such structure refinement and grain growth could be observed at relatively low strain rates. These changes to the material microstructure are common for titanium alloys formed by using hot forming technologies such as superplastic forming.

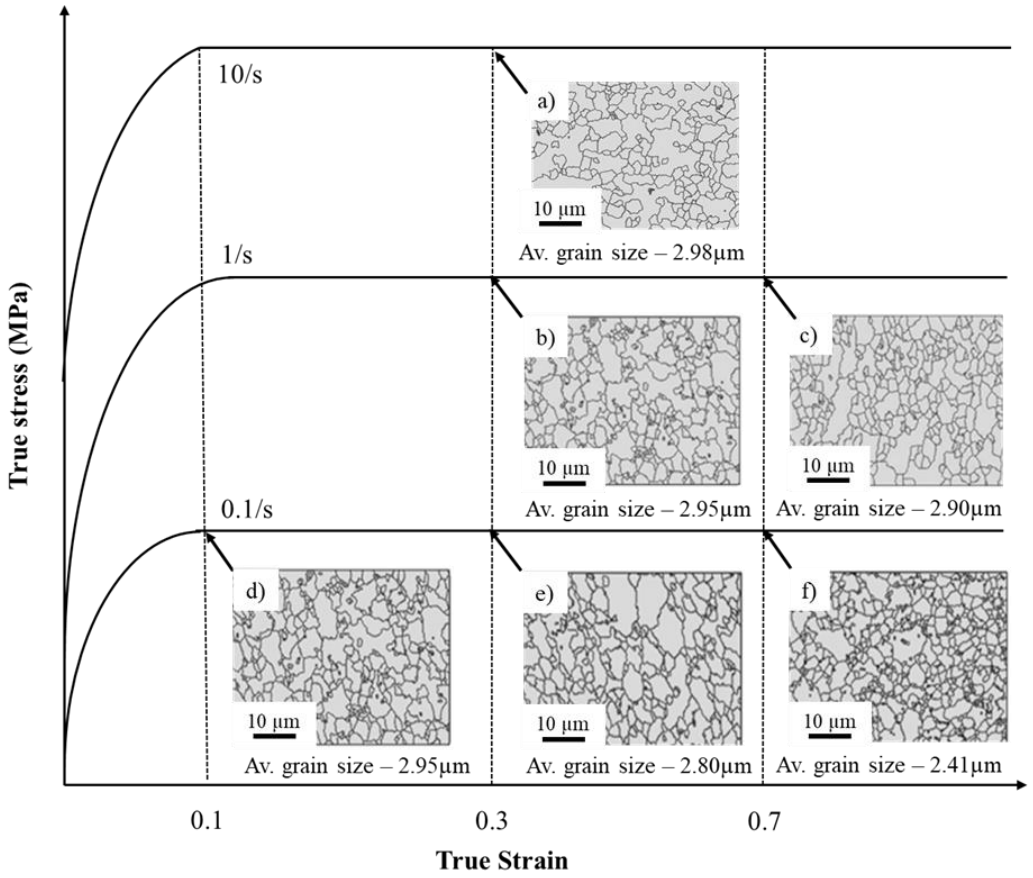

Figure 4-4. Grain size distribution maps of the specimens deformed at 850˚C to different strain values: (a) strain rate 10 s^{-1}, strain 0.3, (b) strain rate 1 s^{-1}, strain 0.3, (c) strain rate 1 s^{-1}, strain 0.7, (d) strain rate 0.1 s^{-1}, strain 0.1, (e) strain rate 0.1 s^{-1}, strain 0.3, (f) strain rate 0.1 s^{-1}, strain 0.7.

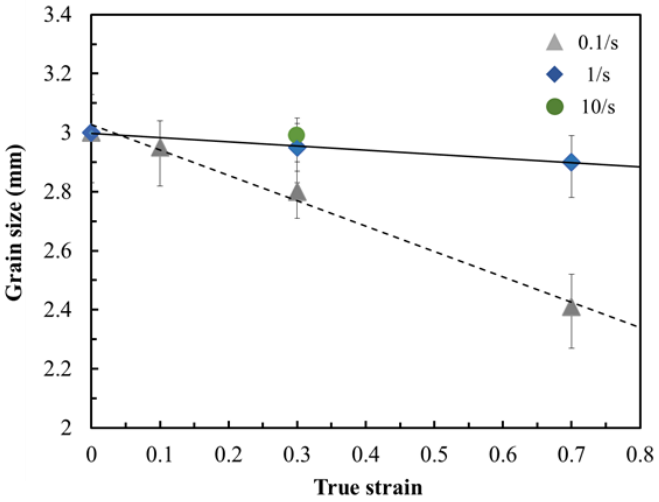

Figure 4-5. Average grain size evolution during deformation at 850˚C.

Based on the results captured, it could be concluded that the microstructure of investigated material is mainly determined by heating temperature. The deformation under temperature of 850°C affect the morphology of β phase, but not its volume fraction. The effect of strain rate on microstructure is more pronounced as a slight drop of average grain size was observed during deformation at strain rate of $0.1s^{-1}$. Such a drop of average grain size was determined by occurrence of dynamic recrystallization resulting in growth of new, fine grains. Deformation under strain rates ranging from 1 to $10s^{-1}$ did not affect the grain size considerably and allow to maintain its initial size.

4.4 Development of unified constitutive equations

The successful modelling of material behavior requires representative equations modelling the key mechanisms involved during deformation. The Johnson–Cook (JC) model and Arrhenius equation are widely used phenomenological models to describe material's stress–strain response. However, these models do not include physical phenomena occurred during titanium deformation such as material recovery or evolution of dislocation density. Based on the microstructural observations and mechanical response of material presented in previous subsections, the material behavior was modelled using mechanism-based viscoplastic constitutive equations to precisely replicate the material and mechanical response of a two-phase titanium alloy Ti6Al4V under hot stamping conditions. In order to improve the accuracy of the model, the behavior of both phases was modelled separately. For metal stamping processes, the viscoplastic flow behavior for both α and β phases can be expressed using Eq. (1):

$$\dot{\boldsymbol{\varepsilon}}_{\boldsymbol{p}} = \left(\frac{\boldsymbol{\sigma - H - k}}{\boldsymbol{K}}\right)^{\boldsymbol{n}} \tag{1}$$

where $\dot{\boldsymbol{\varepsilon}}_{\boldsymbol{p}}$ - plastic strain rate, σ - flow stress, H - stress due to dislocation hardening, k - initial yield stress, K - material parameter . In order to model material behavior of two phase Ti6Al4V titanium alloy with equiaxed initial microstructure accurately, the material model presented by Bai et al. (Bai et al.

2013) was modified by neglecting the spheroidizing.

The hardening parameter H defined in Eq.(1) is determined by dislocation density for both phases separately:

$$\boldsymbol{H_\alpha = 0.5 B_\alpha \bar{\rho}_\alpha^{0.5}} \quad (2)$$

$$\boldsymbol{H_\beta = 0.5 B_\beta \bar{\rho}_\beta^{0.5}} \quad (3)$$

where B is a material parameter. Titanium alloys exhibit the viscoplastic behavior at elevated temperature. The total flow stress during deformation at high temperatures consists of three parameters: the initial yield stress k, dislocation hardening parameter H and the stress caused by viscoplastic behavior which can be calculated by $\sigma - H - k$. The investigated Ti6Al4V titanium alloy is a two-phase material, and thus, different phases should be considered separately:

$$\boldsymbol{\dot{\varepsilon}_{p\alpha} = \left(\frac{\sigma_\alpha - H_\alpha - k_\alpha}{K_\alpha}\right)^{n_1}} \quad (4)$$

$$\boldsymbol{\dot{\varepsilon}_{p\beta} = \left(\frac{\sigma_\beta - H_\beta - k_\beta}{K_\beta}\right)^{n_2}} \quad (5)$$

Based on the high temperature indentation tests on the Ti6Al4V performed by Bai et al (Bai et al. 2013), it was found that the ratio of $\boldsymbol{\beta}$ yield stress over $\boldsymbol{\alpha}$ yield stress is approximately 0.8. As a consequence, it was assumed that $\boldsymbol{k_\beta = 0.8 k_\alpha}$.

Total viscoplastic flow behavior is expressed in the following way:

$$\boldsymbol{\dot{\varepsilon}_p = \dot{\varepsilon}_{p\alpha}\left(1 - f_\beta\right) + \dot{\varepsilon}_{p\beta} f_\beta} \quad (6)$$

The flow stress can be obtained according to the Hooke's law

$$\boldsymbol{\sigma = E(\varepsilon_t - \varepsilon_p)} \quad (7)$$

where ε_t is the total strain, ε_p is the plastic strain, and E is the Young's modulus.

The dislocation evolution involves dislocation accumulation and concurrent dislocation annihilation, which for different phases can be calculated by Eqs. (8) and (9).

$$\boldsymbol{\dot{\bar{\rho}}_\alpha = A_\alpha(1 - \bar{\rho}_\alpha)\dot{\varepsilon}_{p,\alpha} - C_\alpha \bar{\rho}_\alpha^{n_\alpha}} \quad (8)$$

$$\boldsymbol{\dot{\bar{\rho}}_\beta = A_\beta(1 - \bar{\rho}_\beta)\dot{\varepsilon}_{p,\beta} - C_\beta \bar{\rho}_\beta^{n_\beta}} \quad (9)$$

where $\bar{\rho_\alpha}$ and $\bar{\rho_\beta}$ is the normalized dislocation density for α and β phase, respectively, and $\boldsymbol{A_\alpha}$, $\boldsymbol{C_\alpha}$, n_α, $\boldsymbol{A_\beta}$, $\boldsymbol{C_\beta}$ and n_β, are the material parameters.

The Ti6Al4V titanium alloy used in the present research consists of primary HCP α phase, with a dispersion of BCC β phase within the structure. In this paper, the Eq. (10) was used to express the volume function of β phase fraction rate and temperature:

$$\boldsymbol{\dot{f}_\beta = 0.5X\left(f_\beta\right)^m (1 - f_\beta)^\gamma T} \quad (10)$$

where X and m are the material constants; T is the instantaneous temperature. The variation of β phase volume fraction with temperature is based on previously obtained experimental results. Experimental data of the β phase fraction and results computed by using Eq. (10) are presented in **Figure 4-6**, showing

a good agreement between the experiment and predicted results.

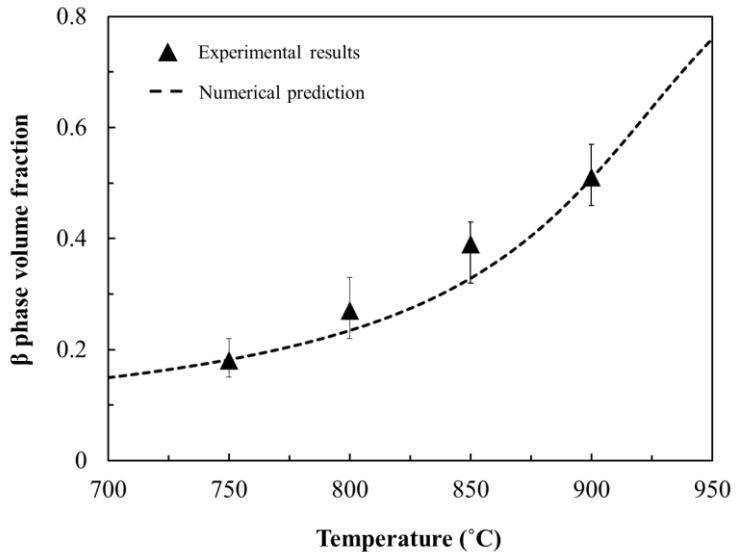

Figure 4-6. Evolution of β phase volume fraction.

The stability of β phase depends on the vanadium concentration and its size. The higher the temperature, the greater the α phase that transforms into β phase and the vanadium diffusing into β phase (Souza et al. 2015). As titanium alloys are highly temperature sensitivity, the flow behavior during deformation of the Ti6Al4V alloy at temperatures greater than 800°C depends on the combined effect of both dynamic recrystallization and phase evolution. However, by using the hot stamping technology (high strain rate deformation at 850°C), the dynamic recrystallization is not observed, thus, the material model was developed to predict the flow behavior within the work hardening/dynamic recovery regime.

4.5 Model calibration

In order to model material behavior under hot stamping conditions, the developed model does not include grain size evolution and softening caused by dynamic recrystallization. The set of constitutive equations (Eqs. 1 – 10) developed to characterise this behavior and the material constants calibrated via experimental data are presented in **Table 4-1.**

Table 4-1. Material parameters in the model.

Parameter	n_1 (-)	n_2 (-)	A_α (-)	C_α (-)	n_α (-)	A_β (-)	C_β (-)	n_β (-)
Value	1.007	1.636	26.975	0.390	4.162	5.991	2.847	20.243
Parameter	K_α (MPa)	k_α (MPa)	B_β (MPa)	B_α (MPa)	m (-)	X (-)	ɣ (-)	
Value	86.709	22.098	75.500	30.158	2.400	0.005	3.400	

The experimental data and computed results for the developed material model are presented in **Figure 4-7,** where the symbols represent the experimental results and the solid lines represent the modelling results. As can be seen, good agreement between the experimental results and theoretical calculations were achieved.

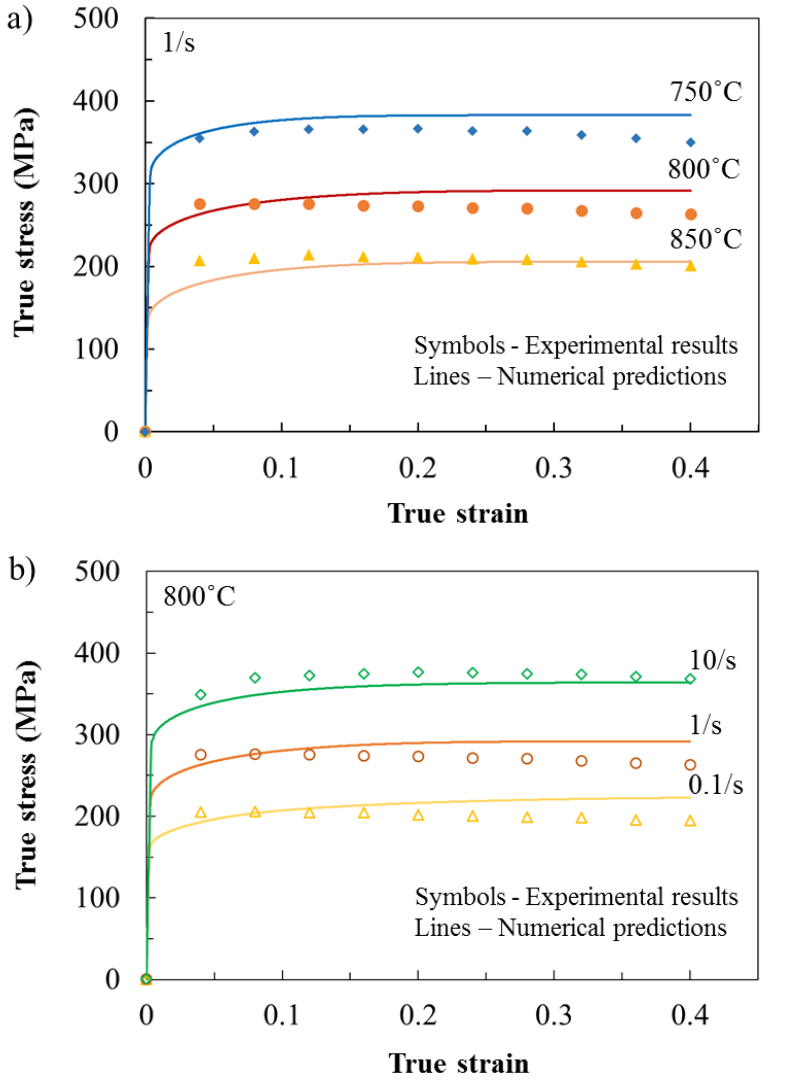

Figure 4-7. Comparison of the true stress - true strain curves obtained from the experiments and numerical calculations at: (a) different temperatures and (b) strain rates.

The above proposed constitutive equations for the Ti6Al4V alloy were developed based on the dominant modes of deformation observed during the high strain rate deformation. However, the response of the Ti6Al4V alloy is highly sensitive to deformation path. The set of constitutive equations proposed has been successful in modelling the stress-strain behavior of the material for the range of strain rates and temperatures encountered in titanium hot forming processes. A temperature and strain rate dependent viscoplastic material model (Eqs. 1 - 10) for the Ti6Al4V alloy were implemented in the

FE simulation as the material card for modelling the hot stamping of a wing stiffener demonstrator component. The results are presented in next chapter.

4.6 Conclusions

The main conclusions stemming from this chapter can be formulated as follows:

- The regime of hot stamping technology for the Ti6Al4V alloy has been determined, using uniaxial tensile tests at temperatures ranging from 750 – 850˚C and at different strain rates in the range of 0.1 – 10 s^{-1}. Optimal conditions were prevalent for the temperature of 850˚C at strain rates between 1 - 10 s^{-1}.
- Microstructural analysis indicates that deformation under high strain rate conditions and temperatures under 900˚C allow for the initial grain size of the material to be maintained. Moreover, the ductility and strength of the Ti6Al4V alloy was strongly dependent on the volume fraction of β phase, which was mainly determined by the heating and soaking stages.
- On the basis of microstructure evolution under high strain rate deformation conditions, the strain-stress relationships of the investigated Ti6Al4V titanium alloy for different temperatures and strain rates were predicted; good agreements between the experimental and theoretical results were obtained.

CHAPTER 5

5. Finite Element (FE) simulation of hot stamping of the Ti6Al4V wing stiffener*

In this chapter, the hot stamping process for a Ti6Al4V wing stiffener component is simulated using the FE commercial software PAM-STAMP. The FE simulation results were validated using experimental results obtained from forming tests. This chapter includes an introduction to the PAM-STAMP software, a description of simulation setup, verification of FE simulation and a discussion of simulation results.

5.1 FE simulation setup PAM-STAMP simulation setup for the Ti6Al4V wing stiffener forming process

In the present research, Finite element (FE) simulations of the hot stamping of the Ti6Al4V wing stiffener were conducted using the commercial software PAM-STAMP and the temperature and strain rate dependent material model developed above. As shown in **Figure 5-1**, the simulation model comprised of a punch, dies, blank and the blank holder sets. The tools, in particular the blank holder, punch and dies were modelled using rigid elements with all degrees of freedom restrained, except for the top blankholder and punch with vertical direction (z-direction) unconstrained. The mesh size used during present FE simulation was set as 1mm. In the present research, the lubricant used was boron nitride and a friction coefficient of 0.2 was chosen to account for surface interaction between the sliding sheet and the die assembly (X. Liu et al. 2017). The main simulation parameters are shown in **Table 5-1**.

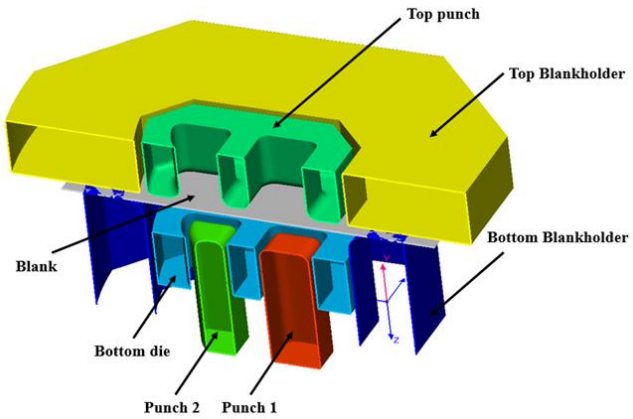

Figure 5-1. Pam-Stamp simulation model

* Chapter 5 is based on paper work - Kopec, M., Wang, K., Qu, H., Politis, D.J., Liu, J., Wang, Y., Kowalewski, Z.L. Wang, L., Lin, J., Experimental and modelling studies on Ti6Al4V under hot stamping conditions and Liu X., Kopec M., El Fakir O., Qu H., Wang Y., Wang L, Characterisation and validation of the interfacial heat transfer coefficient in hot stamping of titanium alloys - International Communications in Heat and Mass Transfer

Table 5-1. Main process and simulation parameters

Initial workpiece temperature (°C)	850
Initial tooling temperature (°C)	20
Punch speed (mm/s)	250
Friction coefficient (−)	0.2
Pressure dependent heat transfer coefficient (kW/m^{2}K)	1.6 – 6 (Liu et al 2020)

The PAM-STAMP software is a sheet metal forming simulation package which allows the numerical evaluation of cold and warm sheet metal forming processes. This software is widely used in the automotive and aerospace industries. In this work, PAM-STAMP was used to simulate the hot stamping of a Ti6Al4V wing stiffener component. The 'PAM-STAMP hot-forming module' was selected to simulate the forming process. The procedure of PAM STAMP simulation is presented in **Figure 5-2**:

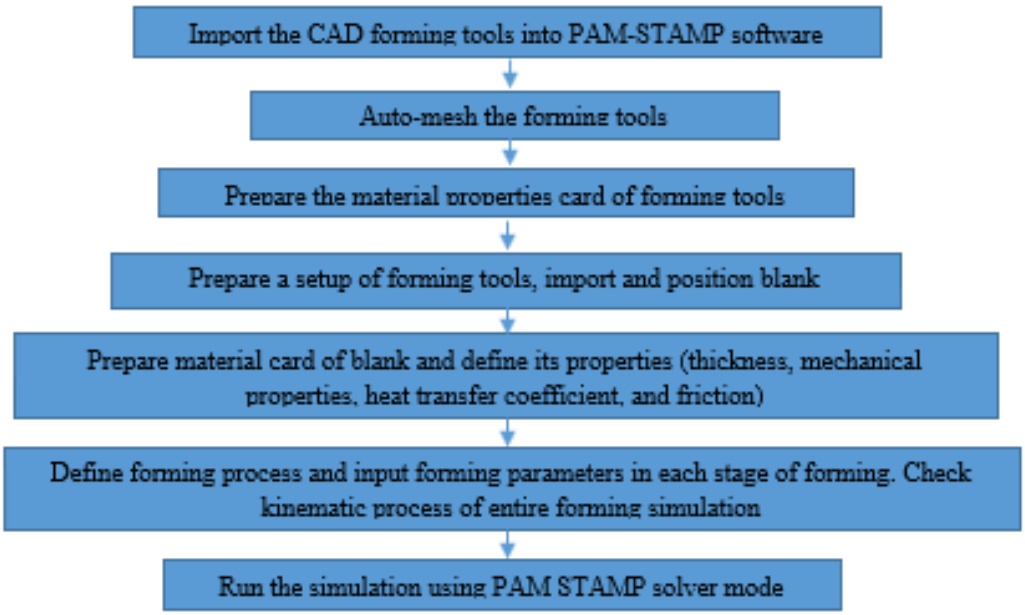

Figure 5-2. The procedure of PAM STAMP simulation

CAD models of forming tools were created by using Solidworks software and then exported to PAM STAMP software. Subsequently, forming tools were meshed automatically by using DeltMesh module. The size of mesh for the blank was obtain by using the PAM-STAMP mesh-size rule described as follows:

$$\boldsymbol{M = 0.5 \times (0.5T + F)}$$

where M is the mesh size, T is the blank thickness and F is the smallest radius in all imported models of the forming tools. According to presented equation, the blank mesh size was set as 1mm. In next step, material properties of forming tools and blank were defined using data presented in **Table 5-1**. The rolling direction of blank was defined as parallel to the longitudinal direction of the blank. In order to

identify the plastic anisotropy, Lankford's coefficients on the basis of uniaxial tensile tests (temperature of 850°C, strain rate of $1s^{-1}$) of specimens cut in three different rolling directions (0°, 45° and 90° angle to the rolling direction) were determined and were set as R_0=0.74, R_{45}=0.69 and R_{90}=0.76. The Lankford coefficients were defined as the plastic width strain divided by the plastic thickness strain in a tensile tested specimenafter unloading.

As all material properties were imported into software, each part of forming tool and blank were assembled and positioned as shown in **Figure 5-1**. Each part of forming tool were set as rigid body without consideration of any deformation during forming. To ensure the consistency of forming trails, forming tools as well as initial blank were in the same size as in real condition forming trials.

Simulation of the viscoplastic response of Ti6Al4V titanium alloys during deformation was based on imported data from stress-strain curves as functions of strain rate and temperature. In order to simulate deformation under hot stamping conditions, the forming temperatures limits were set from 750°C to 950°C and strain rates from $0.1s^{-1}$ to $10s^{-1}$. Stress/strain responses for different temperatures and strain rates were obtained from developed viscoplastic material model presented in previous chapter. Experimental flow stress curves were used to validate the viscoplastic material model. By using this model, the flow behavior of titanium was predicted and stress/strain curves were obtained. These curves were imported to PAM-STAMP software in form of material cards. Besides the material properties of blank and tools, the contact properties between them were defined as well. A constant friction coefficient of 0.2 was used between forming tools and blank for all forming stages. This value was determined by calibration of simulating and experimental results. Due to limitation of PAM-STAMP software, it was impossible to model friction coefficient with combined effect of contact pressure, sliding speed and temperature. In order to model such behaviors, the interfacial heat transfer coefficient (HTC) was introduced as functions of the gap between the blank and tools (before contact of these parts) and then pressure (after contact). These functions were developed and presented by (Liu et al. 2015).

To simulate the hot stamping process, the Hot Forming Process Macro was selected from PAM – STAMPs Process Macro database directory. By using this macro, each stage of forming process was defined. This included gravity stage (initial setup of blank on tools), holding stage (clamping the blank between forming tools) and stamping stage. The boundary conditions used in all forming were listed in **Table 5-2**.

The forming parameters in each stage of hot stamping process of the Ti6Al4V titanium alloy were simultaneously defined. In the gravity stage, the material was positioned on the bottom blankholder. In this stage, the gravity acceleration value was set to $9.81m*s^{-2}$. During holding stage, the top blankholder is clamping the bottom blankholder with the speed of 250mm/s. During stamping stage, initial blank was formed in two pressing stages. In the first stage, blank was deformed by using top punch only. In next stage, blank was deformed with two central punches positioned under the bottom die. Forming speed is determined by the speed of stroke set by user and its value is 250mm/s.

Table 5-2. Boundary conditions for forming stages.

Part / Forming stage	Gravity	Holding	Stamping
Top punch			Translation: X, Y Rotation: X, Y, Z
Top blankholder		Translation: X, Y Rotation: X, Y, Z	Translation: X, Y Rotation: X, Y, Z
Blank	Translation: unlocked Rotation: unlocked	Translation: unlocked Rotation: unlocked	Translation: unlocked Rotation: unlocked
Bottom blankholder	Translation: X, Y, Z Rotation: X, Y, Z	Translation: X, Y, Z Rotation: X, Y, Z	Translation: X, Y, Z Rotation: X, Y, Z
Bottom die			Translation: X, Y Rotation: X, Y, Z
Punches			Translation: X, Y Rotation: X, Y, Z

5.2 Verification of the FE simulation results of formed wing stiffener component

Hot stamping tests were performed for a demonstrator wing stiffener component formed at a speed of 250 mm/s and temperature of 850°C, where the feasibility of complex shaped forming was evaluated. To perform the tests, specimens of size of 200×65×1.6 mm were prepared. Tests were conducted on a 25 ton ESH single action press and wing stiffener forming tool designed by El Fakir et al (El Fakir et al. 2013) and presented in **Figure 5-3**. For the heating stage, the specimen was heated to the required forming temperature and soaked for 60 seconds in order to ensure the target temperature was reached, with the temperature monitored by thermocouples. Once heated, the hot blank was transferred to the cold tool, where the stamping process was activated immediately. The transfer time from the furnace to the cold die was controlled to be approximately 8 seconds and stamping tests were conducted at a forming speed of 250 mm/s. The blank was formed with the punch center aligned to the center of the blank to ensure an evenly distributed load was applied. Forming tests were repeated three times in order to evaluate the repeatability and reliability.

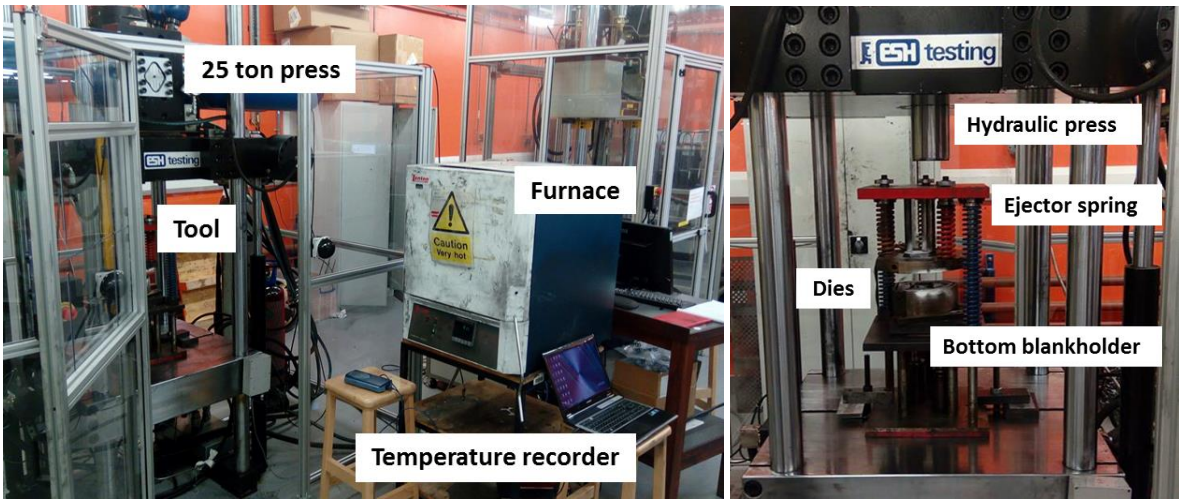

Figure 5-3 Stamping facilities and tool used to form wing stiffener component

Rectangular shaped specimens were used in the forming tests (**Figure 5-4**). Each specimen was prepared using a guillotine cutting machine with its longitudinal direction parallel to the rolling direction. The specimen surface was covered with lubricant to avoid the oxidation. Lubricant was also applied to the forming die and punch before testing to minimise the friction during the forming process. The temperature of the test-piece was monitored by thermocouple attached to its edge.

The simulation results were verified through comparisons of thickness reduction between experiments (**Figure 5-5a**) and simulations (**Figure 5-5b-d**). The experimental results were captured as measurements of thickness in two cross section lines (AB and CD) as shown in **Figure 5-5b**. The formed Ti6Al4V wing stiffener components were sectioned along cross sections using Electrical Discharge Machining (EDM) in order to obtain a material cross-section. The thickness along the cross section was measured every 5 mm by using optical microscopy. Three wing stiffener components were formed, cut and measured for each test condition. The results were presented in the form of thinning distribution as shown in **Figure 5-5c-d**. The thinning value displayed is calculated as follows:

$$\Delta \boldsymbol{l} = (\boldsymbol{t} - \boldsymbol{t_0})/\boldsymbol{t_0}$$

where t is the thickness measured in specific locations post deformation and t_0 is the initial thickness. Simulation results were obtained by exporting the thinning distribution from PAM-STAMP. **Figure 5-5b** shows the 3D thinning reduction contours from the FE simulation and **Figure 5-5c-d** shows the post-forming thinning reduction comparison between experimental and simulation results. Thickness reduction along the curvilinear distance was obtained by taking a 2D cross-sectional view perpendicular to the AB and CD sections. The same cross sections were selected in PAM-STAMP for comparison. Moreover, temperature evolution at two locations was recorded during forming and then compared to simulation results during the quenching stage (**Figure 5-6**).

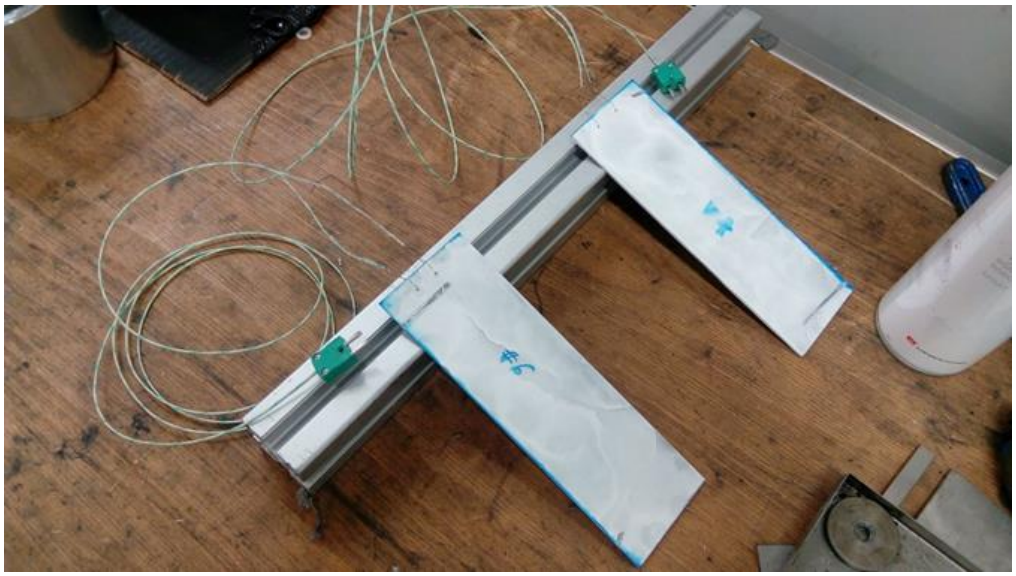

Figure 5-4 Specimens used to form wing stiffener component.

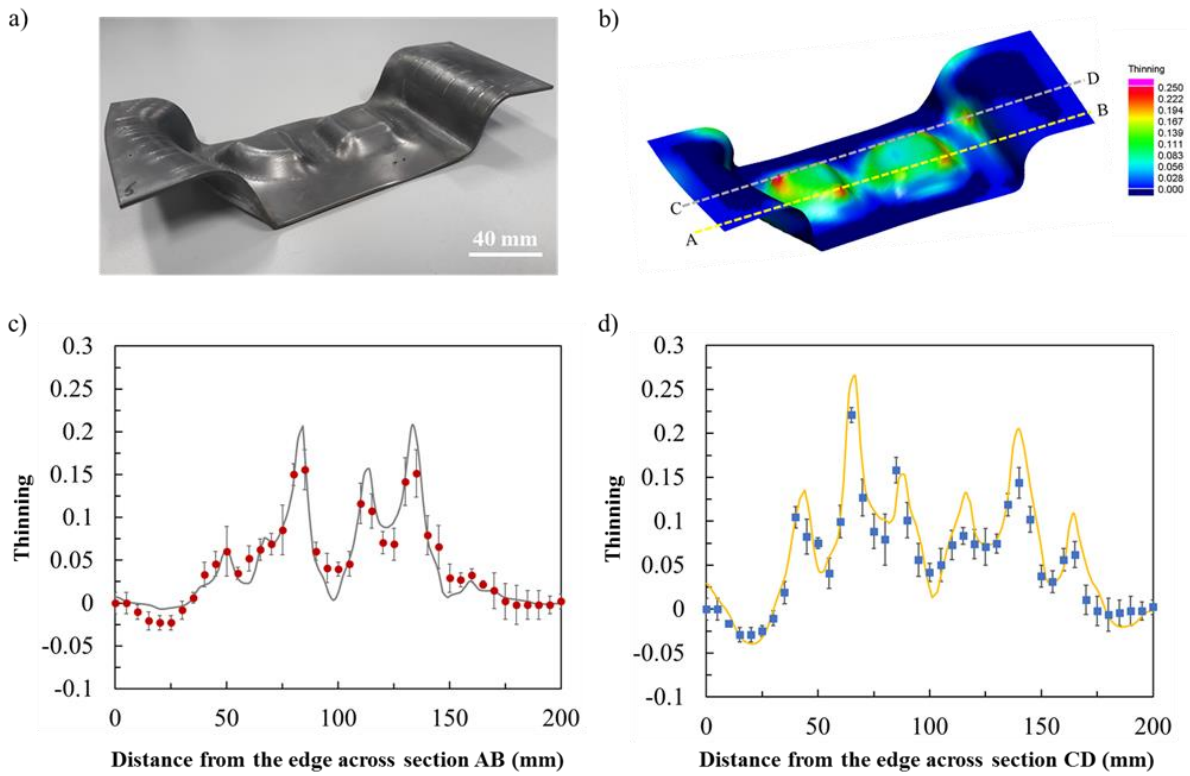

Figure 5-5. TC4 titanium alloy wing stiffener formed by hot stamping technology (a), 3D contours of thinning distributions obtained in the FE simulation (b), and thinning reduction comparison between experimental (symbols) and simulation results (line) for the Ti6Al4V wing stiffener (c – d)

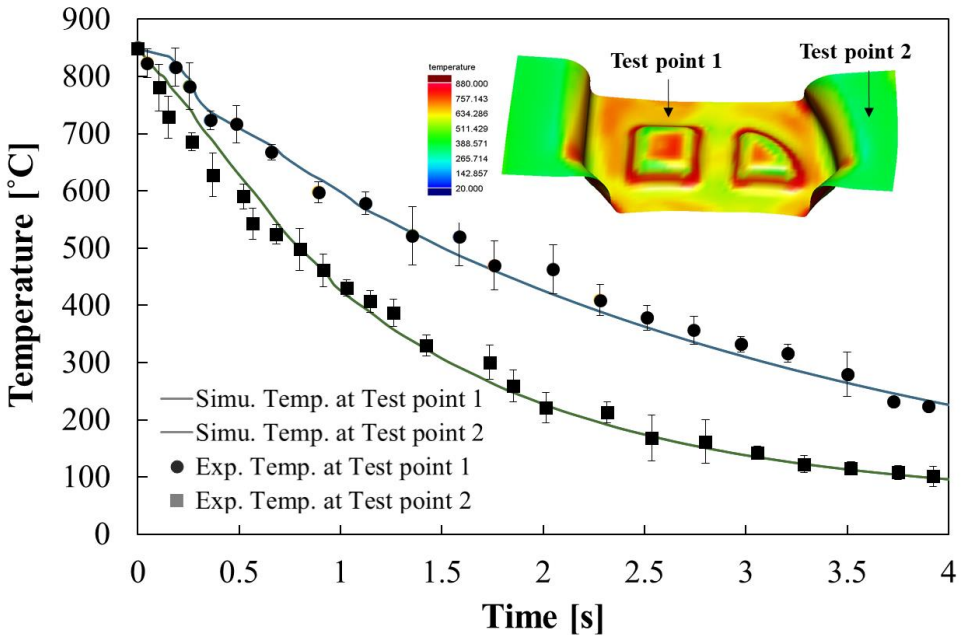

Figure 5-6 Comparison of temperature evolution during quenching stage between experimental (symbols) and simulation results (line)

As shown in **Figure 5-5c-d** and **Figure 5-6**, simulation and experimental results exhibited a very close agreement in terms of the thinning distribution. The largest degree of thinning was initiated around the corners of the central features (**Figure 5-7, 5-8**) which was also captured during thickness measurements

of the specimen's cross-sections. As the punch stroke increased during forming, the blank was first stretched from the central region. Meanwhile, the side area of the blank in contact with the blankholder was quenched rapidly, leading to a higher material strength in this region. Therefore, the severe plastic deformation region shifted towards the central region of the component where a higher blank temperature was maintained. Subsequent forming of the two central features led to the cold die quenching effect which would cause an increase in the thinning as presented in **Table 5-3**. As shown in **Figures 5-5c-d**, the thickness reduction at the corners of central features and the temperature evolution during quenching stage were predicted accurately by the FE simulation.

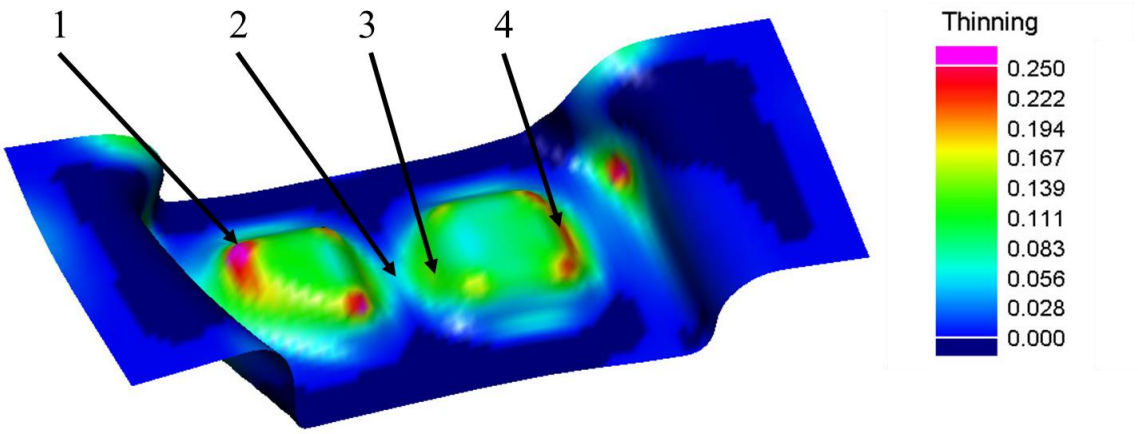

Figure 5-7 Selected regions for thining inspection

Table 5-3 Thining results for selected regions of part

Element	Location	Thining
1	Corner region	0.265
2	Flat region	0.019
3	Thin wall region	0.072
4	Edge region	0.185

Figure 5-8 show that the higher value of thinning was observed in region 1, which was located at one of the corners of the central feature of the wing stiffener component. Suchs high degree of thinning occurred in this region due to the complex geomerical features. Element 2 was located at the flat region of the formed part thus minimal thining of material occured. The thining was also observed on the side wall of central feature however higher values were observed on the edge, where the plastic deformation during forming occurred.

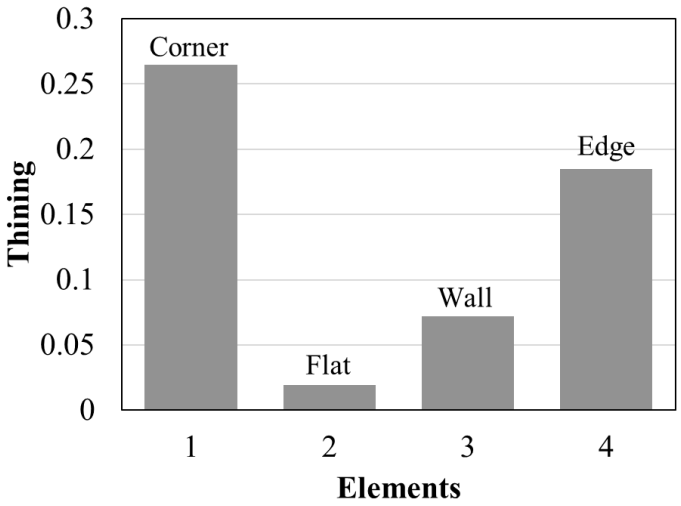

Figure 5-8 Comparison of thining for selected regions

Based on the results from FE simulation, the strain rate and temperature distribution map during the hot stamping process was obtained, as shown in **Figure 5-9**. It could be observed that during the forming at temperature of 850°C, most of deformation was accumulated within the strain rate range between $0.1s^{-1}$ to $10s^{-1}$.

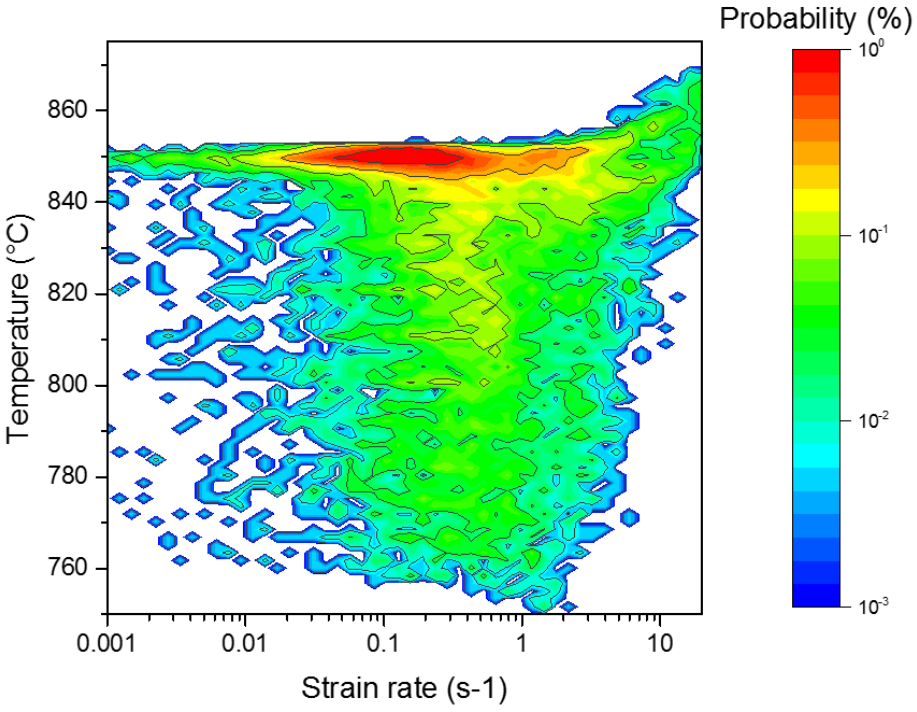

Figure 5-9 The strain rate and temperature distribution during the hot stamping process.

One of the main challenges in the hot forming of titanium alloys is to increase the efficiency of production through the minimization of the forming time and assuring the structural integrity of the component. Conventional hot forming technologies such as superplastic forming utilise low strain rates

(under $0.1s^{-1}$) and high temperatures (above 900°C). During deformation under such conditions, the initial microstructure of titanium alloys changed, thus, affecting the ductility and post form strength.

By using a technology that forms the component at high strain rate conditions and temperatures below 900°C, it is possible to obtain tailored microstructure by controlling the heating temperature. It has been proved that the post form hardness of formed part was reduced only by 5% in comparison to its initial strength. Therefore, hot stamping under high strain rate conditions could further improve the efficiency of hot forming technologies for titanium alloys by reducing the forming cycle time and forming temperature (Gao et al. 2019; Sirvin et al. 2017) thus it should be further studied.

5.3 Conclusions

The main conclusions stemming from this chapter were formulated as follows:

- A FE simulation model was made in accordance with the experimental parameters to study the deformation features of the Ti6Al4V alloy. PAMSTAMP-FE simulations of the hot stamping for forming wing stiffener components were successfully verified experimentally through the hot stamp forming of a demonstrator component and good agreements were obtained between the experimental and FE simulation results. Material thinning and temperature evolution results were accurately predicted.
- The thickness of the formed part at different locations were measured and compared with FE simulation results in form of thining graphs. It was found that the localised necking was initiated around the corners of the central features. Such thining of material was caused by the punch stroke increase during forming leading to stretching of the blank in its central region. During this stage of deformation, the side area of the blank was also in contact with the blankholder which led to rapid quenching and simulatious increase of materal strength in this region.

CHAPTER 6

6. Enhanced formability for titanium alloys by fast heating under FAST condition*

Hot stamping of titanium alloys requires a narrow and carefully controlled processing window, as defined in previous chapter (750°C - 850°C and 60 sec soaking), to successfully form components. Improper forming temperatures result in limited material formability, whereas temperatures approaching the β phase transus lead to a reduction of formability due to phase transformation, grain coarsening and oxidation during the long time heating and subsequent soaking stage. To solve this problem, the Fast light Alloys Stamping Technology (FAST) for titanium alloys was proposed in this chapter, where fast heating of a two-phase titanium alloy sheet with equiaxed microstructure was employed. High-temperature uniaxial tensile tests with varying heating rates and temperatures were conducted to study the effects of heating parameters on the formability and post-form strength of the material. The microstructure after high-temperature uniaxial tensile tests was characterised to reveal the evolution mechanisms of elongation and post-form strength. Forming of a demonstrator wing stiffener component was performed to validate this new process. The test results show that under FAST processing conditions, the phase transformation, grain coarsening and oxidation can be greatly reduced due to the short processing time. The difference between the observed microstructures after slow and fast heating became more pronounced with increasing heating temperature. When the temperature was greater than 850°C, the ductility was improved dramatically by ultra-fast heating. The post-form hardness increased gradually with increasing heating temperature at both slow and fast heating conditions, although the hardness value at slow heating conditions was greater than that at fast heating conditions. A complex shaped wing stiffener panel component was successfully formed from TC4 titanium alloy, demonstrating the great potential of the FAST in forming complex shaped titanium alloy components. The FAST technology promises to reduce the soaking-heating stage from several minutes to few seconds, and thus, be more efficient and economic in comparison to the hot stamping technology.

6.1 Material and experimental procedure

6.1.1 Material

A two-phase TC4 titanium alloy sheet with the thickness of 1.6 mm was employed in this chapter. The initial microstructure was equiaxed to guarantee the thermo-ductility, and the microstructure is shown in **Figure 6-**1, where the white region shows the β phase and the dark region the α phase. The initial

* Chapter 6 is based on paper work - Wang, K., Kopec, M., Qu, H., Politis, D.J., Liu, J., Wang, Y., Liu, G., Wang, L., Lin, J., Enhanced formability for titanium alloys by fast heating under FAST condition - Materials and Desgin

microstructure consists of equiaxed α phase and fine β phase. Both grain size and volume fraction of β phase are much smaller than that of the α phase in the initial microstructure. It should be noted that two-phase titanium alloys with lamella dominant microstructure, near β or β titanium alloys with β phase dominant microstructure are not suitable for this technology.

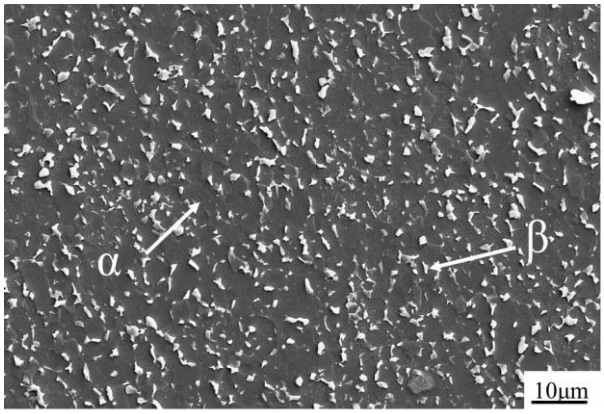

Figure 6-1. Microstructure of the as-received TC4 titanium alloy

6.1.2 High-temperature uniaxial tensile tests and post-form strength examination

To investigate the effect of heating history on the ductility, tensile tests were conducted on a Gleeble 3800 thermo-mechanical simulator to represent the forming processes. The specimens were firstly heated up to the soaking temperature (ranging from 850°C to 950°C) with different heating rates (from 0.5 to 150°C/s). After soaking for various times (0 and 2 min), the specimens were cooled down to 700°C, at which tensile tests were performed at a constant strain rate of 1 s^{-1} as shown in **Figure 6-2**. Each test was performed at least twice to ensure the repeatability. During the tests, a K type thermocouple was welded in the centre of the specimen to accurately control and monitor the heating temperature and heating rate.

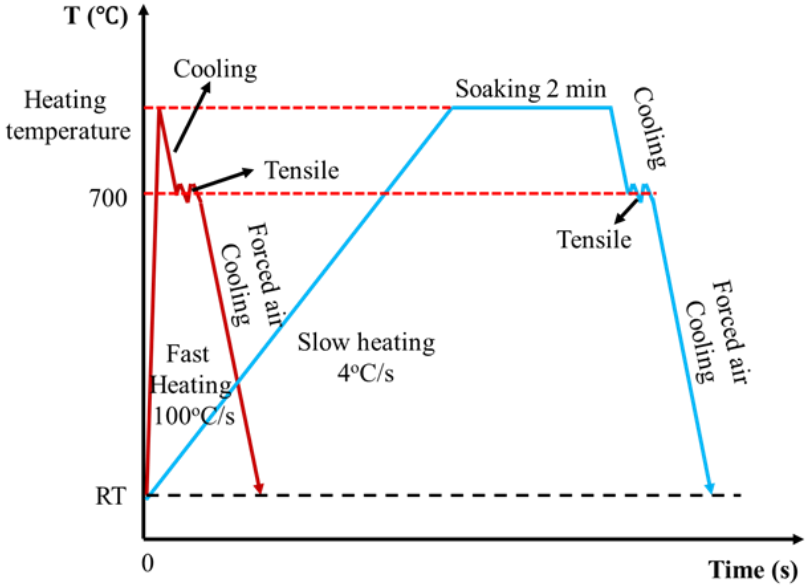

Figure 6-2. High-temperature uniaxial tensile tests program – investigation of the heating history effect on the ductility

To investigate the effect of heating rate on the ductility of the TC4, high-temperature uniaxial tensile tests with different heating rates at a heating temperature of 900°C were performed. During the tests, the specimen was first heated to 900°C with different heating rates, and when the temperature reached the targeted value, the specimen was then cooled to 700°C with a cooling rate of 60°C/s and deformed immediately to failure as shown in **Figure 6-3**. The specimen was subsequently cooled with pressured air to room temperature within 10 s after the failure.

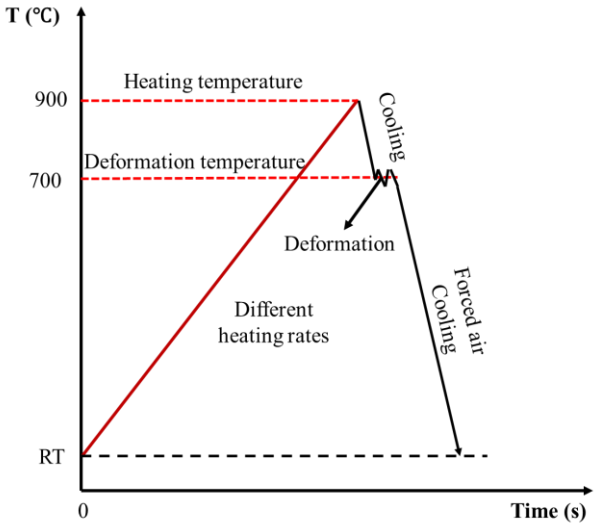

Figure 6-3. High-temperature uniaxial tensile tests: investigation of the heating rate effect on the ductility

The Vickers hardness values of the specimens after the uniaxial tensile tests and FAST forming were measured with the same conditions presented in Chpter 3.1.1. The specimens for SEM characterization were prepared by conventional metallographic procedures presented in Chapter 3.1.1.

6.1.3 Forming of the wing stiffener panel components

To verify the feasibility of the FAST technology and extend the forming processing windows for hot stamping, a complex-shaped wing stiffener component was selected as the demonstrator. A rectangular-shaped initial sheet with thickness of 1.6 mm was machined from the rolled blank with dimensions shown in **Figure 6-4(a)**, where the rolling direction was along the longitudinal direction. The geometry of the component is shown in **Figure 6-4(b)**. To avoid complications arising from optimizing the blank shape, a section of the component containing the most complex features was formed. Further details regarding the full-size wing stiffener can be found in (El Fakir et al. 2014).

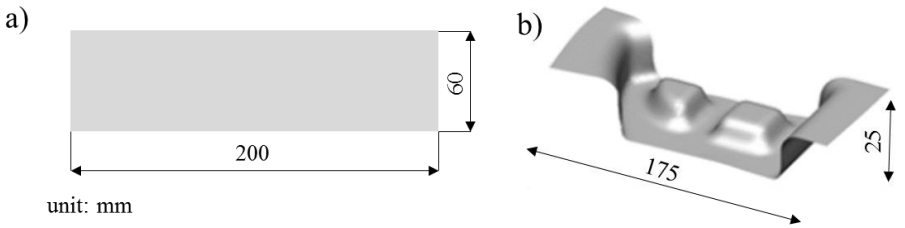

Figure 6-4. The dimensional information of the initial sheet (a) and formed component (b)

The forming tests were performed on a 25-tonne press. The schematic of the forming tool is shown in **Figure 6-5**. The sheet was rapidly heated by the use of contact heaters. The sheet was lubricated by boron nitride on all surfaces and was heated to 900°C at an average heating rate of 15°C/s. A K-type thermocouple was attached to the sheet to monitor the temperature. Once the temperature of the sheet reached 900°C, the blank was transferred from the hot platen to the forming die and immediately formed. The formed specimen was held for 5 s within the die. Then the formed specimen was removed from the stamping tool to allow further cooling in air to room temperature. After the forming, the material thinning and post-form hardness along the cross-section was measured.

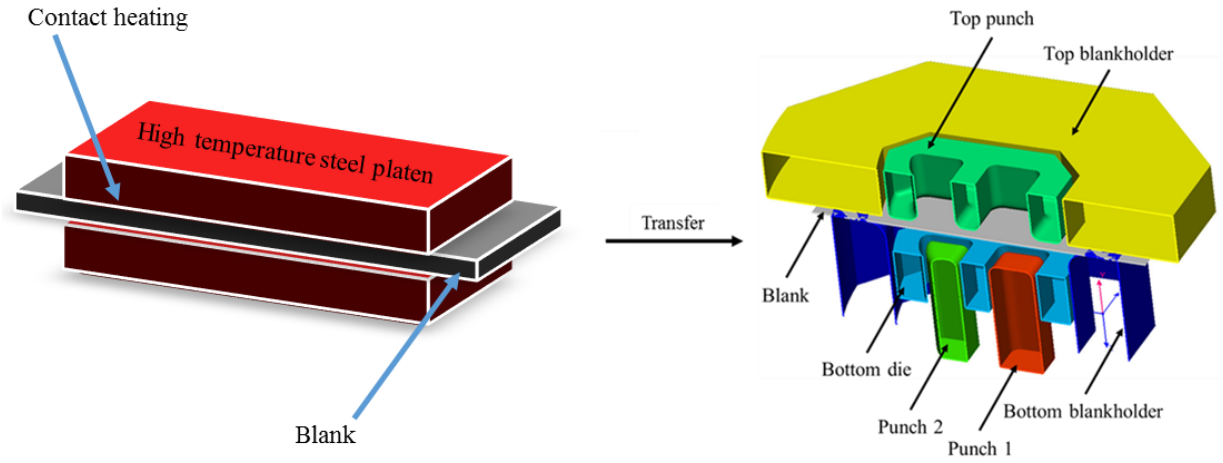

Figure 6-5. The schematic for FAST forming of titanium alloy wing stiffener

6.2 Effect of heating temperature on ductility and post-form strength of TC4 titanium alloy

The formability of the material decreased when the heating temperature was greater than 850°C during the hot stamping. Tensile tests under hot stamping and FAST conditions were first carried out to reveal the failure mechanisms and to investigate the effect of heating temperature on the formability and post-form strength of the TC4 titanium alloy. For the hot stamping condition, the specimen was first heated to the target temperature with a heating rate of 4°C/s, and was followed by soaking for 2 minutes, cooling to 700°C and finally deforming immediately to failure with a strain rate of 1 s^{-1}. The specimen was cooled with high pressure air to room temperature within 10 s after failure. As for the FAST condition, the specimen was first heated to the target temperature with a heating rate of 100°C/s, and when the temperature reached the target value, the specimen was cooled to 700°C and deformed immediately to failure with a strain rate of 1 s^{-1}. After failure, the same cooling rate and method was used, and the stress-strain curves are shown in **Figure 6-6**. It could be observed that the material had a higher failure strain but lower flow stress at FAST conditions, indicating greater ductility. Under the FAST condition, the flow stresses were almost the same; while at hot stamping conditions, the flow stress increased dramatically after heating to 950°C. The elongation and post-form hardness distribution is shown in **Figure 6-7**. It is obvious that the heating temperature affects the elongation significantly.

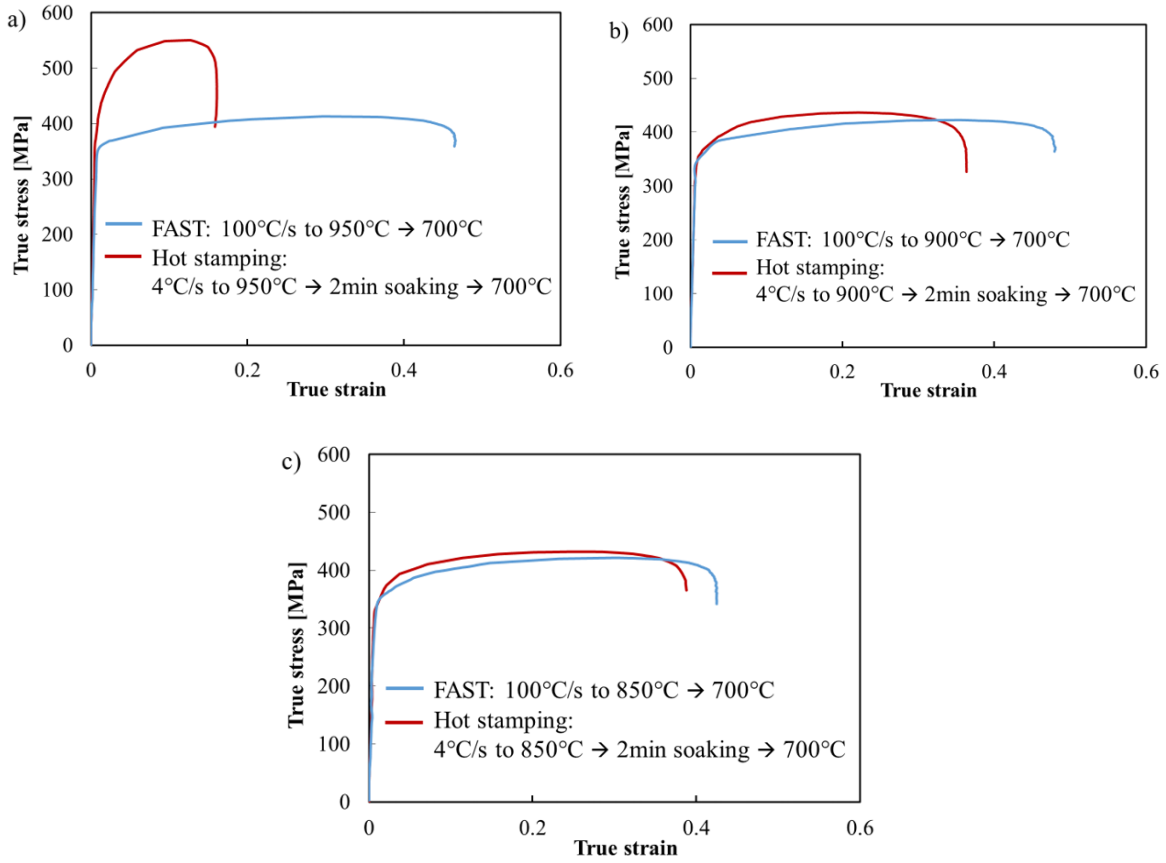

Figure 6-6. Effect of heating temperature a) 950°C; b) 900°C; c) 850°C on the ductility of investigated titanium alloy tested under both hot stamping and FAST conditions

The elongation decreased gradually with increasing heating temperature at hot stamping condition; while the elongation first increased and eventually decreased at FAST condition. The elongation enhancement obtained at FAST condition increased from 17% at 850°C to 241% at 950°C. The post-form hardness increased gradually with the increasing heating temperature at both hot stamping and FAST conditions, although hardness at hot stamping condition is greater than that at FAST condition. The high-temperature uniaxial tensile test results at hot stamping condition were in good agreement with previous forming tests results (Kopec et al. 2018)， where the decreasing ductility with the increasing heating temperature caused forming failure when the temperature was greater than 850°C.

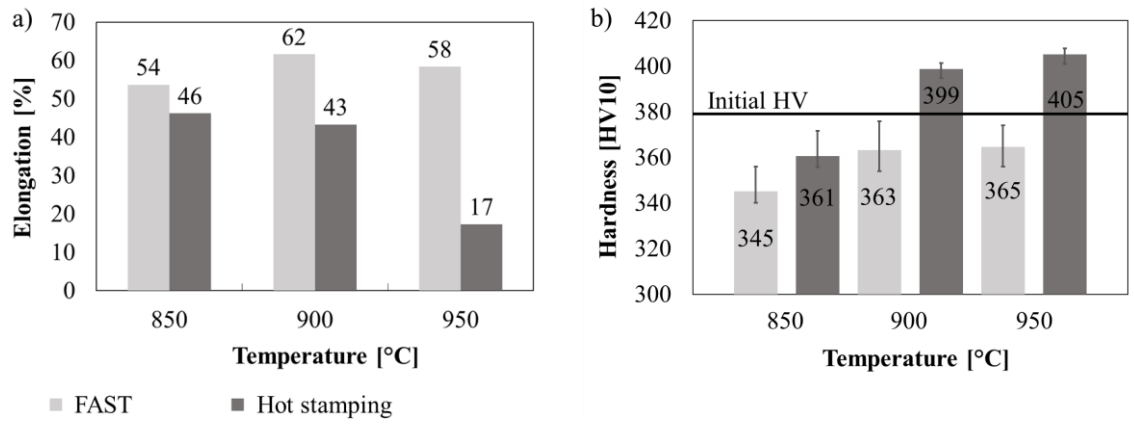

Figure 6-7. Effect of heating temperature on elongation (a) and post-form hardness (b)

To reveal the evolution mechanism of elongation and post-form hardness, the post-form microstructure near the fracture area and fracture morphology were characterised and the results are shown in **Figure 6-8** and **Figure 6-9** respectively. With the increase of heating temperature, the volume fraction and size of β phase increased. Under the FAST condition, the volume fraction of prior β phase at elevated temperature is much lower than that under the hot stamping condition. It can also be found that the difference between the microstructures after fast heating and slow heating became larger with increasing temperature. When the temperature was greater than 850°C, secondary α appeared under the hot stamping condition; while no visible secondary α could be found in the SEM figures under the FAST condition. This is because of the insufficient time for element diffusion under the FAST condition to generate more β phase, although the β phase grew coarser than the initial state (Semiatin et al. 2019). Therefore, the elongation enhancement by fast heating would be more obvious at higher temperature range (> 850°C) for titanium alloys at hot stamping condition.

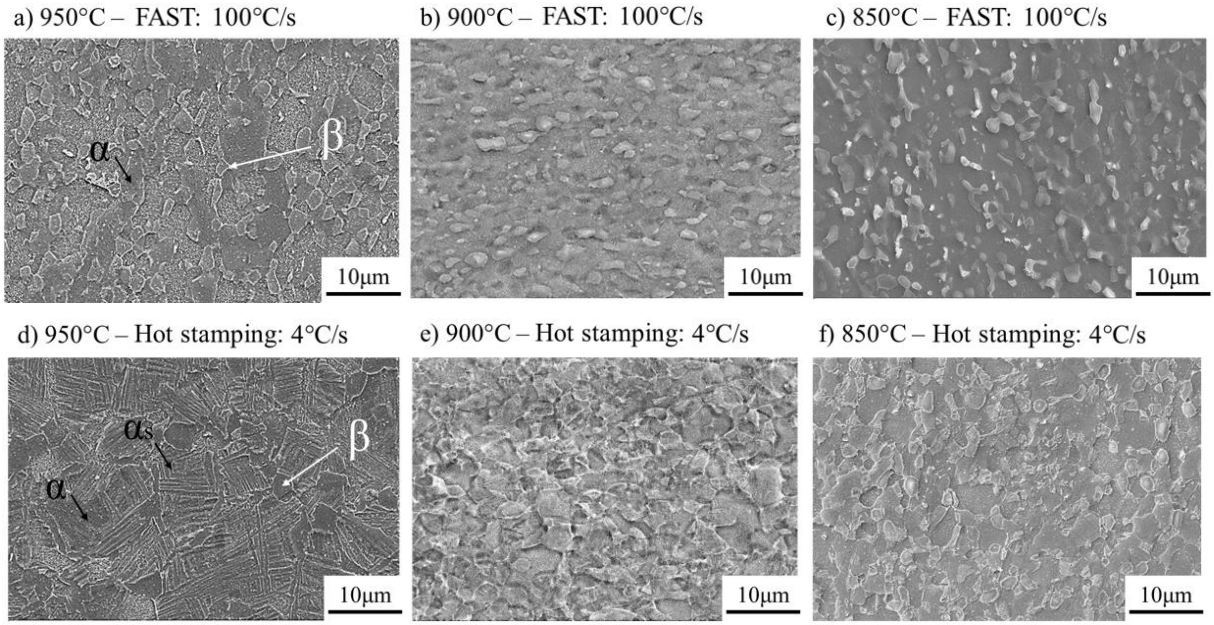

Figure 6-8. Microstructure of the investigated titanium alloy after deformation at different conditions

The fracture morphology demonstrated ductile fracture with various dimples at all conditions is presented in **Figure 6-9**. More larger and deeper dimples were observed in FAST condition than under the hot stamping condition, indicating that more plastic deformation occurred under the fast heating condition. However this difference reduced at 900 and 850°C which is in good agreement with the stress-strain curves. Based on the above results, it can be concluded that the fast heating could restrain the phase transformation of α to β during the heating and therefore improve the formability of the TC4 titanium alloy under hot stamping condition.

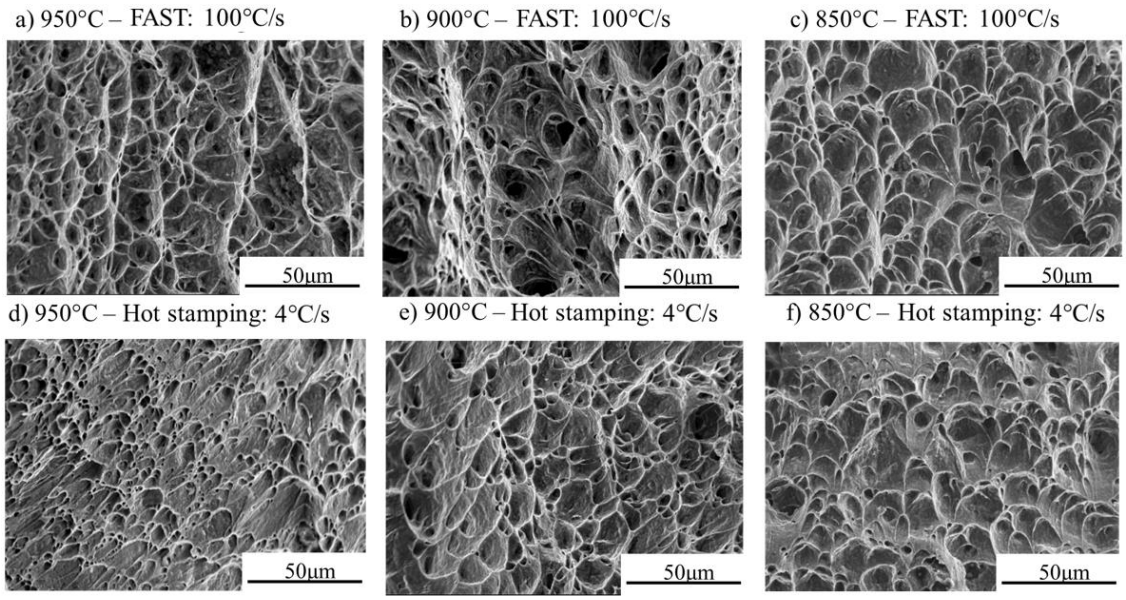

Figure 6-9. Fracture morphology of the Ti6Al4V alloy after deformation at different conditions

6.3 Effect of heating rate on the ductility and post-form strength of TC4 titanium alloy

From the above results, 900°C is an effective heating temperature for TC4 titanium alloy at FAST condition. The investigated material was tested under different heating rates conditions ranging from 0.5 to 150°C/s. It can be seen from **Figure 6-10** that heating rate affects the ductility of the material, where an increased heating rate increases the tensile elongation.

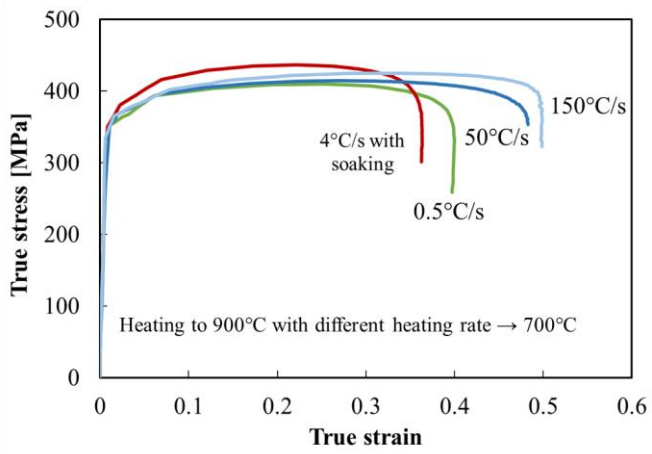

Figure 6-10. Stress-strain curves for the material heated to 900°C at different heating rates, quenched and tested at 700°C

The distribution of elongation-to-failure with different heating rates is shown in **Figure 6-11a**. The elongation increased from 49.2% at the heating rate of 0.5°C/s to 64.9% at the heating rate of 150°C/s, which was increased by 31.9%. However, the elongation enhancement decreased with the increasing heating rate. When the heating rate is greater than 50°C/s, the elongation exhibits negligible changes. The specimen demonstrating the lowest elongation was at a heating rate of 4°C/s followed by two minutes soaking. Therefore, it would be very important to avoid extensive soaking during hot stamping to guarantee formability. The post-form strength was evaluated by Vickers hardness and the result is

shown in **Figure 6-11b**. The post-form strength decreased with the increasing heating rate. Approximately 94.7% of the original hardness was retained even after deformation at a heating rate of 150°C/s. Therefore, it could be concluded that FAST could maintain the post-form strength.

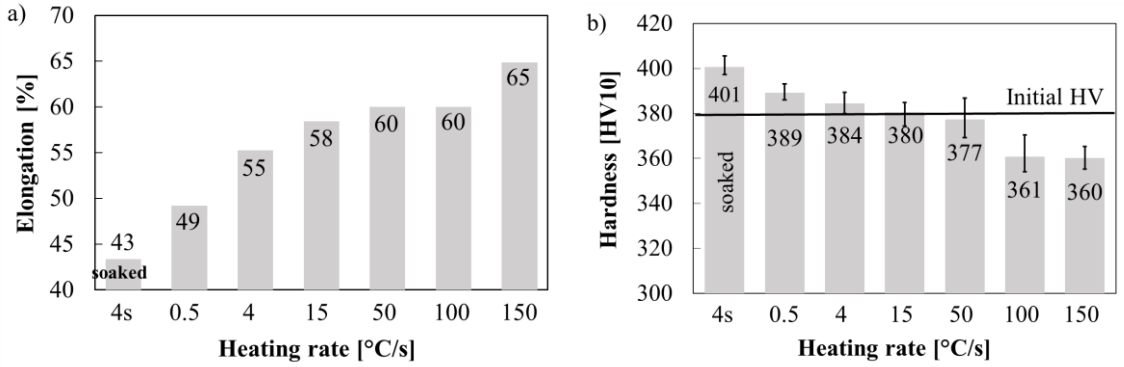

Figure 6-11. Effect of heating rate on elongation (a) and post-form hardness (b)

The microstructures near the fracture area after tensile tests are shown in **Figure 6-12**. It can be seen that both volume fraction and size of β phase increased with decreasing heating rate, and fine secondary α phase formed at heating rates of 0.5 and 4°C/s with 2 min soaking. Hence, it can be summarised that more phase transformation of α to β occurred during the hot stamping condition, and the β phase formed increased the hardness but decreased the ductility. Based on the above discussion, it was concluded that when the TC4 titanium alloy was heated at a high temperature range in the two-phase zone (e.g. > 850°C), the formability and efficiency will be improved under the FAST condition, although post-form strength may decrease slightly; under the hot stamping condition, the post-form strength may be improved, but this may negatively impact the formability and efficiency. Hence, an appropriate heating rate is very important. According to the elongation and post-form hardness distribution, heating rates ranging from 4°C/s to 50°C/s at 900°C is suggested for the investigated TC4 titanium alloy.

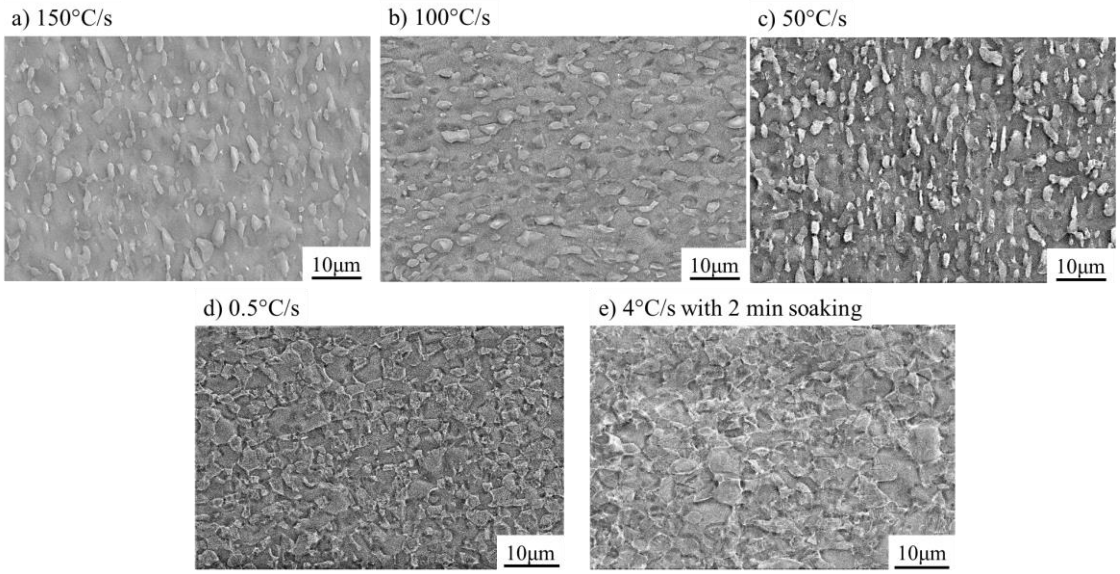

Figure 6-12. Microstructure near the fracture area of the specimen after tensile tests with a heating rate of 150°C/s (a), 100°C/s (b), 50°C/s (c), 0.5°C/s (d) and 4°C/s with 2 min soaking (e)

6.4 Validation of FAST by forming of a wing stiffener

To validate the feasibility of FAST for titanium alloys, forming tests of a wing stiffener were performed. According to the high-temperature uniaxial tensile tests, a relatively good forming condition was determined to be a heating rate ranging from 4°C/s to 50°C/s at 900°C, because in this range, the material exhibited a relatively good elongation and the post-form strength was similar with the initial material. In the actual forming, the blank was heated to 900ºC with an average heating rate of 15°C/s through contact heating. After reaching the target heating temperature, the blank was immediately transferred and formed. A qualified wing stiffener without visible cracks was successfully formed with fully formed local features as shown in **Figure 6-13**. However, when the initial sheet was soaked in the furnace for 2 minutes at target temperature of 900°C, the formed part failed due to the cracks occurring on the surface as shown in **Figure 6-13**. The longer heating time led to more phase transformation, grain coarsening and surface oxidation, which resulted in the cracks. In order to investigate the post-form hardness of the as-formed part, hardness tests were conducted on wing stiffener shaped components. Hardness measurements were performed in the longitudinal direction of formed parts as shown in **Figure 6-14**. The post-form hardness distributed uniformly along the longitudinal direction and the average value was 370HV±10, which was almost the same as the initial material.

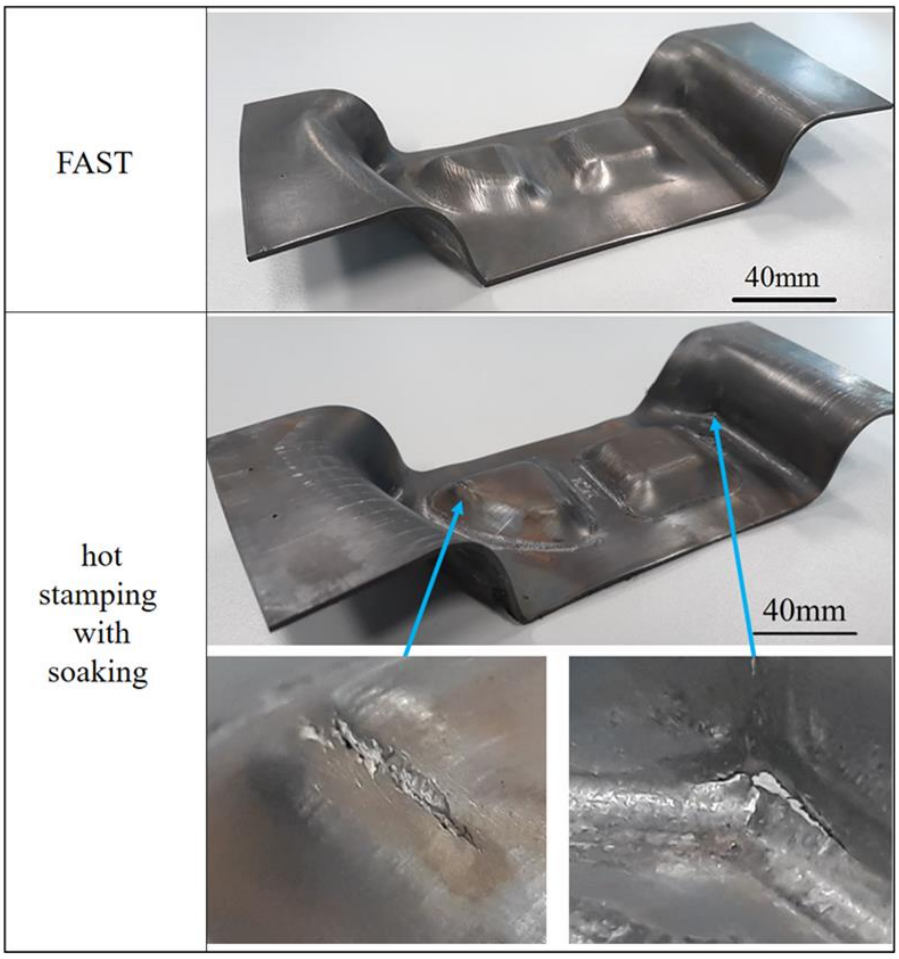

Figure 6-13. Comparison of parts formed by FAST and hot stamping with soaking (heating temperature 900°C)

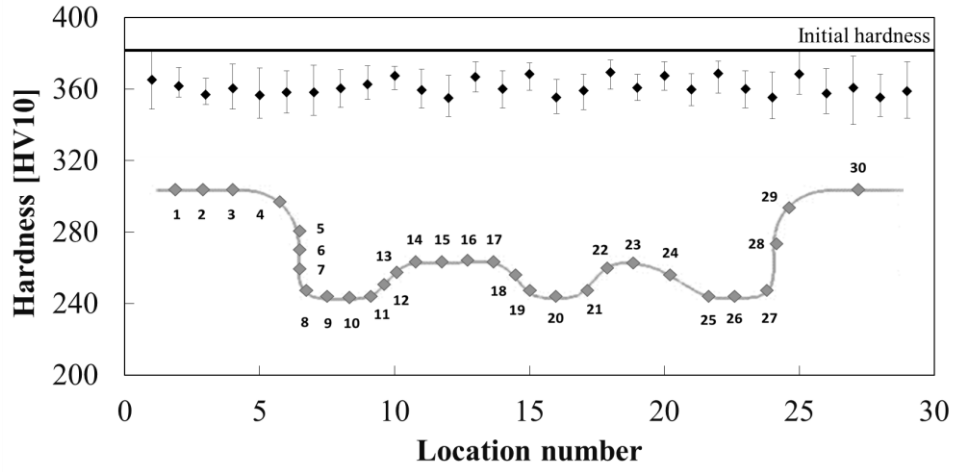

Figure 6-14. Post-form strength distribution of the investigated TC4 titanium alloy wing stiffener formed by FAST

The thickness distribution along sections AB and CD from the wing stiffener is shown in **Figure 6-15**. It can be seen that the thickness was distributed non-uniformly. In the flange area, there was some thickening; whereas localized thinning can be observed in other areas. With an initial thickness of 1.6 mm, the minimum wall thickness is approximately 1.27 mm resulting in a 20% thickness reduction. The maximum thickness reduction occurred at the corner regions due to the local deformation.

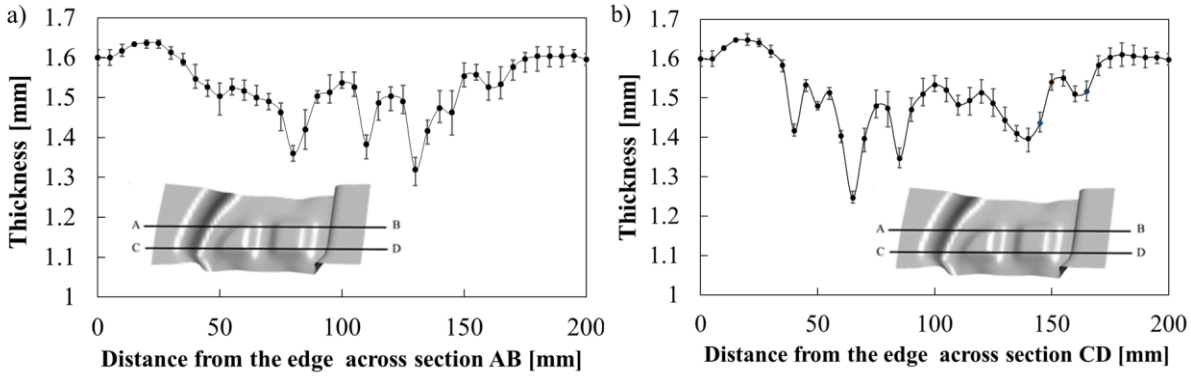

Figure 6-15. Thickness distribution along the cross sections of AB (a) and CD (b)

6.5 Conclusions

In this chapter, FAST was proposed to extend the processing windows for titanium alloys with a tailored initial microstructure under hot stamping conditions. High-temperature uniaxial tensile tests with different heating rates and different heating temperatures were performed in Gleeble to study the effects of heating parameters on the ductility and post-form strength. Forming tests of a TC4 titanium alloy wing stiffener were performed to verify this new process. The main conclusions obtained in this study are as follows:

(1) Under the fast heating condition, the heating time was too short for full element diffusion, which could reduce the phase transformation, grain coarsening and oxidation for titanium alloys, and therefore the formability of the TC4 titanium alloy could be improved.

(2) When the heating temperature was 900°C, the elongation was increased by 31.9% when the heating rate increased from 0.5°C/s to 150°C/s. However, the elongation enhancement decreased with the increasing heating rate. When the heating rate is greater than 50°C/s, the elongation change was negligible.

(3) The elongation decreased gradually with increasing heating temperature at slow heating condition; while it first increased and was followed by a reduction at fast heating conditions. The elongation enhancement obtained at fast heating condition improved from 17% at 850°C to 241% at 950°C. The post-form hardness also increased gradually with increasing temperature at both slow and fasting heating conditions, although the hardness values were greater at slow heating conditions.

(4) A qualified TC4 titanium alloy wing stiffener part without visible cracks could be formed successfully at 900°C with an average heating rate of 15°C/s. The post-form hardness was distributed uniformly and the as-formed part had almost the same strength as the initial material. The proposed FAST process demonstrates the great potential in forming complex shaped titanium alloy components.

CHAPTER 7

7. Final conclusions and futurework

7.1 Conclusions

In this thesis, an innovative forming technology to shape the Ti6Al4V titanium alloy utilizing low temperature forming tools and a hot blank was studied through uniaxial tensile test and hot stamping process. The uniaxial tensile properties of the Ti6Al4V alloy at temperatures ranging from 600°C to 900°C with the various strain rate ranging from 0.1 to $10s^{-1}$ where investigated to define the optimal processing window for hot stamping of titanium alloys. The comprehensive studies of the Ti6Al4V microstructure evolution and flow behavior under hot stamping conditions were performed. Characterisation of material behavouir allowed to develop a viscoplastic constitutive model in order to precisely describe the response of the material under high temperature deformation. The developed material model was calibrated through various uniaxial tensile tests with good agreements between the experimental and theoretical results. Simultaneously, the data from material modelling was transfered into the Finite Element (FE) simulation software (PAM-STAMP) in the form of material card to study the deformation characteristics of investigated Ti6Al4V alloy under hot stamping conditions.

The key findings from the project are summarised below:

1. The optimal temperature for the hot stamping of titanium parts were prevalent in a range from 750°C to 850°C at strain rates between 1 - 10 s^{-1}. Forming at temperatures up to 750°C led to surface cracks. Such occurrence of cracks was related to limited ductility of the material. On the other hand, the forming at heating temperatures above 850°C led to excessive $\alpha \rightarrow \beta$ phase transformation. During the following transfer and forming, temperature reduction occurred resulting in a formation of transformed β phase and simultanious reduction of the formability. It was found that deformation condition influenced both the mechanical properties and microstructure of the material. The post-form hardness and microstructure were mainly determined by heating temperature and soaking time. Through the proper adjustment of these parameters, the formability and post-form hardness of the material could be tailored during the forming process.
2. Microstructural analysis of the Ti6Al4V titanium alloy indicates that deformation under high strain rate conditions and temperatures under 900˚C allow for the initial grain size of the material to be maintained. The ductility and post-form strength of the Ti6Al4V alloy was determined by the volume fraction of β phase formed within the structure during the heating and soaking stages.

3. On the basis of the Ti6Al4V flow behavior and its microstructure evolution under high strain rate deformation conditions, the strain-stress relationships for different temperatures and strain rates were predicted with good agreements between the experimental and theoretical results. The data obtained from calculations performed using the material model developed was imported into FE simulation software (PAM-STAMP) in the form of material card, and subsequently, FE simulation model was elaborated. Such model allows to reflect the forming conditions and simulate each step of material deformation. FE model was successfully verified experimentally through the hot stamp forming of a demonstrator component. Good agreement was achieved between the experimental and FE simulation results, especially with regard to the thinning and temperature history during forming.
4. Deformation of material under the FAST conditions led to the elongation enhancement from 17% at 850°C to 241% at 950°C. A qualified TC4 wing stiffener part without visible cracks could be formed successfully at 900°C within the heating rate ranging from 15 to 50°C/s. The proposed FAST process demonstrates the great potential in forming complex shaped titanium alloy components. The FAST technology allows to reduce the soaking-heating stage from several minutes to few seconds, and thus, be more efficient and economic in comparison to hot stamping technology.

7.2 Suggestions for futurework

A number of aspects involved in the modelling and simulation of the hot stamping process and FAST forming that could to be further improved were listed below :

1. Improved modelling of the heating rate dependent viscoplastic behaviors & post-form microstructure/strength prediction of the Ti6Al4V alloy under hot stamping conditions;
2. Improved modelling of the FAST forming by detailed characterisation of microstructure evolution of investigated titanium alloy during fast heating and high strain rate deformation;
3. Development of multi-objective simulations of a forming process using a cloud computing environment for titanium alloys components;
4. Implementation and comerialisation of FAST technology to industrial scale. Forming a big scale components;

REFERENCES

Adamus, J. 2009. "Theoretical and Experimental Analysis of the Sheet-Titanium Forming Process." Archives of Metallurgy and Materials Vol. 54, i: 705–9.

Arun, J.V. 2006. "Titanium Alloys. An Atlas of Structures and Fracture Features" CRC Press Taylor & Francis Group.

Astarita, A., Armentani, E., Ceretti, E,. Giorleo, L., Mastrilli, P., Paradiso, V., Scherillo, F., Squillace, A. and Velotti, C., 2013. "Hot Stretch Forming of a Titanium Alloy Component for Aeronautic: Mechanical and Modelling." Key Engineering Materials 554–557 (January): 647–56. https://doi.org/10.4028/www.scientific.net/KEM.554-557.647.

Babu, B., and Lindgren,. L.-E., 2013. "Dislocation Density Based Model for Plastic Deformation and Globularization of Ti-6Al-4V." International Journal of Plasticity 50: 94–108. https://doi.org/10.1016/j.ijplas.2013.04.003.

Bai, Q., Lin, J., Dean, T. A., Balint, D. S., Gao, T. and Zhang. Z. 2013. "Modelling of Dominant Softening Mechanisms for Ti-6Al-4V in Steady State Hot Forming Conditions." Materials Science and Engineering A 559: 352–58. https://doi.org/10.1016/j.msea.2012.08.110.

Bariani, P. F., Bruschi, S., Ghiotti, A. and Michieletto, F., 2013. "Hot Stamping of AA5083 Aluminium Alloy Sheets." CIRP Annals - Manufacturing Technology 62 (1): 251–54. https://doi.org/10.1016/j.cirp.2013.03.050.

Barrett, C. S. 1952. "Structure of Metals." McGraw-Hill.

Beal, J. D, Boyer, R., Sanders, D. and The Boeing Company, 2006, "Forming of Titanium and Titanium Alloys." ASM Handbook : Metalworking: Sheet Forming 14B: 656–69. https://doi.org/10.1361/asmhba0005146.

Blanc, M., 1999, " High- Rate Deformation in Metals", Third Biennial Tri-Laboratory Engineering Conference on Modelling and Simulation, Pleasanton, CA (US), 11/03/1999--11/05/1999;

Boyer, R. R., 1996. "An Overview on the Use of Titanium in the Aerospace Industry." Materials Science and Engineering A 213 (1–2): 103–14. https://doi.org/10.1016/0921-5093(96)10233-1.

Bridges, P J, and Magnus, B., 2001, "Manufacture of Titanium Alloy Components for Aerospace and Military Applications." RTO AVT Specialists' Meeting on "Cost Effective Application of Titanium Alloys in Military Platforms" 069 (II): (SM2)2-1-2-11.

Bruschi, S., Ghiotti, A., 2014a., "Hot Stamping." Comprehensive Materials Processing 3: 27–54.

https://doi.org/10.1016/B978-0-08-096532-1.00303-4.

Bruschi, S., Altan, T., Banabic, D., Bariani, P. F., Brosius, A., Cao, J., Ghiotti, A., Khraisheh, M., Merklein, M. and Tekkaya, A. E. 2014b. "Testing and Modelling of Material Behavior and Formability in Sheet Metal Forming." CIRP Annals - Manufacturing Technology 63 (2): 727–49. https://doi.org/10.1016/j.cirp.2014.05.005.

Cahn, R. W., Haasen, P., Kramer, E.J. 1995. Materials Science and Technology. New York: VCH.

Cai, Z.-H., Fakir, O.E., Sun, Y.-H., Zhang, Q.-L., Dhawan, S., Luan, X., Wu, G., Wang, L.-L. 2019. A data guided approach to manufacturing light-weight components., patent issued 2019.

Chang, L., Yu, Z., and Hua, X. 2017. "The Effects of Prestrain and Subsequent Annealing on Tensile Properties of CP-Ti." Metals 7 (3). https://doi.org/10.3390/met7030099.

Chen, C., Chen, M., Xie, L., Gong, Z. and Ye, J. 2019. "Numerical and Experimental Investigations of the Hot Stamping Process for Complex Aircraft Skin Parts Composed of TA32 High-Temperature Titanium Alloy Using an Arrhenius-Type Constitutive Model." International Journal of Advanced Manufacturing Technology 103 (1–4): 807–17. https://doi.org/10.1007/s00170-019-03568-7.

Chen, J., Li, X., Han, X., 2014. "Hot Stamping." Comprehensive Materials Processing 5: 351–70. https://doi.org/10.1016/B978-0-08-096532-1.00526-4.

Cui, C., Hu, B.M., Zhao, L., and Liu, S. 2011. "Titanium Alloy Production Technology, Market Prospects and Industry Development." Materials and Design 32 (3): 1684–91. https://doi.org/10.1016/j.matdes.2010.09.011.

Deng, T., D. Li, X. Li, P. Ding, and K. Zhao. 2014. "Hot Stretch Bending and Creep Forming of Titanium Alloy Profile." Procedia Engineering 81 (October): 1792–98. https://doi.org/10.1016/j.proeng.2014.10.234.

Destefani, J. D. 1990." Introduction to Titanium and Titanium Alloys. Vol. 2". ASM International. https://doi.org/10.31399/asm.hb.v02.a0001080.

Donachie, M. J., 2000. "Titanium: A Technical Guide". ASM International.

Donachie, M. J., 2001, "Heat Treating Titanium and Its Alloys." ASM International.

Elmer, J. W., Palmer, T. A., Babu, S. S., and Specht, E. D. 2005. "In Situ Observations of Lattice Expansion and Transformation Rates of α and β Phases in Ti-6Al-4V." Materials Science and Engineering A 391 (1–2): 104–13. https://doi.org/10.1016/j.msea.2004.08.084.

Elmer, J. W., Palmer, T. A., Babu, S. S., Zhang, W. and DebRoy, T. 2004. "Phase Transformation Dynamics during Welding of Ti-6Al-4V." Journal of Applied Physics 95 (12): 8327–39. https://doi.org/10.1063/1.1737476.

Ermachenko, A. G., Ya Lutfullin, R. and Mulyukov, R. R. 2011. "Advanced Technologies of Processing Titanium Alloys and Their Applications in Industry." Reviews on Advanced Materials Science 29 (1): 68–82.

Fakir, O.El, Chen, S. H., Wang, L., Balint, D., Dear, J. P. and Lin, J. 2013. "Numerical Investigation on the Hot Forming and Cold-Die Quenching of an Aluminium-Magnesium Alloy into a Complex Component." Materials Science Forum 765 (July): 368–72. https://doi.org/10.4028/www.scientific.net/msf.765.368.

Fakir, O.El, Wang, L., Balint, D., Dear, J. P., Lin, J. and Dean, T. A. 2014. "Numerical Study of the Solution Heat Treatment, Forming, and in-Die Quenching (HFQ) Process on AA5754." International Journal of Machine Tools and Manufacture 87: 39–48. https://doi.org/10.1016/j.ijmachtools.2014.07.008.

Fiorentino, A., Ceretti, E. and Giardini, C. 2015. "Experimental and Numerical Method for the Analysis of Warm Titanium Sheet Stamping of an Automotive Component." Advances in Materials Science and Engineering 2015. https://doi.org/10.1155/2015/137964.

Fitzner, A., Palmer, J., Gardner, B., Thomas, M., Preuss, M. and da Fonseca, J. Q. 2019. "On the Work Hardening of Titanium: New Insights from Nanoindentation." Journal of Materials Science 54 (10): 7961–74. https://doi.org/10.1007/s10853-019-03431-w.

Froes, F.H. 2015. "Titanium: Physical Metallurgy Processing and Application". ASM International. Vol. 53. Ohio: ASM International. https://doi.org/10.1017/CBO9781107415324.004.

Furuhara, T., Poorganji, B., Abe, H. and Maki, T. 2007. "Dynamic Recovery and Recrystallization in Titanium Alloys by Hot Deformation." Jom 59 (1): 64–67. https://doi.org/10.1007/s11837-007-0013-8.

Gao, M., He, K., Li, L., Wang, Q. and Liu, C. 2019. "A Review on Energy Consumption , Energy E Ffi Ciency and Energy Saving of Metal Forming Processes From Different Hierarchies." Processes,7, 357; doi:10.3390/pr7060357

Guleryuz, H. and Cimenoglu, H. 2009. "Oxidation of Ti-6Al-4V Alloy." Journal of Alloys and Compounds 472 (1–2): 241–46. https://doi.org/10.1016/j.jallcom.2008.04.024.

Guo, M.L., Liu, J., Tan, M.J. and Chua, B.W. 2014. "Microstructure Evolution of Ti-6Al-4V during

Superplastic-like Forming." Procedia Engineering 81 (October): 1090–95. https://doi.org/10.1016/j.proeng.2014.10.146.

Hamedon, Z., Mori, K., Maeno, T ., 2013. "Hot Stamping of Titanium Alloy Sheet Using Resistance," NMSTU 5:12–15. URL: https://cyberleninka.ru/article/n/hot-stamping-of-titanium-alloy-sheet-using-resistance-heating (òàòà îáðàùåíèÿ: 16.07.2020).

Hu, M., Dong, L., Zhang, Z., Lei, X., Yang, R. and Sha, Y. 2018. "Correction of Flow Curves and Constitutive Modelling of a Ti-6AL-4V Alloy." Metals 8 (4): 1–15. https://doi.org/10.3390/met8040256.

Inagaki, I., Takechi, T., Shirai, Y. and Ariyasu, N. 2014, "Application and Features of Titanium for the Aerospace Industry." Nippon Steel & Sumitomo Metal Technical Report 106 (106): 22–27.

Jadhav, S., Powar, A., Patil, S., Supare, A., Farane, B. and Singh, R. 2017, "Effect of Volume Fraction of Alpha and Transformed Beta on the High Cycle Fatigue Properties of Bimodal Ti6Al4V Alloy." IOP Conference Series: Materials Science and Engineering 201 (1). https://doi.org/10.1088/1757-899X/201/1/012035.

Jha, J. S., Tewari, A., Mishra, S. and Toppo, S. 2017. "Constitutive Relations for Ti-6Al-4V Hot Working." Procedia Engineering 173: 755–62. https://doi.org/10.1016/j.proeng.2016.12.089.

Jiao, L. 2010. "Microstructure Evolution during High Temperature Deformation of Ti-6Al-4V Alloy." Rare Metal Materials and Engineering 39 (8): 1323–28. https://doi.org/10.1016/S1875-5372(10)60114-2.

Karasevskaya, O. P., Ivasishin, O. M., Semiatin, S. L. and Matviychuk, Y. V.. 2003. "Deformation Behavior of Beta-Titanium Alloys." Materials Science and Engineering A 354 (1–2): 121–32. https://doi.org/10.1016/S0921-5093(02)00935-8.

Karbasian, H., Tekkaya, A.E., 2010. "A Review on Hot Stamping." Journal of Materials Processing Technology 210 (15): 2103–18. https://doi.org/10.1016/j.jmatprotec.2010.07.019.

Knauer, E., Freudenberger, J., Marr, T., Kauffmann, A. and Schultz, L. 2013. "Grain Refinement and Deformation Mechanisms in Room Temperature Severe Plastic Deformed Mg-AZ31." Metals 3 (3): 283–97. https://doi.org/10.3390/met3030283.

Kopec, M., Wang, K., Politis, D.J., Wang, Y., Wang, L. and Lin, J. 2018. "Formability and Microstructure Evolution Mechanisms of Ti6Al4V Alloy during a Novel Hot Stamping Process." Materials Science and Engineering A 719. https://doi.org/10.1016/j.msea.2018.02.038.

Kopec, M., Wang, K., Wang, Y., Wang, L. and Lin, J. 2018. "Feasibility Study of a Novel Hot

Stamping Process for Ti6Al4V Alloy." In MATEC Web of Conferences. Vol. 190. https://doi.org/10.1051/matecconf/201819008001.

Lee, W. S., and Huang, S. Z.. 2005. "Deformation and Failure Behavior of Ti-6Al-4V Alloy under High Rate Shear Loading." Computational Ballistics II 40: 229–38.

Lee, W.-S. and Lin, C. 1998. "High-Temperature Deformation Behavior of Ti6Al4V Alloy Evaluated by High Strain-Rate Compression Tests." Journal of Materials Processing Technology 75 (1–3): 127–36. https://doi.org/10.1016/S0924-0136(97)00302-6.

Leo Prakash, D. G., Ding, R., Moat, R. J., Jones, I., Withers, P. J., Quinta da Fonseca J. and Preuss, M. 2010. "Deformation Twinning in Ti-6Al-4V during Low Strain Rate Deformation to Moderate Strains at Room Temperature." Materials Science and Engineering A 527 (21–22): 5734–44. https://doi.org/10.1016/j.msea.2010.05.039.

Liu, J., Tan, M., Aue-u-lan, Y. 2013. "Superplastic-like Forming of Ti-6Al-4V Alloy." International Journal of Advanced Manufacturing Technology 69 (5–8): 1097–1104. https://doi.org/10.1007/s00170-013-5101-z.

Liu, J., Gao, H., Fakir, O. El., Wang, L. and Lin, J. 2015. "HFQ Forming of AA6082 Tailor Welded Blanks." MATEC Web of Conferences 21. https://doi.org/10.1051/matecconf/20152105006.

Liu, X., Ji, K., Fakir, O. El, Fang, H., Gharbi, M. M. and Wang, L. 2017. "Determination of the Interfacial Heat Transfer Coe Ffi Cient for a Hot Aluminium Stamping Process." Journal of Materials Processing Tech. 247 (April): 158–70. https://doi.org/10.1016/j.jmatprotec.2017.04.005.

Liu, X., Kang, J., Fakir O.El, Liu J., Qunli, Z. and Wang, L. 2015. "Determination of the Interfacial Heat Transfer Coefficient in the Hot Stamping of AA7075 Determination of the Interfacial Heat Transfer Coefficient in the Hot Stamping of AA7075," no. January. https://doi.org/10.1051/matecconf/20152105003.

Lutjering, G. and Williams, J.C. 2007. "Titanium." Springer.

Ma, B. L., X. D. Wu, X. J. Li, M. Wan, and Z. Y. Cai. 2016. "Investigation on the Hot Formability of TA15 Titanium Alloy Sheet." Materials and Design 94: 9–16. https://doi.org/10.1016/j.matdes.2016.01.010.

Maeno, T., Mori, K., Yachi, R. 2017. "Hot Stamping of High-Strength Aluminium Alloy Aircraft Parts Using Quick Heating." CIRP Annals - Manufacturing Technology 66 (1): 269–72. https://doi.org/10.1016/j.cirp.2017.04.117.

Maeno, T., Tomobe, M., Mori, K. and Ikeda, Y. 2018. "Hot Stamping of Titanium Alloy Sheets Using Partial Contact Heating." Procedia Manufacturing 15: 1149–55. https://doi.org/10.1016/j.promfg.2018.07.375.

Maeno, T., Yamashita, Y. and Mori, K. 2016. "Hot Stamping of Titanium Alloy Sheets into u Shape with Concave Bottom and Joggle Using Resistance Heating." Key Engineering Materials 716: 915–22. https://doi.org/10.4028/www.scientific.net/KEM.716.915.

Majorell, A., Srivatsa, S. and Picu, R. C. 2002a. "Mechanical Behavior of Ti-6Al-4V at High and Moderate Temperatures-Part I: Experimental Results." Materials Science and Engineering A 326 (2): 297–305. https://doi.org/10.1016/S0921-5093(01)01507-6.

Majorell, A, Srivatsa, S. and Picu, R. C. 2002b. "Mechanical Behavior of Ti-6Al-4V at High and Moderate Temperatures - Part II: Constitutive Modelling." Materials Science and Engineering A-Structural Materials Properties Microstructure and Processing 326 (2): 306–16. https://doi.org/Pii s0921-5093(01)01507-6\r10.1016/s0921-5093(01)01507-6.

Meng, M., Fan, X. G., Gao, P. F., Guo, L. G., Zhan, M. and Wei, K. 2017. "Microstructure Evolution in near Isothermal Forming of Titanium Alloy Component." Procedia Engineering 207: 2173–78. https://doi.org/10.1016/j.proeng.2017.10.977.

Mises, Von.L., 1928. "Mechanik Der Plastischen Formanderung von Kristallen." Zeitschrift For Angewandte Mathematik Und Mechanik 1.

Moćko, W., Kostrzewski, C. and Brodecki, A. 2017. "Anisotropic Properties of Ti6Al4V Titanium Sheet under Quasi-Static and Dynamic Loading Conditions." Materials Today: Proceedings 4 (5): 5883–88. https://doi.org/10.1016/j.matpr.2017.06.063.

Mosleh, A. O., Mikhaylovskaya, A. V., Kotov, A. D., Kwame, J. S. and Aksenov. S. A. 2019. "Superplasticity of Ti-6Al-4V Titanium Alloy: Microstructure Evolution and Constitutive Modelling." Materials 12 (11). https://doi.org/10.3390/ma12111756.

Ning, Y. Q., Luo, X., Liang, H. Q., Guo, H. Z., Zhang, J. L. and Tan, K. 2015. "Competition between Dynamic Recovery and Recrystallization during Hot Deformation for TC18 Titanium Alloy." Materials Science and Engineering A 635: 77–85. https://doi.org/10.1016/j.msea.2015.03.071.

Odenberger, E. L., Oldenburg, M., Thilderkvist, P., Stoehr, T., Lechler, J. and Merklein, M. 2011. "Tool Development Based on Modelling and Simulation of Hot Sheet Metal Forming of Ti-6Al-4V Titanium Alloy." Journal of Materials Processing Technology 211 (8): 1324–35. https://doi.org/10.1016/j.jmatprotec.2011.03.001.

Oh, S., Woo, K., Lee, T. and Lee, H. 2015. "Effects of Heat Treatment on Mechanical Properties of VAR- Cast Ti-6Al-4V Alloy," Proceedings of the World Congress on Mechanical, Chemical, and Material Engineering (MCM 2015)

Ozturk, F., Ece, R.E., Polat, N. and Koksal, A. 2010. "Effect of Warm Temperature on Springback Compensation of Titanium Sheet." Materials and Manufacturing Processes 25 (9): 1021–24. https://doi.org/10.1080/10426914.2010.492056.

Ozturk, F., Ece, R.E., Polat, N. and Koksal, A. 2011, "Assessment of Electrical Resistance Heating for Hot Formability of Ti-6Al-4V Alloy Sheet." Key Engineering Materials 473 (October 2015): 130–36. https://doi.org/10.4028/www.scientific.net/KEM.473.130.

Ozturk, F., Ece, R.E., Polat, N., Koksal, A., Evis, Z. and Polat, A. 2013. "Mechanical and Microstructural Evaluations of Hot Formed Titanium Sheets by Electrical Resistance Heating Process." Materials Science and Engineering A 578: 207–14. https://doi.org/10.1016/j.msea.2013.04.079.

Ozturk, F., Ece, R.E., Polat, N., Koksal, A., Evis, Z. and Sheikh-Ahmad, Y. 2016. "Application of Electric Resistance Heating Method on Titanium Hot Forming at Industrial Scale." Arabian Journal for Science and Engineering 41 (11): 4441–48. https://doi.org/10.1007/s13369-016-2159-6.

Peters, M., 2003a. "Titanium and Titanium Alloys". WILEY-VCH Verlag GmbH & Co. KGaA, Weinheim. DOI:10.1002/3527602119

Peters, M., Kumpfert, J., Ward, C. H. and Leyens, C. 2003b. "Titanium Alloys for Aerospace Applications." Advanced Engineering Materials 5 (6): 419–27. https://doi.org/10.1002/adem.200310095.

Quan, G., Luo, G., Liang, J., Wu, D., Mao, A. and Liu, Q. 2015. "Modelling for the Dynamic Recrystallization Evolution of Ti – 6Al – 4V Alloy in Two-Phase Temperature Range and a Wide Strain Rate Range." Computational Materials Science 97: 136–47. https://doi.org/10.1016/j.commatsci.2014.10.009.

Raghu, T., Balasundar, I. and Sudhakara Rao, M. 2011. "Isothermal and near Isothermal Processing of Titanium Alloys." Defence Science Journal 61 (1): 72–80. https://doi.org/10.14429/dsj.61.321.

Raja, A., Jayaganthan, R., Tiwari, A. and Srinivasa Rakesh, Ch. 2020. "Effect of Grain Size on Superplastic Deformation of Metallic Materials." In Aluminium Alloys and Composites, edited by Kavian Omar Cooke. Rijeka: IntechOpen. https://doi.org/10.5772/intechopen.86017.

Rhaipu, S. 2002. "The Effect of Rapid Heat Treatment on the High-Temperature Tensile Behavior of Superplastic Ti-6Al-4V." Metallurgical and Materials Transactions A: Physical Metallurgy and Materials Science 33 (1): 83–92. https://doi.org/10.1007/s11661-002-0007-7.

Rollett, A, Humphreys, F, Rohrer, G.S, Hatherly, M. 2013. "Recrystallisation and Related Annealing Phenomena." Journal of Chemical Information and Modelling 53 (9): 1689–99. https://doi.org/10.1017/CBO9781107415324.004.

Sandala, R. S.. 2012. "Deformation Mechanisms of Two-Phase Titanium Alloys." PhD Thesis. https://doi.org/10.1533/9780857093844.1.63.

Sergent, P., Ahsby, M., 1982, "Deformation maps for titanium and zirconium", Scripta Matellurgica, 16 (12) 1415-1422 DOI: 10.1016/0036-9748(82)90439-2

Semiatin, S. L., Obstalecki, M., Payton, E. J., Pilchak, A. L., Shade, P. A., Levkulich, N. C., Shank, J. M., Pagan, D. C., Zhang, F. and Tiley, J. S. 2019. "Dissolution of the Alpha Phase in Ti-6Al-4V During Isothermal and Continuous Heat Treatment." Metallurgical and Materials Transactions A: Physical Metallurgy and Materials Science 50 (5): 2356–70. https://doi.org/10.1007/s11661-019-05164-6.

Semiatin, S. L., Seetharaman, V. and Weiss, I. 1998. "Hot Workability of Titanium and Titanium Aluminide Alloys — an Overview" 243: 1–24.

Sengupta, B., Shekhar, S. and Kulkarni, K. N. 2017. "A Novel Ultra-High Strength and Low-Cost as-Cast Titanium Alloy." Materials Science and Engineering A 696 (April): 478–81. https://doi.org/10.1016/j.msea.2017.04.106.

Serra, D. 2009. "Superplastic forming applications on aero engines " uroSPF08, Sep 2008, Carcassonne, France. hal-00359685

Sieniawski, J., Ziaja, W., Kubiak, K. and Motyka, M. 2013. "Microstructure and Mechanical Properties of High Strength Two-Phase Titanium Alloys." Titanium Alloys - Advances in Properties Control. https://doi.org/10.5772/56197.

Sikirica, S. 2016. "Low-Cost Titanium Alloy Production Titanium for Energy Efficient mechanical systems" https://www.energy.gov/sites/prod/files/2016/08/f33/Low%20Cost%20Titanium%20Alloy%20Production_0.pdf

Singh, P., Pungotra, H., Kalsi, N. S. 2017. "On the Characteristics of Titanium Alloys for the Aircraft Applications." Materials Today: Proceedings 4 (8): 8971–82.

https://doi.org/10.1016/j.matpr.2017.07.249.

Sirvin, Q., Velay, V., Bonnaire, R. and Penazzi, L. 2017. "Mechanical Behavior and Modelisation of Ti-6Al-4V Titanium Sheet under Hot Stamping Conditions." AIP Conference Proceedings 1896. https://doi.org/10.1063/1.5007973.

Soutis, C. 2005. "Carbon Fiber Reinforced Plastics in Aircraft Construction." Materials Science and Engineering A 412 (1–2): 171–76. https://doi.org/10.1016/j.msea.2005.08.064.

Souza, P. M., Beladi, H., Singh, R., Rolfe, B. and Hodgson, P. D. 2015. "Constitutive Analysis of Hot Deformation Behavior of a Ti6Al4V Alloy Using Physical Based Model." Materials Science and Engineering A 648: 265–73. https://doi.org/10.1016/j.msea.2015.09.055.

Takaki, T., Yamanaka, A. and Tomita, Y. 2015. "Phase-Field Modelling for Dynamic Recrystallization Phase-Field Modelling for Dynamic Recrystallization," no. June. https://doi.org/10.1007/978-3-319-19440-0.

Tan, K., Li, J., Guan, Z., Yang, J. and Shu, J. 2015. "The Identification of Dynamic Recrystallization and Constitutive Modelling during Hot Deformation of Ti55511 Titanium Alloy." Materials and Design 84: 204–11. https://doi.org/10.1016/j.matdes.2015.06.093.

Vanderhasten, M., Rabet, L. and Verlinden, B. 2007. "Deformation Mechanisms of Ti-6Al-4V during Tensile Behavior at Low Strain Rate." Journal of Materials Engineering and Performance 16 (2): 208–12. https://doi.org/10.1007/s11665-007-9033-3.

Velay, V., Matsumoto, H., Vidal, V. and Chiba, A. 2016. "Behavior Modelling and Microstructural Evolutions of Ti-6Al-4V Alloy under Hot Forming Conditions." International Journal of Mechanical Sciences 108–109: 1–13. https://doi.org/10.1016/j.ijmecsci.2016.01.024.

Wang, A., Liu, J., Gao, H., Wang, L. and Masen, M. 2017. "Hot Stamping of AA6082 Tailor Welded Blanks : Experiments and Knowledge- Based Cloud – Fi Nite Element (KBC-FE) Simulation ☆." Journal of Materials Processing Tech. 250 (March): 228–38. https://doi.org/10.1016/j.jmatprotec.2017.07.025.

Wang, K., Liu, G., Huang, K., Politis, D. J. and Wang, L. 2017. "Effect of Recrystallization on Hot Deformation Mechanism of TA15 Titanium Alloy under Uniaxial Tension and Biaxial Gas Bulging Conditions." Materials Science and Engineering A 708 (June): 149–58. https://doi.org/10.1016/j.msea.2017.09.128.

Wang, K., Liu, G., Zhao, J., Huang, K. and Wang, L. 2018. "Experimental and Modelling Study of an Approach to Enhance Gas Bulging Formability of TA15 Titanium Alloy Tube Based on Dynamic

Recrystallization" Journal of Materials Processing Tech. 259 (October): 387–96. https://doi.org/10.1016/j.jmatprotec.2018.05.002.

Williams, J. C., and Starke, E. A. 2003. "Progress in Structural Materials for Aerospace Systems." Acta Materialia 51 (19): 5775–99. https://doi.org/10.1016/j.actamat.2003.08.023.

Wu, F., Xu, W., Jin, X., Zhong, X., Wan, X., Shan, D. and Guo, B. 2017. "Study on Hot Deformation Behavior and Microstructure Evolution of Ti55 High-Temperature Titanium Alloy." Metals 7 (8). https://doi.org/10.3390/met7080319.

Yang, H., Fan, X. G., Sun, Z. Ch., Guo, L.G. and Zhan, M. 2011. "Recent Developments in Plastic Forming Technology of Titanium Alloys." Science China Technological Sciences 54 (2): 490–501. https://doi.org/10.1007/s11431-010-4206-y.

Yang, L., Li, N., Wang, B., Lin, J., Zhao, H. and Ma, W. 2016. "Unified Constitutive Modelling for Two-Phase Lamellar Titanium Alloys at Hot Forming Conditions." Manufacturing Review 3. https://doi.org/10.1051/mfreview/2016016.

Zhang, Q., Luan, X., Dhawan, S., Politis, D. J., Du, Q., Wang, M., Wang, K., Gharbi, M.M. and Wang, L. 2019. "Development of the Post-Form Strength Prediction Model for a Highstrength 6xxx Aluminium Alloy with Pre-Existing Precipitates and Residual Dislocations." International Journal of Plasticity 119: 230–48. https://doi.org/10.1016/j.ijplas.2019.03.013.

Zherebtsov, S. V., Kudryavtsev, E. A., Salishchev, G. A., Straumal, B. B. and Semiatin, S. L. 2016. "Microstructure Evolution and Mechanical Behavior of Ultrafine Ti[Sbnd]6Al[Sbnd]4V during Low-Temperature Superplastic Deformation." Acta Materialia 121: 152–63. https://doi.org/10.1016/j.actamat.2016.09.003.

APPENDIX A

The length of isothermal zone of tensile speicmen in the Gleeble tensile test was measured by using three set of thermocouples spot welded and positioned on the tensile specimen. Thermocouple TC1 was welded in the centre of the specimen while thermocouples TC2 and TC3 were welded in 5 milimiters distance from the centre of specimen on its left and right side, respectively (Figure A-1).

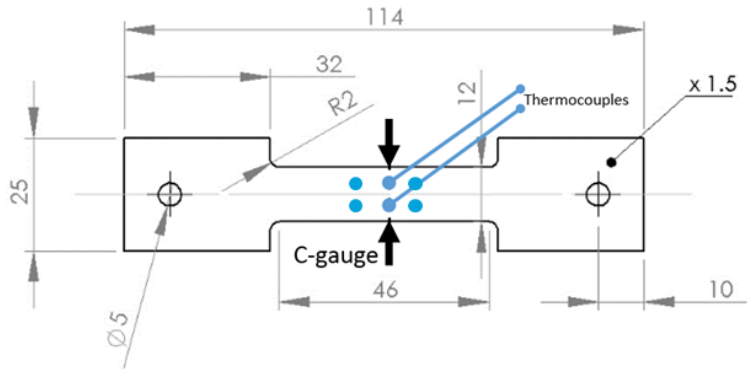

Figure A-1. The location of thermocouples on tensile specimen

In the Gleeble heating test, the target temperature was set to 700°C. The temperatures of three defined positions in each time were recorded simultaneously by Gleeble. The temperature profiles against time were shown in Figure A-2. The relatively uniform temperature distribution was recorded within 5 mm from centre of the specimen in each direction and the gauge length of 10 mm was selected.

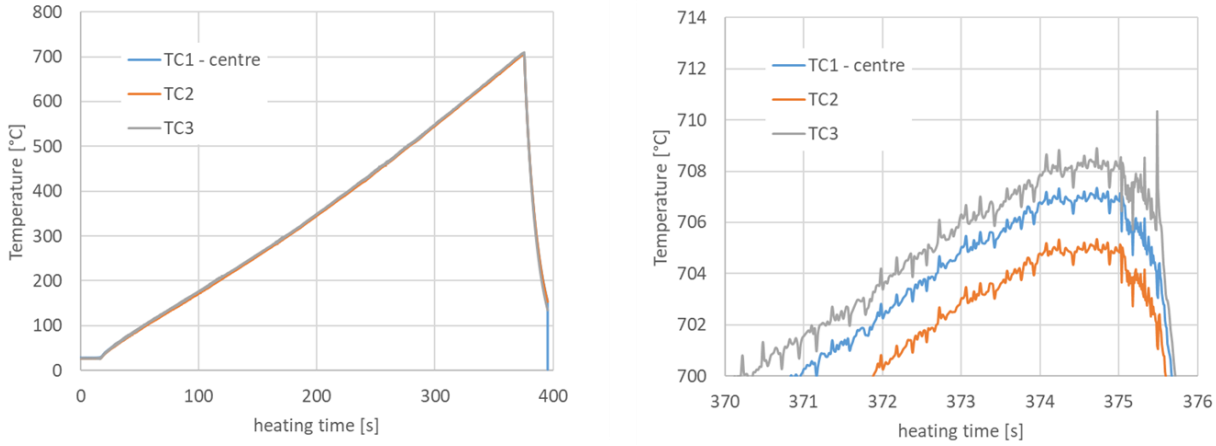

Figure A-2. Temperature recordings from 3 set of thermocouples at testing temperature of 700°C

APPENDIX B

The hardness values of the specimens after the uniaxial tensile test were measured by means of a Zwick hardness tester (Figure B-1) at room temperature with 6 measurements per condition. Each hardness measurement was performed using a 10 kgf force and the dwelling time of 10 seconds. Detailed results of hardness measurements could be found in Table B1.

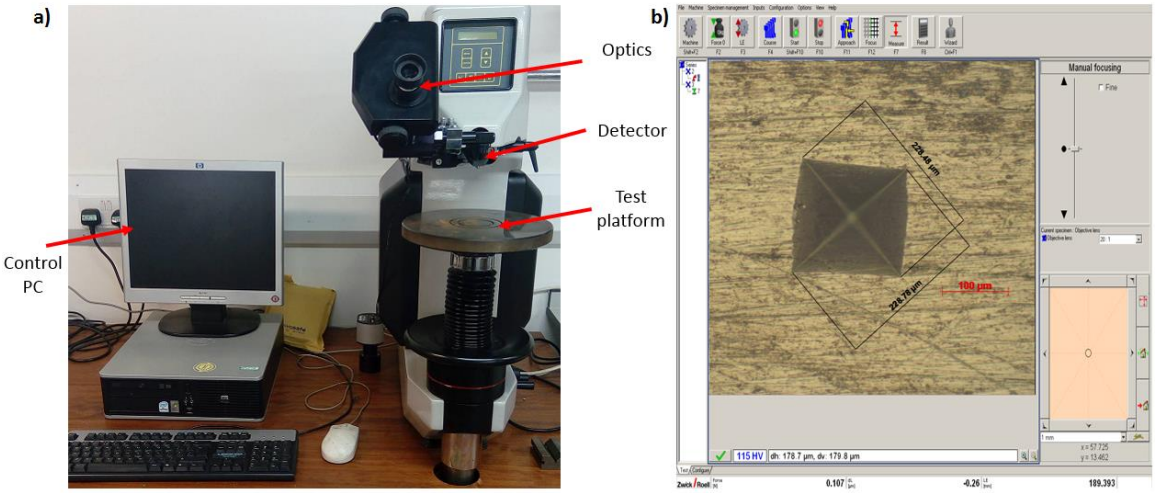

Figure B-1. Zwick ZHU hardness test machine (a) and measurement of indentation (b)

Table B-1 Hardness measurements of Ti6Al4V specimens tested in temperatures ranging from 600°C - 900°C

Heating temperature [ºC]	Hardness [HV10]						Average HV10
600	350	347	348	353	351	350	350
650	345	345	340	339	338	339	341
700	337	333	335	339	335	340	337
750	332	336	335	333	335	334	334
800	338	336	337	339	334	337	337
850	344	340	344	340	340	341	341
900	352	356	352	351	353	351	352

The hardness of m-shaped parts were evaluated in 20 different positions as presented in Figure B-2. The detailed hardness measurements of formed parts were presented in Table B-2.

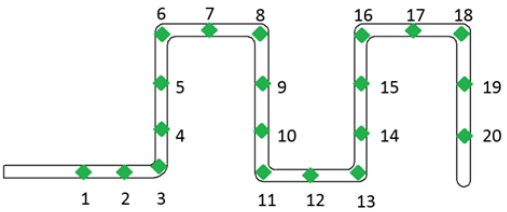

Figure B-2 Visual presentation of hardness measurement points

Table B-2 Hardness measurements of m-shaped parts

Heating temperature [°C]	600	750	850	900
Hardness [HV10]	360	342	362	376
	359	338	353	374
	358	341	358	388
	365	344	361	381
	361	343	365	383
	363	347	366	383
	357	345	370	373
	360	340	364	385
	361	349	351	372
	357	335	367	365
	359	339	354	373
	355	336	361	384
	362	347	359	365
	364	331	363	372
	355	347	356	373
	361	339	360	381
	362	341	354	381
	360	340	361	385
	360	337	352	378
	354	339	365	379
AVG HV10	359	341	360	377